Antimicrobial activity of ciprofloxacin-coated gold nanoparticles on selected pathogens

---

Nivrithi Moodley

Submitted in complete fulfillment for the Degree of Master of Technology (Biotechnology) in the Department of Biotechnology and Food Technology, Durban University of Technology, Durban, South Africa

***SUBMISSION APPROVED FOR EXAMINATION**

SUPERVISOR **Professor B. Odhav (PhD)**	**DATE**

REFERENCE DECLARATION

I, Ms N. Moodley – student number: 20924875 and Prof Bharti Odhav (full name of promoter/ supervisor) do hereby declare that in respect of the following dissertation:

Title: **Antimicrobial activity of ciprofloxacin-coated gold nanoparticles on selected pathogens**

1. As far as we ascertain:

a) no other similar dissertation exists;

the only similar dissertation(s) that exist(s) is/are referenced in my dissertation as follows:

_____

_____

_____

2. All references as detailed in the dissertation are complete in terms of all personal communication engaged in and published works consulted.

Signature of student	**Date**
Signature of promoter/ supervisor	**Date**
Signature of co-promoter/ co-supervisor	**Date**

AUTHORS DECLARATION

This study presents original work by the author. It has not been submitted in any form to another academic institution. Where use was made of the work of others, it has been duly acknowledged in the text. The research described in this dissertation was carried out in the Department of Biotechnology and Food Technology, Faculty of Applied Sciences, Durban University of Technology, South Africa, under the supervision of **Prof Bharti Odhav**.

_____

Student's signature

ACKNOWLEDGEMENTS

I would like to extend thanks to the following people and organizations:

To my supervisor, Prof. Bharti Odhav, for providing invaluable assistance, knowledge and guidance through all my years of study. This project would not have come to fruition without her constant encouragement and kindness.

To my family, for all their love, support, encouragement and belief in me (and for giving me a shove in the right direction when required!).

To Dr. Venugopal, Dr. Rajangum, Prof. Baijnath, Kaminee and Dr. Puri, for their ready assistance and expert advice on my research.

To Dr. J. Wesley-Smith and colleagues at the National Centre for Nano-structured Materials (NCNSM), CSIR, for the characterization and TEM work in this study.

To Dr. F. Swalaha, for his great assistance with the statistical analysis of the results of this study.

To Alicia, Ashira, Kabange, John, Farnaaz, Naazlene, Kriya, Evashni, Khadija, Venessa and the rest of my friends and colleagues at the Department of Biotechnology and Food Technology, DUT. Your advice, companionship, conversation, warmth and humour never failed to brighten my day.

To the National Research Foundation (NRF) for funding this project.

Lastly, to all staff at the Department of Biotechnology and Food Technology for their help and guidance.

ABSTRACT

Antibiotic resistance amongst bacterial pathogens is a crisis that has been worsening over recent decades, resulting in serious and often fatal infections that cannot be treated by conventional means. Diseases caused by these drug resistant agents result in protracted illnesses, greater mortality rates and increases in treatment costs. Improvements to existing therapies and the development of novel treatments are urgently required to deal with this escalating threat to human health. One of the more promising strategies to combat antibiotic resistance is the use of metallic nanoparticles. Research into this area has shown that the binding of antibiotics to nanoparticles enhances their antimicrobial effects, reduces side-effects due to requirement of lower dosages of the drug, concentrates the drug at the interaction site with bacterial cells and in certain cases, has re-introduced susceptibility into bacterial strains that have developed drug resistance. Furthermore, these nanoparticles can be used in cancer treatment in similar drug delivery roles.

Based on the promising data that demonstrated the synergistic effects of antimicrobial agents with nanoparticles, the aim of our research is to determine the effect of ciprofloxacin-conjugated gold nanoparticles as antimicrobial agents. To achieve this aim our objectives were: (i) to synthesize citrate-capped and ciprofloxacin-conjugated gold nanoparticles; (ii) to determine the physical and chemical characteristics of the ciprofloxacin-nanoparticle hybrid molecule; (iii) to investigate the antimicrobial activity of the conjugated nanoparticles against various species of common pathogens and (iv) to investigate the anti-cancer potential of the citrate-capped nanoparticles against a Caco-2 cell line.

In this study, citrate-capped gold nanoparticles were conjugated to the antibiotic, ciprofloxacin, and their antibacterial and anti-cancer activity was evaluated. Initial experiments involved the synthesis and characterization of gold nanoparticles and ciprofloxacin conjugated nanoparticles. The gold nanoparticles were synthesized using the Turkevich citrate reduction technique which has been extensively used in studies thus far. The synthesized nanoparticles were characterized for specific absorbance using a UV-Spectrophotometer. The bond between the nanoparticles and ciprofloxacin

was characterized by FTIR. Ultra structural details of the gold nanoparticles were established by TEM. The colloidal stability of the nanoparticles was determined by spectroscopic analysis. The antibacterial activity of the ciprofloxacin-conjugated gold nanoparticles was studied by exposure to pathogenic bacteria (*Staphyloccocus aureus*, *E. coli*, *Klebsiella pneumoniae*, *Enterococococcus* spp., *Enterobacter* spp., and *Psuedomonas* spp.). MIC values were measured to give indication of antimicrobial effect. These bactericidal properties of the conjugate nanoparticles were further investigated by electron microscopy. To evaluate the action of the citrate capped gold nanoparticles on cancer cells, we exposed Caco-2 cells to various concentrations of the nanoparticles and its effect was evaluated by measuring the viability of the cells.

The results showed that 0.5 mM trisodium citrate reduced gold chloride to yield gold nanoparticles, which were spherical and 15 to 30 nm (by TEM characterization) and had an absorption maxima of 530 nm. The ciprofloxacin conjugated nanoparticles had an absorption maxima of 667nm. The colloidal stability, which is used to assess whether the synthesized particles will retain their integrity in solution showed that citrate-capped GNPs were most stable at 37°C over a 14 day storage period while ciprofloxacin-conjugated GNPs were found to be most stable at 4°C over a 14 day period. The FTIR results showed that chemical bonding in the conjugated nanoparticles occurs between the pyridone moiety of ciprofloxacin and the nanoparticle surface. The antimicrobial results of ciprofloxacin-conjugated GNPs had a significantly improved killing response compared to ciprofloxacin on both Gram positive and Gram negative bacteria. The citrate-capped GNPs are shown to exert a similar cytotoxic effect to gemcitabine on the Caco-2 cell line at a concentration of 0.5 mM.

These results indicate that combining gold nanoparticles and ciprofloxacin enhances the antimicrobial effect of the antibiotic. The conjugate nanoparticles increase the concentration of antibiotics at the site of bacterium-antibiotic interaction, and thus enhance the binding and entry of antibiotics into bacteria. This has great implications for treatment of infection, as these antibiotic-conjugated nanoparticles can be incorporated into wound dressings, be administered intravenously as drug delivery agents, be engineered to possess multiple functionalities in addition to antibacterial activity and act as dual infection tracking and antimicrobial agents. Likewise, in this study, gemcitabine, an anticancer drug and gold nanoparticles were shown to kill

cancer cells. In addition to their use in photothermal therapy and as drug delivery agents, the nanoparticles themselves possess anti-cancer activity against the Caco-2 cells. Thus, they have potential to act alone as a form of cancer treatment if functionalized with certain targeting agents that are specific to cancer cells, reducing the side-effects that come with regular chemotherapeutic drugs.

It can be concluded that ciprofloxacin-conjugated gold nanoparticles enhance antibacterial effects of the antibiotic ciprofloxacin against bacterial cells and citrate-capped gold nanoparticles have anti-cancer activity against the Caco-2 cell line.

TABLE OF CONTENTS

LIST OF FIGURES

LIST OF TABLES

LIST OF ABBREVIATIONS

Caco-2: Human colon carcinoma cell line

GNP: Gold nanoparticle

GNWA: Gold nano wire arrays

DNA: Deoxyribonucleic acid

IR: Infrared

SAMs: Self-assembled monolayers

SERS: Surface enhanced Raman scattering

UV: Ultraviolet

EPR: Enhanced permeability and retention

NIR: Nuclear imaging resonance

TNF: Tumour necrosis factor

tRNA: Transfer ribonucleic acid

MRSA: Methicillin-resistant *Staphyloccocus aureus*

MIC: Minimum inhibitory concentration

PIBCA: Polyisobutylcyanoacrylate

PEBCA: Polyethylbutylcyanoacrylate

PLGA: Poly(lactide-co-glycolide)

FTIR: Fourier Transform Infrared

OD: Optical density

INT: p-iodonitrotetrazolium chloride

NCNSM: National Centre for Nano-structured Materials

MRC: Medical Research Council

DMEM: Dulbecco's Modified Eagle Medium

FCS: Foetal calf serum

PBS: Phosphate saline buffer

DMSO: Dimethyl sulfoxide

MTT: 3-(4,5-dimethylthiazol-2-yl)-2,5-diphenyltetrazolium bromide

ELISA: Enzyme-linked immunosorbent assay

EPS: Exo-polysaccharide

1. INTRODUCTION

Drug resistance and re-emerging diseases are challenges which modern medical research and drug development struggle to adapt to. Such infections lead to high morbidity and mortality rates amongst the patients infected (Freire-Moran *et al.*, 2011). The key to efficient and effective treatment of emerging diseases lies in the early identification, diagnosis and treatment of the infection caused. In this sense, drug development remains the most prominent area of research focus and demand. Drug development itself faces a number of different challenges, the most significant being the acquirement of antibiotic resistance amongst many bacterial strains.

Modern drug delivery techniques operate on the highly beneficial principle of site-specific or targeted therapy. This area of research has been revolutionized by the development of nanotechnology. The use of nanoparticles in various medical applications has allowed for huge advances in cancer treatment, drug therapy and various applications related to visualization, sensing and gene delivery (Shrivastava *et al.*, 2007). There is much to be gained from the use of nanoparticles for drug delivery, as this form of treatment has many advantages over conventional drug therapy. A significant factor is the ability of nanoparticles to target specific areas, thus avoiding non-specific interactions of the drug with unaffected tissue and thus prevention of undesired side effects (Gindy and Prud'homme, 2009). Furthermore, nanoparticles have numerous favourable properties, which include the ability to self-assemble, high stability in biological systems, specificity with regard to tissue targeting, the ability to encapsulate drugs and providing image contrast for visualization purposes (Gindy and Prud'homme, 2009). Thus nanoparticle-oriented research will play a major role in the advancement of medical treatment enhanced by technological aspects.

Antibiotics are currently being rendered obsolete by the rising incidence of drug resistance amongst pathogenic bacteria. Research has been focused on developing solutions to this problem by creating new antibiotics and chemically altering existing ones. However, the rate of evolution of drug resistance far outstrips efforts to impede this phenomenon in the laboratory (Boucher *et al.*, 2009). Strains of *Staphylococcus aureus*, *Pseudomonas aeruginosa* and *Klebsiella pneumoniae* are the agents of 16 % of

critical infections in hospitals and clinics and have evolved drug resistance to many of the established antimicrobial compounds on the market at present (Brown *et al.*, 2012).

Conventional cancer treatment is another aspect of medical therapy which has numerous limitations, the first and foremost being the debilitating side-effects that occur after and during chemotherapy. These side effects are largely due to the non-specificity of the chemotherapeutic drugs and the manner in which they affect healthy tissues in the human body, along with the cancerous tissue or tumours. Treatment can often only be administered at later stages in cancer development and metastatic disease (the drug resistant form) is a common cause of mortality (Heath and Davis, 2008).

Nanotechnology offers a solution to these limitations in current treatment methods due to the relatively small size of nanoparticles in comparison to biological molecules. Engineered biological compatibility is a possibility and the level of control that can be exerted over nanoparticle synthesis as well as their physical and chemical properties allows for far greater flexibility to be exercised in treatment methods, ideal for drug resistant infection control and combating cancer in its advanced form (Blecher *et al.*, 2011).Gold nanoparticles in particular have achieved a firmly established status with regard to molecule and gene delivery into cells. Some of the most significant benefits to using gold nanoparticles include their resistance to corrosion over time as well as their inert nature which makes them highly compatible with regular biological systems (Sperling *et al.*, 2008). They have been extensively employed in cancer treatment (photodynamic therapy as well as their role as drug delivery agents) and have had similar effectiveness in treatment of bacterial infections. Their mechanisms of delivery to bacterial cells have not yet been fully elucidated (Pissuwan *et al.*, 2010).

This study primarily aims to determine the effect of gold nanoparticles hybridized to an antibiotic on bacterial pathogens. Furthermore, we examined the effect of the gold nanoparticles on cancer cells. Objectives of the study were as follows:

- To synthesize citrate-capped and ciprofloxacin-conjugated gold nanoparticles
- To determine the physical and chemical characteristics of the ciprofloxacin-nanoparticle hybrid molecule

- To investigate the antimicrobial activity of the conjugated nanoparticles against various species of common pathogens
- To investigate the anti-cancer potential of the citrate-capped nanoparticles against a Caco-2 cell line.

These objectives are covered in six chapters. Chapter 1 is the introduction to the thesis, which presents the overview of the study. Chapter two (literature review) is an overview of nanotechnology, its therapeutic application, with emphasis on gold nanoparticles, its value to biomedicine and biocompatibility with human and animal systems. This section also contains a brief discussion on the antibiotic ciprofloxacin, its mechanism of destroying bacterial cells and the role of conjugating ciprofloxacin with nanoparticles. In Chapter three, the methodology used to synthesise and characterize nanoparticles, conjugate them to ciprofloxacin and evaluate the effect of the conjugated nanoparticle on bacterial pathogens is described. This is followed the methodology used to grow and maintain a cancer cell line (Caco-2) and testing of the effect of nanoparticles on these. Chapter four presents the results obtained and these are discussed in chapter five and six. The detailed layout of the thesis is outlined in Figure 1.

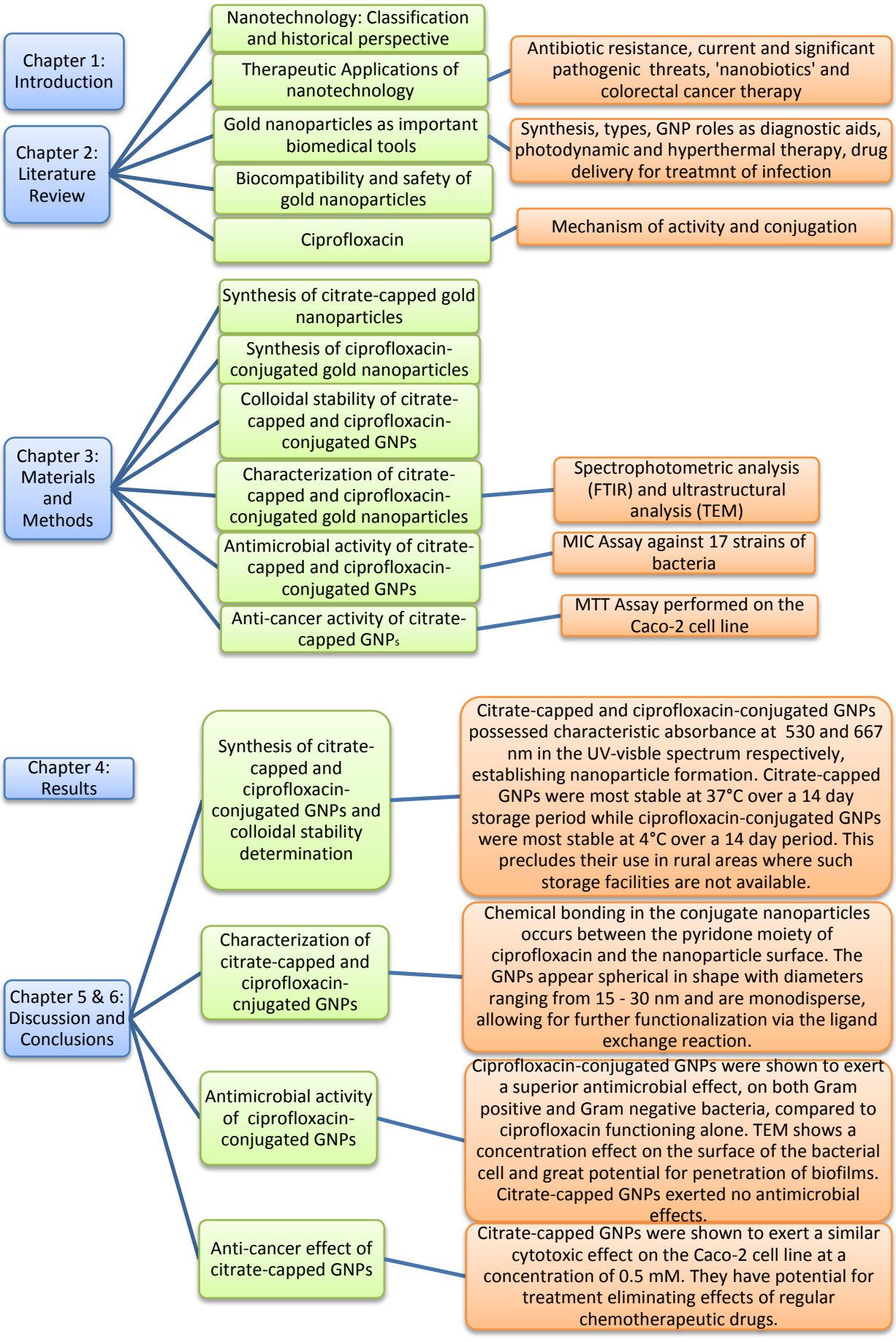

Figure 1: Layout of dissertation.

2. LITERATURE REVIEW

2.1. Nanotechnology: Classification and historical perspective

Nanotechnology is a research field that spans a broad range of research areas, including the fields of physics, chemistry, molecular biology, mechanical, chemical and electrical engineering, thus making it both multi-disciplinary and interdisciplinary (Parveen *et al.*, 2012). The field of nanotechnology, in this broad sense, involves the "synthesis, design, characterization, production and application of structures, devices and systems by controlling shape and size at the nanometer scale as well as applications of nanoparticles" (Sharon, 2012).

The definition of 'nanoscale' refers to matter within the size range of one billionth of a meter (1×10^{-9} m). Nanoparticles and other nanodevices are generally agreed to have at least one of three dimensional measurements within the size range of 1 to 100 nm (Shatkin, 2012). Nanoparticles are generally comparable, in terms of size, to biological molecules such as cell-surface receptors, enzymes and antibodies. The most well-researched and applied nanoparticle types, in terms of biomedical applications, are liposomes (Torchilin, 2005), gold nanoparticles (Ghosh *et al.*, 2008), carbon nanotubes (Shvedova *et al.*, 2009), quantum dots (Smith *et al.*, 2006) and numerous other newly emerging nanoparticles.

The concept of nanotechnology was first introduced in 1959, in a talk given by Nobel laureate, Dr. Richard Feynman. In his seminar, "There's Plenty of Room at the Bottom", he highlights the possibilities of being able to manoeuvre matter on the atomic scale and the massive implications of such work on all aspects of science (Papazoglou and Parthasarathy, 2007). This revolutionary idea led to the subsequent coining of the term 'nanotechnology' by Prof. Norio Taniguchi of Tokyo Science University, who attempted the engineering of different materials on the nanoscale level (Sharon, 2012).

Over the years, the potential of nanoscience grew with advancements in technology, providing the instruments needed to manipulate matter on the nanoscale level

envisioned by Dr. Feynman. The year 1996 witnessed a major boost to the investment in nanotechnology research. One of the most essential principles of nanotechnology application was that various materials can be, and have been in the past, re-structured in nano-form to present a whole range of unique properties and novel enhancements to existing properties (Mudshinge *et al.*, 2011).

2.2. Antimicrobial resistance and therapeutic applications of nanotechnology

The use of penicillin in the 1940's was the first highly successful form of antibiotic use. It proved to be effective right up until the 1970's and 1980's when other, stronger, broad spectrum antibiotic agents were developed (Taubes, 2008). In recent years, due to the exponential rise in antibiotic resistance amongst many bacterial species responsible for highly infectious and life-threatening diseases (Petrenko and Sorokulova, 2004; Levy, 2005) the fields of novel drug development and drug delivery have come under close scrutiny. With the increasingly problematic mutations that occur within bacterial species that allow them to develop drug-resistance mechanisms, less and less time, funding and effort is channeled into drug development. Many pharmaceutical institutions have abandoned this area of study in favour of the treatment of chronic disease (Projan, 2003).

The treatment of bacterial and viral infections with antibiotics is a route which is rapidly becoming more and more difficult to achieve. The start of the twentieth century saw infectious disease as the leading cause for mortality worldwide (Cohen, 2000). These diseases were treatable, for a time, with antibiotic development and research coming to the fore in medical focus at this time. However, with increased use of antibiotics and their integration into other branches of human employment, antibiotic resistant strains of bacteria began to emerge (Wood *et al.*, 1996; Walsh, 2000). In addition to the constant development of resistance, the genes coding for resistance to antibiotics are not easily lost once evolved in a bacterial population. Upon integration, these genes become a stable component of the bacterial genome. As further resistance mechanisms are developed, it becomes harder to provide treatment which is able to effectively combat this multi-drug resistant phenomenon (Livermore, 2003).

With the introduction of flouroquinolones to the drug market, there was renewed hope amongst medical researchers and practitioners with regards to the scope of treatment possible, as these antibiotics were broad-spectrum and could be employed effectively against a variety of infectious diseases, even those caused by drug-resistant agents. However, this optimism was short-lived when strains resistant to many of these new generation drugs, including ciprofloxacin, emerged. Bacterial species implicated in these cases included *S. aureus*, *P. aeruginosa* and *E. coli* (Piddock, 1999).

The constant evolution of antibiotic resistance amongst many of these causative bacterial strains creates complications with the upkeep of parallel development of drugs to combat their effects (Rice, 2009). To emphasize the need for this constant evolution of treatment techniques, the alternation between bacterial types in each round of epidemic challenge facing populations all around the world is a good example. MRSA (methicillin resistant *Staphylococcus aureus* was first detected as a resistant strain in patients and vancomycin was found to be an effective agent in treatment of infections caused by these bacteria (Bozdogan *et al.*, 2003). However, in addition to the development of vancomycin resistance (VRSA), current bacterial resistance challenges are far more serious with Gram negative strains of bacteria as the causative agents. These scenarios raise an important issue; that there is a great need for an enhancement of existing technology and techniques in the field of drug development, as well as the pressing requirement for development of new and innovative treatment methods for infectious diseases. These new research foci need to be directed towards creating a long-term solution to these resistance issues, one that can, and will, be implemented as a framework for future medical work in these areas (Taylor *et al.*, 2002).

The answer to this problem may lie in the relatively recent discovery of antimicrobial nanomaterials, technology against which the pathogens may not be able to develop a resistance mechanism. The nanomaterials themselves would act as precisely engineered platforms from which drugs may be delivered to target physiological sites (Nirmala Grace and Pandian, 2007). Recent studies involving metal nanoparticles shows that they possess antimicrobial activity and thus have a potential for enhancement of treatment of infection, if properly adapted into existing procedures (Schaller *et al.*, 2003; Goodman *et al.*, 2004; Weir *et al.*, 2008; Rai *et al.*, 2009). Some of the other

problematic areas of medical treatment, and the solutions offered by nanotechnology, are outlined in Table 1.

Table 1: Challenges and solutions to current diseases (Couvreur and Vauthier, 2006).

Disease	Therapeutic Challenge	Nanotechnology Solution
Infections	• Increase efficacy of delivery • Reduce toxicity by ➢ Enhancing intracellular penetration ➢ Control of biodistribution	• Nanoparticles • Liposomes • Micelles • PEGylated nanoparticles • PEGylated liposomes
Cancer	• Increase efficacy of delivery • Reduce toxicity by ➢ Enhancing intracellular penetration ➢ Control of biodistribution	• Nanoparticles • Liposomes • PEGylated nanoparticles • PEGylated liposomes • Antigen-presenting devices
Metabolic Disease	• Controlled and sustained release of drug • Protection of molecules against degradation • Improvement of mucosal absorption	• Nanoparticles • Liposomes
Gene Therapy-related diseases	• Protect DNA against degradation • Condensation of DNA • Enhance the cellular uptake of DNA	• Cationic nanospheres • Cationic liposomes • Cationic lipids

Thus far metal nanoparticles have been adapted for the applications of immunisation, detection and treatment of infection and cross infection control (Allaker and Ren, 2008). A number of advantages conferred by using these nanoparticle-based systems are evident, namely: (i) enhancement of the rate and efficiency of drug absorption by means of epithelial diffusion; (ii) prevention of degradation of the drug during its passage to the target tissues; and (iii) enhancement of the efficiency of intracellular penetration and subsequent distribution (Couvreur and Vauthier, 2006). Furthermore,

the large surface-to-volume ratio of these nanoparticles allow for greater interaction with the surface of the target molecule, whether a specific biological molecule or bacterial cell. Their relative small size also allows for bypassing many types of biological membranes (such as the blood/brain barrier), a feat that cannot be accomplished by conventional therapeutic methods (Blecher *et al.*, 2011).

The term 'nanobiotic' is used to describe nanomaterials which possess antimicrobial activity themselves, or enhance the antimicrobial activity of currently used treatments and compounds (Rai *et al.*, 2009). Use of many of the antimicrobials currently on the market leads to adverse and acute side-effects, a drawback that employment of 'nanobiotics' may be able to overcome. The long term effects of exposure to such treatment, in conjunction with nanobiotics, remains to be seen, as clinical trials have not yet covered such risks (Medina *et al.*, 2007).

2.2.1. 'Nanobiotic' types and current applications

Over the years, a very wide range of nanoparticles engineered from different nanomaterials have been created via innovative synthetic techniques, yielding a plethora of unique properties and potential applications (Parveen *et al.*, 2012). Controlling drug resistance brought about through genetic mutation of bacterial pathogens is the area of focus towards which use of these 'nanobiotics' are targeted. They are able to target biological pathways in a broad spectrum sense, as these pathways occur in most bacteria. Thus, in order for resistance to develop against the nanomaterials, a great number of synchronized mutations amongst these species would have to occur (Huh and Kwon, 2011). Further advantageous aspects of use of nanomaterials for their antimicrobial properties include their stability, ensuring a longer shelf-life once manufactured (Weir *et al.*, 2008), and their greater degree of resistance to other physical storage and preparation conditions (such as sterilization at high temperatures), to which regular antibiotics display great susceptibility.

Most nanomaterials described in current research have antimicrobial activity based on at least one of the following mechanisms: inhibiting cell wall/membrane synthesis; interrupting energy transduction; production of highly toxic reactive oxygen species;

through photocatalysis; and inhibiting the production of enzymes and DNA (Li *et al.*, 2008; Weir *et al.*, 2008). Some of the well researched and characterized antimicrobial nanomaterials and their applications in industry and medical treatment are outlined in Table 2.

Table 2: Types of antimicrobial nanomaterials and their applications (Huh and Kwon, 2011).

Nanomaterial	Antimicrobial Mechanism	Application	Reference
Silver	Damages DNA; disruption of cellular membrane and thus, electron transport	Antibacterial and antifungal agent; incorporation into wound dressings; incorporation into portable water filters	(Pal *et al.*, 2007), (Li *et al.*, 2008)
Zinc oxide	Damage to cell membrane; accumulation inside the cell; production of toxic H_2O_2	Surface coatings of surgical instruments; incorporation into antimicrobial topical ointments; mouthwash	(Huang *et al.*, 2008), (Dastjerdi and Montazer, 2010)
Titanium dioxide	Damage to cell membranes/walls; production of toxic reactive oxygen species	Water treatment; sterilization of food; antibacterial agent; air purifying agent	(Maness *et al.*, 1999), (Pratap Reddy *et al.*, 2007)
Gold	Heavy electrostatic attraction to cell surfaces; accumulation at and interaction with cell membrane/wall	Photothermal therapy using near-IR irradiation source; adjuvants in antimicrobial treatments; antifungal agent	(Chamundeeswari *et al.*, 2010), (Johnston *et al.*, 2010)
Chitosan	Disruption of cell membranes; inactivation of enzymes; chelation of trace metals	Antimicrobial agent in biomedical products; purification of drinking water; immobilization of bacteria	(Rabea *et al.*, 2003), (Li *et al.*, 2008)
Fullerenes	Disruption of cell membranes; enhances activity of infiltrating neutrophil	Potential application in disinfection	(Lyon *et al.*, 2005)
Carbon nanotubes	Production of reactive oxygen species; oxidation of lipids and protein occurring in cell membrane	Incorporation into water filters; antibacterial agent; surface coatings	(Kang *et al.*, 2007)
Nitric oxide-releasing nanoparticles	Release of nitric oxide and production of reactive oxygen species	Incorporation into wound dressings	(Weller, 2009)
Nano emulsion	Disruption of cell membranes; disruption of spore coats	Delivery vehicles in vaccines; antimicrobial inhaler; anti-biofilm agent	(Hamouda *et al.*, 1999)

Silver nanomaterials were re-examined in terms of their antimicrobial activity with the advent of antibiotic resistance. Previously, incorporation of silver into disinfection and treatment of wounds had been rendered obsolete by the use of penicillin (Taubes, 2008). As shown in Table 2, silver nanoparticles cause disruption of the microbial cell membrane. They also inhibit the respiratory process and cell division (Klasen, 2000). Silver nanoparticles have been best characterized, compared to other metal nanoparticles, in terms of conjugation to various antibiotics and enhancement of their activity (Shahverdi *et al.*, 2007; Fayaz *et al.*, 2010). In these cases the integration of silver nanoparticles was found to have a synergistic effect on antimicrobial activity against both Gram negative and Gram positive bacterial species. Although certain research suggests that silver nanoparticles have minimal cytotoxic effects when tested on mammalian cell lines, other studies highlight the potential risks of long term exposure, leaving much to be evaluated before full-scale use in certain medical applications (Oberdörster *et al.*, 2005).

Encountering similar issues, is the use of **carbon nanotubes** and **nitrogen oxide-releasing nanoparticles**. Both exhibit effective antimicrobial properties, by inhibiting membrane function and production of reactive oxygen species. However, taking into consideration their toxic effects, this points to the conclusion that their relative cytotoxicity outweighs their potential application (Tian *et al.*, 2006).

Zinc oxide, **titanium dioxide** and **gold** are the metal nanomaterials that show most promise in treatment of bacterial infections. Zinc oxide nanoparticles display no cytotoxic effects and are thus biocompatible and have already been incorporated into a number of biomedical and industrial processes. Their application in the food industry has been highly successful, with antimicrobial activity noted against *E. coli* (Liu *et al.*, 2009) and *Staphylococcus aureus* (Uğur *et al.*, 2010).

They have been extensively applied in wastewater treatment, as they are non-toxic, stable in aqueous medium and have a low production cost (Li *et al.*, 2008). Gold nanoparticles are most effective in antimicrobial treatment when used as agents of the hyperthermic effect. This form of antimicrobial application involves the irradiation of gold nanoparticles with light in the near-infrared wavelength range, causing them to heat up and selectively kill bacterial cells which they adhere to (Huang *et al.*, 2009).

The strong electrostatic interactions between gold nanoparticles and the negatively charged bacterial cell membrane are the founding principle for many subsequent drug delivery strategies, which will be discussed in further detail.

2.2.2. Strategies for treatment of infection with nanotechnology-related therapies

The need for novel drug delivery strategies has led to the exploration of nanodevices and nanoparticles as agents for encapsulation, attachment and release of drugs to target areas. The myriad variety of nanoparticle types, their tunable and engineered properties, size-related advantages and emerging potential in biomedical applications has resulted in the rapid expansion of these ideas (Jain, 2005). The control of infectious diseases is one instance in which nanotechnology has proven an invaluable aid. Diseases can be targeted in one of three key areas, or with potential combined functionalities which are able to minimize or eliminate the problem in short, sequential steps.

The first target area, **detection**, has been widely developed using nanotechnology to overcome time-consuming and cumbersome methods of pathogen diagnosis. Antibody-conjugated nanoparticles (Look *et al.*, 2010) and gold nano wire arrays (GNWA) (de la Escosura-Muñiz and Merkoçi, 2011) are examples of technologies developed for rapid detection of pathogenic bacteria, reducing the time taken for diagnosis to 20 minutes in the case of the former. In terms of the actual **antibacterial properties** of nanomaterials, metal and metal oxide nanoparticles have received increasing attention, with silver nanoparticles already being incorporated into wound dressings (Rai *et al.*, 2009) and polymeric nanoparticles displaying more effective antimicrobial activity against methicillin-resistant *Staphylococcus aureus* in comparison with general antibiotics (Turos *et al.*, 2007a; Turos *et al.*, 2007b). Furthermore, nanoparticles have also been used in the **prevention** of infectious disease, incorporated into vaccines as colloidal carriers and adjuvants (Kreuter, 1995; Jiang and Koganty, 2003).

2.2.3. Selection of bacterial strains based on current pathogenic threats

Infections caused by common pathogenic bacterial strains, such as Staphylococcus *aureus*, *Escherichia coli* and *Klebsiella pneumoniae*, take on a new significance once these microorganisms develop some form of drug resistance. Cases in point of such incidences are the *E. coli* outbreak in Walkerton, Ontario (the pathogen's presence being noted in the area's drinking water supply) (Ali, 2004) and *Enterobacter sakazakii*, an emerging opportunistic pathogen in South Africa, which has been noted to be the causative agent of severe infections, including meningitis, sepsis and necrotizing enterocolitis in premature and immuno-compromised infants (Cawthorn *et al.*, 2008).

This study focuses on six different isolated species, *Staphylococcus aureus*, *Escherichia coli*, *Pseudomonas* spp., *Enterococcus faecalis*, *Enterobacter* spp. and *Klebsiella pneumoniae*. Seventeen different isolates were obtained for all species in total, from different types of infectious material, by the supplier of the cultures, Lancet Laboratories. These species were chosen as the basis of the antimicrobial testing due to their widespread and common occurrence as disease-causing microbial agents in both the community and nosocomial settings (Zetola *et al.*, 2005).

Staphylococcus aureus, a Gram positive bacterial species, has come under close scrutiny over the past few years as it is a major cause of serious infections and pathogenicity, in both hospital and community-acquired diseases. The resistant strains of this bacterium present a problem in terms of medical treatment, the most commonly encountered being MRSA (methicillin-resistant *Staphylococcus aureus*) (Pereira *et al.*, 2009). The number of hospitalizations and deaths resulting from *Staphylococcus aureus* infections has been reported as approximately 500 000 and 20 000 in the year 2005, respectively. These figures relate to the United States alone (Peres and Madrenas, 2013).

Klebsiella pneumonaie, a Gram negative bacterial species belonging to the Enterobacteriaceae is also a significant pathogen in both hospital and community environments, being the cause of community-acquired pneumonia. The K1/K2 capsular

serotypes have been identified as particularly resistant strains, resulting in liver abscesses and meningitis (Keynan and Rubinstein, 2007). In previous years, *E. coli* had been marked as the leading cause of pyogenic liver abscesses, however, *Klebsiella* spp. has now assumed this role in both the United States and Taiwan (Pope *et al.*, 2011). These surveys in no way eliminate *E. coli* as a pathogenic threat, however, with both resistant and highly infectious strains of this bacterial species also being reported worldwide. STEC (Shiga toxin-producing *E. coli*) are one such instance, causing infections in both humans and animals that rate on the infectious scale from mildly infectious to life-threatening (Prager *et al.*, 2009). Yet another member of the family Enterobacteriaceae, and cause for concern in terms of its relative pathogenicity, is the *Enterobacter* spp. Outbreaks of *Enterobacter cloacae* have been reported in neonatal units, being transferred amongst patients within these wards through nutrition solutions, medical equipment and intravenously delivered fluids (Talon *et al.*, 2004).

Pseudomonas aeruginosa and related species (*Pseudomonas flourescens* and *Pseudomonas putida*, for instance) are known to be important causes of infection and subsequent death, despite the development of numerous vaccines and treatment methods. These bacteria target the central nervous system (CNS) and infection leads to development of meningitis and encephalitis (Picot *et al.*, 2003). They display classic features of opportunistic pathogens and were found, in studies conducted by Picot *et al.* (2003), to bind with a high degree of specificity to the cell membranes of glial cells and neurons. Once attached, the bacteria appear to induce cell death through a possible apoptotic mechanism.

All of the bacterial species tested against in this study present a serious threat to the healthcare sector in terms of their infectious potential, pathogenicity and the development of drug resistance. Besides the diseases caused by direct infection with these bacterial agents, secondary infections in immuno-compromised patients also creates huge cause for concern. Current treatment methods involving drug development and efficient drug delivery to sites of infection, all the while maintaining minimal side effects and faced with widespread drug-resistance, is an issue that the pharmaceutical industry struggles to keep abreast with. Thus, the need for efficient, novel drug delivery techniques and drug delivery vehicles has become of paramount importance in the case of treatment of such diseases and infections.

2.2.4. Colorectal cancer and incorporation of nanotechnology-based treatment

Cancer therapy has also, to a greater degree than all other branches of the medical field, incorporated nanomaterials into treatment procedures. The use of nanoparticles allows for tumour-specific delivery of chemotherapeutic drugs. Taking into account the acute side-effects of chemotherapy, nanoparticle-based delivery systems provide significant advantages. These include the reduction of drug passage to healthy tissue due to tumour-specific delivery, as well as the ability of the nanoparticle carriers to escape clearance by the reticulo-endothelial system, allowing for a longer circulation time in the system (Moghimi *et al.*, 2005).

Colorectal cancer is the focus in this study, being the third most commonly diagnosed cancer type in the world (Parkin *et al.*, 2005). Statistics reveal that 40 to 50% of patients that have been newly diagnosed with the disease soon after develop the metastatic form, while 25% of diagnosed patients undergoing treatment develop the overt metastatic form (Van Cutsem *et al.*, 2009). Conventional chemotherapy based methods of treatment include fluorouracil combined with leucovorin and irinotecan (Saltz *et al.*, 2000). An alternative therapeutic route involves administration of cetuximab (the immunoglobulin G1 monoclonal antibody acting against the epidermal growth factor receptor) in combination with irinotecan (Cunningham *et al.*, 2004). All these chemotherapeutic agents however, as in the case of all non-specific cancer therapies, have a number of undesirable side-effects, including nausea, diarrhoea and skin reactions (Van Cutsem *et al.*, 2009).

The recent approval of antibody-based targeted therapy for treatment of this cancer type has led to greater focus being directed towards research into targeted delivery systems. Nanoparticles, in particular, have been heralded as ideal dual action therapy agents, allowing for both delivery of conjugated drugs and binding to and inhibiting colorectal cancer pathways. Despite the potential benefits of further research into this treatment area, there have been relatively few ventures into nanoparticle-mediated therapy of colorectal cancer (Byrne *et al.*, 2008). Research thus far into nanocarrier treatment techniques include targeting based on peptide ligands for detection of cancerous tissue (Kelly and Jones, 2003), the targeting of guanylyl cyclase C receptors (over-expressed

in colorectal cancer tissue) and subsequent thermal ablation of tumour cells using gold nanoshells (Fortina *et al.*, 2007).

2.3. Gold nanoparticles as important biomedical tools

The unique chemical and physical properties of gold nanoparticles make them ideal for a variety of applications which have great significance in terms of biology. The advantages conferred by the employment of gold nanoparticles are: (i) the fact that they are biologically inert; (ii) they can be synthesized with a great degree of specificity and control with regard to sizes and shapes; (iii) they can be surface functionalized through a variety of techniques; (iv) they can be stabilized such that they maintain their colloidal stability for the maximum time required to perform their specific function and; (v) the surface functionalization make possible specific targeting of biological molecules, cell surface receptors, bacterial cell walls, etc. (Rastogi *et al.*, 2012).

The following sections detail the significant aspects of gold nanoparticle application in the biomedical field, including the manner in which they are synthesized and the resultant physical properties (2.3.1. and 2.3.2.), the various ways in which medical treatment incorporating gold nanoparticles is effected (2.3.3., 2.3.4. and 2.3.5.) and the proposed mechanisms by which they carry out these activities (2.3.6.), as described in literature.

2.3.1. Synthesis of gold nanoparticles

Following the same principles as synthesis of silver nanoparticles, the formation of gold nanoparticles requires the reduction of a gold salt, such as $HAuCl_4$ by an appropriate reducing agent. This reduction results in nucleation of ionic gold in solution and leads to the production of gold nanoparticles (Turkevich *et al.*, 1951). This is a ‘bottom up’ synthesis of gold nanoparticles (Figure 1, A), in which there is seed growth of the nanoparticles over time. The reduction step results in the formation of nucleated gold nanoparticles from ionic gold present in solution, originating from the gold salt. As the reaction continues, there is further collision between ions, atoms and clusters, thus resulting in both nucleation and incremental growth of the nanoparticles. Once a suitably sized nucleus of nanogold has formed, which is colloidally stable enough to act

as a platform for further growth, the synthetic parameters can be optimized and controlled to achieve a specific end result with regard to the shape and size of the nanoparticles formed. Controlling synthesis results in a number different nanoparticle sizes and shapes, including nanorods, nanocages and hollow particles which have been most applied in medical research (Figure 1, B) (Kimling *et al.*, 2006; Kim and Kim, 2011). Synthesis of gold nanoparticles has been established in both organic solvents and aqueous medium. Solvent-based synthesis requires a separate reducing and stabilizing agent, whilst aqueous synthesis allows for use of a single chemical acting in both capacities (Sperling *et al.*, 2008).

Turkevich *et al.* (1951) was the first to demonstrate the synthesis of colloidal gold by means of the citrate reduction technique. As this technology reached greater advancement in terms of control of parameters, the citrate ligand on these synthesized nanoparticles was replaced with other molecules that would have great impact on biomedical application.

The surface chemistry of gold allows for the formation of self-assembled monolayers (SAMs), which, in this case, refers to a single, uniform layer of a specific type of molecule on the surface of the gold particle. These molecules, which are characterized by an affinity to the gold molecules, do not react with the gold surface. Rather, they form weak chemical bonds with the surface (van der Waals force interactions) (Mani *et al.*, 2008; Cademartiri and Ozin, 2009). Such chemical properties thus make gold an ideal nanocarrier or drug delivery vehicle, taking into account the nature of formation of these SAMs and the inert nature of gold molecules' surfaces.

The biomolecules which are able to form SAMs on the surface of GNPs are characterized by the presence of thiol moieties (R-SH where R represents any organic chemical group), due to the affinity which gold possesses for sulphur (Cademartiri and Ozin, 2009). Many of the functionalization studies carried out employing GNPs as the carrier molecules first make use of this chemical interaction in a thiolation step to ensure efficient binding of the desired chemical group to the nanoparticles (Sperling *et al.*, 2008; Bastús *et al.*, 2009; Alanazi *et al.*, 2010; Pissuwan *et al.*, 2010; Bach *et al.*, 2012).

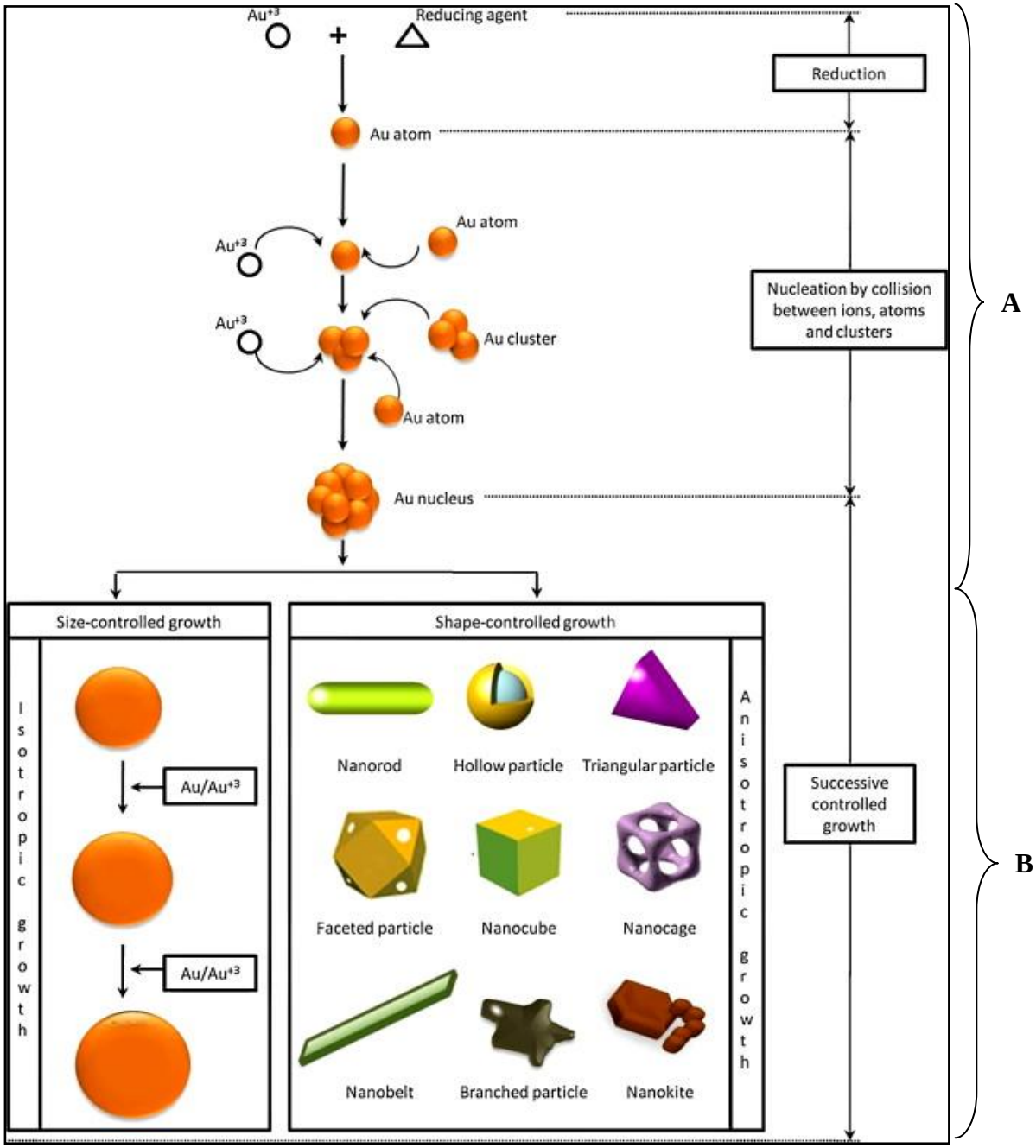

Figure 2: 'Bottom up' synthesis of gold nanoparticles by the reduction of a gold salt, followed by nucleation (A) and progressive growth, in terms of both size and shape (B).

The specifics of this reaction are yet to be fully elucidated, however, the most common line of thought directs us towards an oxidation/reduction reaction in which there is an elimination of a hydrogen atom from the thiol group (R-SH to $R\text{-}S^-$) and the simultaneous oxidation of gold to Au^+ (Cademartiri and Ozin, 2009).

The surface functionalization of gold nanoparticles has led to a number of confirmed and potential multi-disciplinary applications. A commonly exploited phenomenon in experiments dealing with coating GNPs with particular molecule types and colloidal stability studies is the "ligand exchange" reaction (Sperling *et al.*, 2008). Cademartiri and Ozin (2009) state that in the instance of a SAM-protected gold surface being placed into the solution form of another alkanethiol, a state of equilibrium is reached between the thiols present on the surface and those in solution. When one of these thiol moieties is present in greater quantities than the other, a shift in the equilibrium will result which would lead to the thiol group present in excess almost completely replacing the original SAM.

Taking into account this principle of ligand exchange, there are two separate ways of attaching biological molecules to the gold nanoparticles' surfaces. The first involves the exchange reaction, in which thiol or other moieties on the surface of the gold nanoparticles are replaced with the desired molecules (Nirmala Grace and Pandian, 2007) which possess functional groups that are able to bind to the gold surface. The second method of attachment is through bio-conjugation, namely, the formation of chemical bonds between the biological molecule and stabilizer molecules attached to the surface of the gold nanoparticles (Figure 3) (Sperling *et al.*, 2008). The attachment of antibiotics and anti-cancer drugs, such as aminoglycosides and methotrexate respectively, to the surface of citrate-capped gold nanoparticles is one instance of such a binding application (Paciotti *et al.*, 2004; Tom *et al.*, 2004; Nirmala Grace and Pandian, 2007; Pissuwan *et al.*, 2010).

Stabilization is another essential aspect of nanoparticle synthesis. Stabilizing agents, also referred to as surfactants, are generally adsorbed or bound chemically to the surface of the nanoparticle. These agents are typically charged so that they confer this collective charge to the nanoparticle surface and cause the nanoparticles in aqueous suspension to repel each other, due to like charges. This ensures colloidal stability in the sense that no aggregation occurs and the nanoparticles maintain their discrete form (Singh *et al.*, 2011).

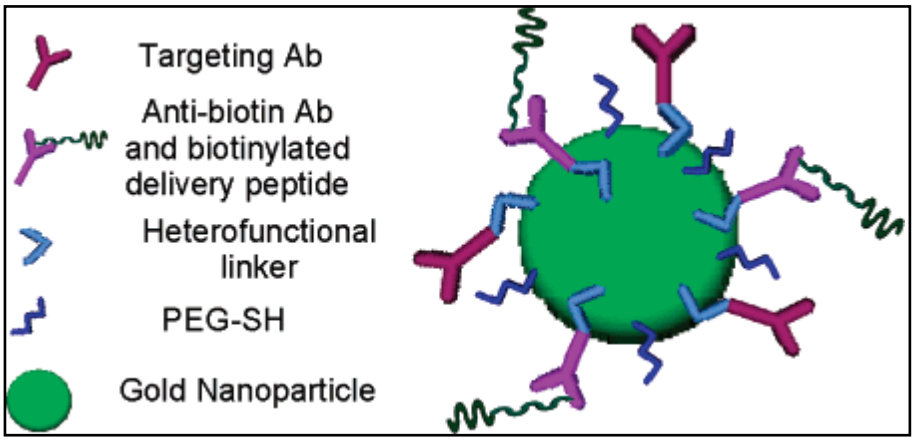

Figure 3: A gold nanoparticle contrast agent with multi-functional ligands, including components which allow for both targeting and drug delivery (Kumar *et al.*, 2007).

Various stabilizing agents have been tested with gold nanoparticles in direct comparison with citrate, which is the most commonly employed reagent for the synthetic procedure, as it behaves as both reducing and stabilizing agent (Tom *et al.*, 2004). Other agents that have been used for such stabilizing properties include starch, gum arabic (Kumar *et al.*, 2010), sodium borohydride, tannic acid/citrate mixtures (Hayat, 1989) and zwitterionic disulphide ligands (Rouhana *et al.*, 2007).

Due to the variations and control exerted over the types of surface functionalizations of gold nanoparticles, a wide range of biological molecules can be attached to their surfaces (Figure 4). Bioconjugation reactions, in most cases, have not been optimized, such that attachment of the desired molecule to the nanoparticle surface is guaranteed.

After the conjugation process, thorough characterization is carried out to ensure attachment or encapsulation. This stage is carried out to rule out the aggregation phenomenon, where the molecules produced are no longer classified within the nano-scale and further, to prevent unspecific binding during the conjugation process. In many studies, the number of molecules bound to the surface of the nanoparticles is merely a rough estimate, as there is currently no standard protocol via which the number of molecules attached can be accurately determined (Demers *et al.*, 2000; Pellegrino *et al.*, 2008). This is relevant to many current drug delivery strategies using nanoparticles as

drug delivery vehicles, where a more accurate and standardized manner of determination of the number of molecules bound to the nanoparticle surface is required.

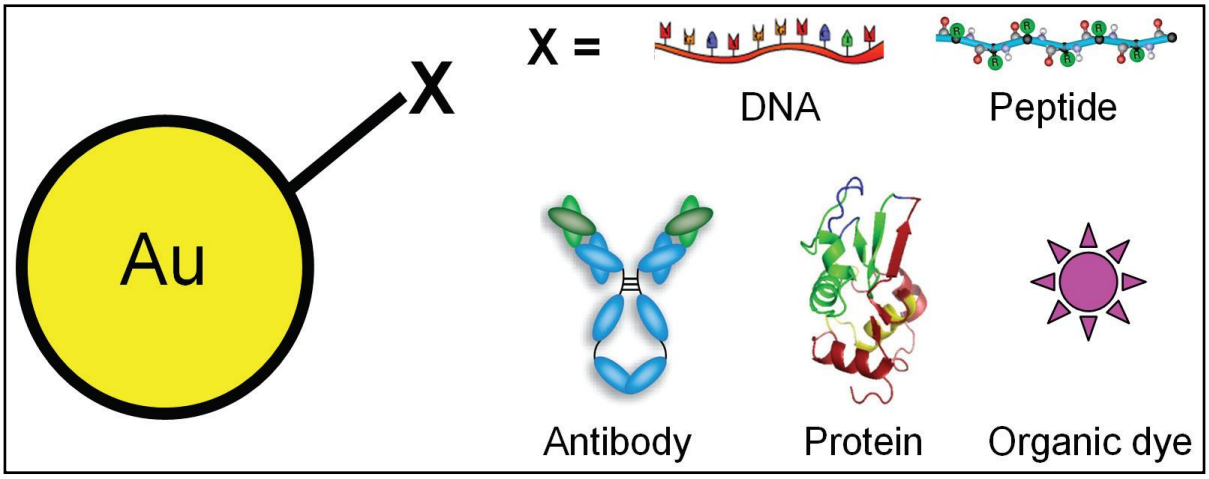

Figure 4: Representation of the potential surface functionalizations for gold nanoparticles, including ligation to nucleic acids and various protein molecules (Cai *et al.*, 2008).

2.3.2. Types of gold nanoparticles

The first reported synthesized gold nanoparticles were conventionally spherical, with subsequent modifications of the synthetic procedure resulting in the formation of gold nanorods, nanoshells and nanocages, respectively (Figure 5). The Surface Enhanced Raman Scattering (SERS) nanoparticle type, one with exceptional surface-enhanced Raman scattering properties, has been reported in work performed by Keren *et al.* (2008). Further advancement of these techniques, in terms of controlling synthetic conditions, has led to the optimization of production protocols. This allows for the manufacturing of specific nanoparticle types within specific size ranges with a great deal of precision (Cai *et al.*, 2008).

The most significant in terms of biomedical application are (Figure 5): (left to right) Top row: very small nanoparticles, generally 4 nm in diameter, synthesized by means of a strong reducing agent (sodium borohydride); larger nanoparticles, 15 nm in diameter, synthesized by a weaker reducing agent (trisodium citrate); nanocages, which are formed through a galvanic replacement reaction with silver. Bottom row: Gold

nanoshells formed surrounding an inert core, 100-200 nm in diameter and hollow nanoshells, both large and small (Pissuwan *et al.*, 2010).

Gold nanospheres are most commonly synthesized and employed in biomedical applications. Variations of the citrate-reduction technique (predominant synthesis route for these nanoparticles) have been introduced, as modifications of the original procedure described by Turkevich *et al.* (1951). These changes in production parameters come in the form of changes in citrate/gold ratios and result in smaller or larger nanospheres. The use of sodium citrate as the reducing agent is preferred as it results in the formation of monodisperse gold nanoparticles (Frens, 1973). Other techniques for producing gold nanospheres have been researched, with positive results (Weare *et al.*, 2000; Hiramatsu and Osterloh, 2004). Detection of presence of gold nanospheres after synthesis is relatively simple, with a single absorption peak on the UV-visible spectrum appearing between 510 and 550 nm. Increases in nanoparticle size result in a shift of this plasmon resonance peak to a longer wavelength (Cai *et al.*, 2008).

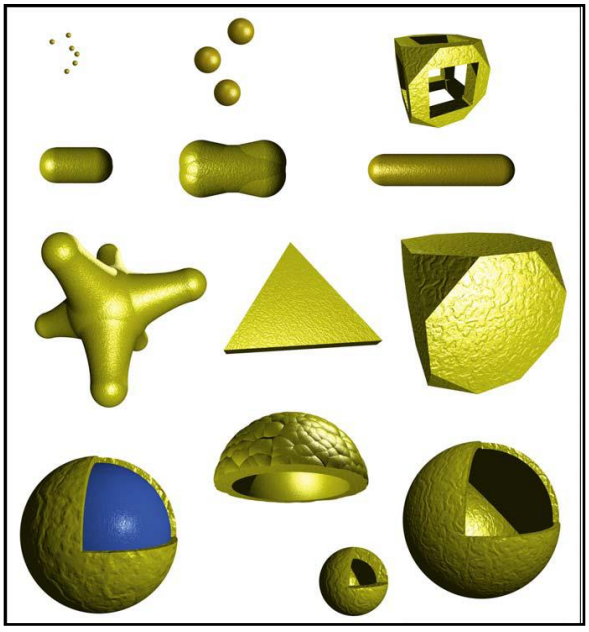

Figure 5: 3D representations of different types of gold nanoparticles, including the gold nanosphere (first row, second position), nanorods (second row), nanoshells (last row) and nanocages (first row, third position) (Pissuwan *et al.*, 2010).

Gold nanorods are synthesized via a template technique, in which gold is electrochemically deposited in pores present in nanoporous alumina or polycarbonate templates (Van der Zande *et al.*, 1997). This overcomes the problems encountered in seed-mediated growth, brought about by reduction procedures, where extensive separation of the gold nanorods from spheres and shells has to be conducted (Busbee *et al.*, 2003). However, despite the advantages conferred by template synthesis, the drawbacks include the relatively low yields of nanorods synthesized, making this techniques unsuitable for mass production. Seed-mediated growth of gold nanorods results in exponentially higher yields, despite the separation limitations (Jana *et al.*, 2001).

Gold nanoshells have immense potential as contrast agents, for detection on the UV-visible spectrum. Frangioni (2003) showed that all biomolecules experience a phenomenon of minimal absorbance in the near-infrared region (700-900 nm). Gold nanoshells can be designed such that their surface plasmon maxima lie within the near-infrared region, thus making detection simple and clearly visible (Oldenburg *et al.*, 1999). In terms of synthesis, the diameter of a gold nanoshell is dependent on the diameter of the inert silica core. Thickness of the nanoshell can be brought to a desired measurement by controlling the amount of gold deposited on the core (Suzuki and Kawaguchi, 2005).

Gold nanocages, synthesized via the galvanic replacement reaction with silver nanocubes, are characterized by the presence of controlled pores on their surfaces. As with gold nanoshells, these nanoparticles can be designed such that their surface plasmon resonance maxima fall within the near-infrared region (700-900 nm) (Chen *et al.*, 2010). Due to their well-characterized surface properties, molecules such as specific antibodies can be attached, allowing for targeting of specific biological sites. Work in this respect has been performed in targeting and destruction of cancerous tissue (Skrabalak *et al.*, 2007).

The synthesis of **Surface Enhanced Raman Scattering** (SERS) **gold nanoparticles** have also been described in numerous imaging and diagnostic studies (Keren *et al.*, 2008). These nanoparticles have a tunable plasmon resonance, ideal for imaging applications, along with many other engineered advantages that add to their application

potential (Oldenburg *et al.*, 1999). As nanoshell modifications, they are detectable in the near-infrared region of radiation with minimal interference. They possess great robustness in terms of their reactivity and bonding with biological matrices. Chemiluminescence and fluorescence are among the properties which confer significant advantages on these nanoparticles in comparison to conventional imaging and detection technology (Michael *et al.*, 2007).

These gold nanoparticle types lend themselves to applications where their unique physical and chemical properties, especially shape, structure and surface functionalization, give them an advantage (Figure 6). This study focuses on two biological applications of spherical nanoparticles, namely, their drug delivery and anti-cancer properties.

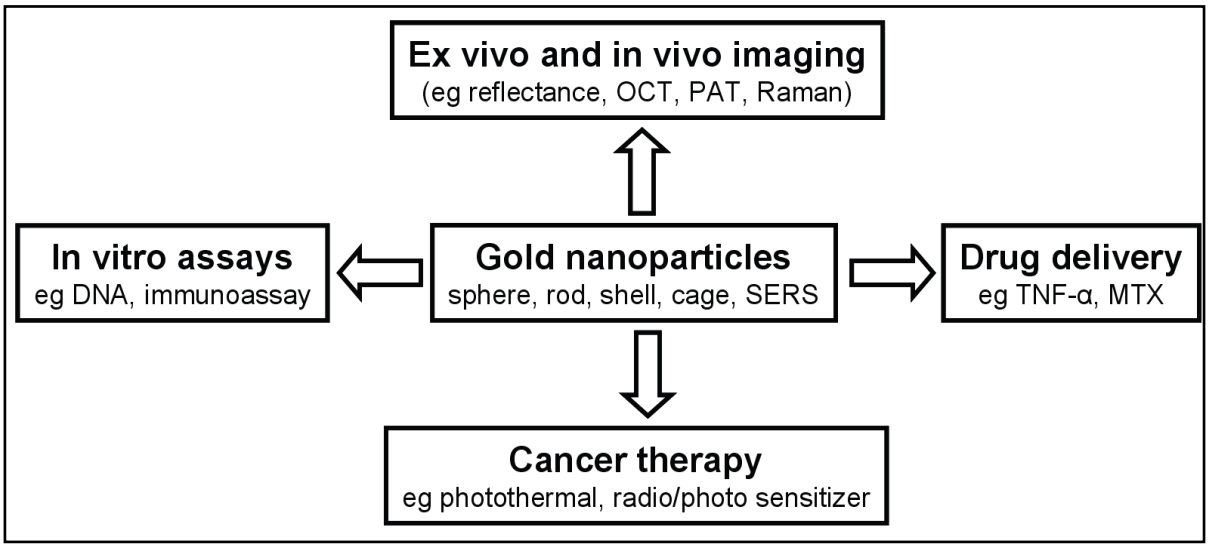

Figure 6: The applications of gold nanoparticles in the biomedical field, including their applications in cancer treatment, drug delivery, imaging of disease and their employment in various assays (Cai *et al.*, 2008).

2.3.3. Gold nanoparticles as diagnostic aids

GNPs make very valuable visualization and molecular **labeling** aids, mainly due to their surface plasmon resonance frequency. This is a very significant property of GNPs, which determines many of their unique applications in biosensing and imaging. As a metal, electrons within the GNP metal lattice structure can move freely, in accordance

with the 'electron sea' model. When a GNP is exposed to an electromagnetic wave, it results in the formation of a transient dipole, with the positive and negative charges oscillating between one pole of the particle and the other (Figure 7). This oscillatory movement of the electron cloud is referred to as a **plasmon** of which the oscillation itself occurs at a specific frequency (the **resonance frequency**) (Cademartiri and Ozin, 2009; Bolla *et al.*, 2011).

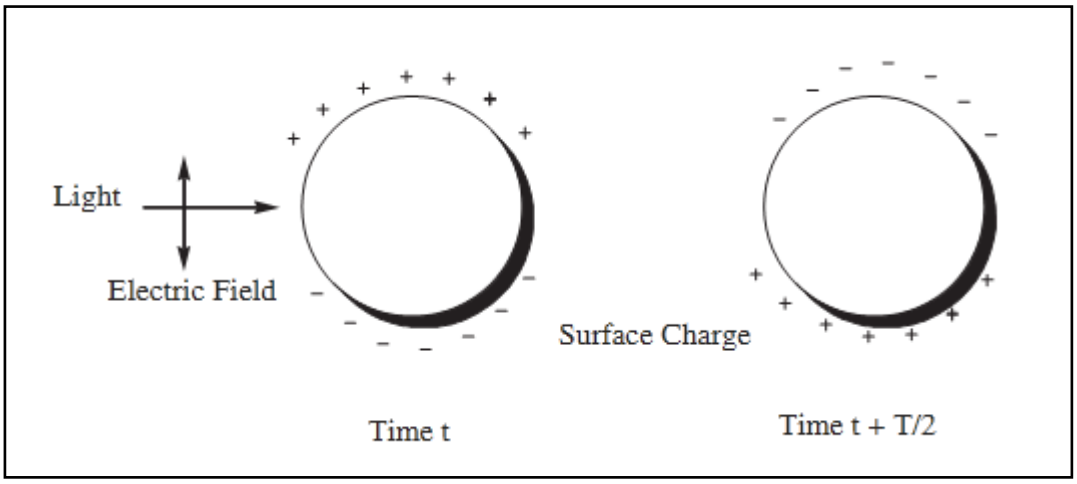

Figure 7: Diagram showing the oscillation of the electron cloud from one pole of the particle to the other, resulting in the phenomenon of detectable plasmon resonance.

In addition to their unique light scattering properties, the interaction of the GNPs with X-rays and electron waves allows for their detection and visualization. The high atomic weight of the GNPs, when viewed by transmission electron microscopy, provides a contrast of very high clarity (Sperling *et al.*, 2008). Various studies utilizing this labeling efficiency of nano-gold involve the tracking and treatment of various types of cancer, infection and disease. Immunochromatographic testing has allowed for the rapid and efficient diagnosis of bacterial and viral infections through the indication of presence of a specific antibody or antigen, or by hybridization with DNA (Pingarrón *et al.*, 2008). These techniques have the advantages of being, besides time-efficient, sensitive and inexpensive (Tallury *et al.*, 2010).

Further applications involving the use of GNPs as labeling aids include: 'immunostaining', the labeling of specific cellular components or molecules; single particle tracking, in which GNPs are conjugated with antibodies specific to molecules

on the surface of the cell, thus enabling mapping of these molecules' positions; their use as contrast agents for X-rays (Sperling *et al.,* 2008) and 'phagokinetic tracks' describes a way to track the movement of cells adhering to a particular substrate, a method first developed by Albrecht-Buehler (1979).

Labeling of biological molecules makes use of GNPs as 'passive' reporters, in which case, no changes occur to the structure of the nanoparticles. This type of passive targeting has great implications in the detection of cancerous tissues, and providing contrast to the surrounding healthy tissue. This application takes advantage of what is known as the EPR (Enhanced Permeability and Retention) effect, where the vasculature of tumour tissue is 'leaky', thus allowing for greater retention of circulating nanoparticles as compared to their retention in healthy tissue (Maeda *et al.,* 2000).

In contrast, the sensing function utilizes GNPs as 'active' reporters. In this form of application, a specific target molecule can be detected, as well as the concentration in which it is present, by reading changes in the optical properties of the GNPs after their interaction with the molecule (Pingarrón *et al.*, 2008; Gullotti and Yeo, 2009; Pissuwan *et al.*, 2010). Such a study was carried out by Kumar *et al.* (2007), in which multifunctional GNPs were synthesized, having both delivery and specific attachment functionalities. The changes in optical properties of these GNPs were used to track the rearrangement of actin in live fibroblast cells. GNPs are also used as electron donors in redox reactions, where the nanoparticles are bound to enzymes which catalyze these reactions. The flow of electrons can be measured and quantified as an electric current, which would give an indication of the presence and concentration of the target molecule that participates in the redox reaction (Willner *et al.,* 2006; Pingarrón *et al.*, 2008).

2.3.4. Gold nanoparticles in photodynamic and hyperthermal therapy

Photodynamic cancer treatment using GNPs was developed as an exploitation of the ability of the nanoparticles to produce heat when bombarded with specific types and wavelengths of radiation. The surface plasmon resonance plays a crucial role in determining the extent of heat energy released from the nanoparticles once their

electrons have been elevated to an excited state. Under plasmon resonance conditions, this heating effect is most pronounced, when the energy of the incident photons is closest to the plasmon frequency of the GNPs (Govorov *et al.*, 2006; Cademartiri and Ozin, 2009).

Hyperthermia refers to the effect of heating on living cells. Humans develop a fever when body temperature exceeds 37°C, and temperatures over 42°C are lethal in nature. Using this principle, cancer cells can be targeted by attaching GNPs to ligands which are specific to receptors expressed in excess on the surface of cancer cells. Once accumulated on the surface of, or internalized within the cell, these GNPs can be stimulated to a higher energy state by an external source of radiation. Once the GNPs have returned to their lower energy level, the energy required to reach the excited state is then released in the form of heat. This results in a heating effect on the cells and tissues in which the GNPs are closely situated, causing cell death in the target cancerous tissue (Hirsch *et al.*, 2003; El-Sayed *et al.*, 2005; Moghimi *et al.*, 2005; Pissuwan *et al.*, 2006; Huff *et al.*, 2007; Gindy and Prud'homme, 2009).

2.3.5. Gold nanoparticles as drug delivery vehicles

GNPs have been widely described as effective agents of drug delivery for numerous medical conditions, including various types of cancer, microbial infections and chronic disease. Since, in comparison to other metallic candidates for nanoparticle synthesis, gold has the most favourable properties for biological applications, it is most often encountered in literature as a stable, non-toxic and biocompatible drug carrier (Tsoli *et al.*, 2005). Nanoparticles that are monodisperse in aqueous medium and functionalized with various ligands (in certain cases imparting multiple functionalities) can be synthesized by a number of different techniques (Schmid and Hornyak, 1997).

Size-controlled synthesis is also possible, an essential aspect in this case, as the size of nanoparticles play a crucial role in their effectiveness as drug delivery vehicles. The submicron size of nanoparticles creates a number of advantages in terms of drug delivery and cellular uptake as opposed to microparticles. A study involving use of a rat intestinal in situ loop model, performed by Panyam and Labhasetwar (2003), indicated

that microparticles tend to accumulate in the epithelial lining, whereas the smaller-sized nanoparticles demonstrated the ability to penetrate the sub-mucosal layer, thus offering concrete evidence of this size advantage. They describe the favourable properties of nanogold as the following: i) The relative toxicity of these particles is low (supported by the findings of Tsoli *et al.* (2005)); ii) Optical resonance frequencies can be tailored to correspond with a specific nuclear imaging resonance (NIR) frequency, as a function of nanoparticle size and shape; iii) The small size of the nanoparticles, largely less that 100 nm, is favourable for adsorption to, and uptake by cells; and iv) their plasmon resonance frequency allows for a dual functionality, both drug delivery and biological imaging by acting as contrast agents. Furthermore, nanocarriers possess a high surface to volume ratio, allowing for attachment of a much larger number of the desired molecules to the nanoparticle surface. When bound to biological compounds, such as oligonucleotides and peptides, the nanoparticles have been found to improve the overall stability of these compounds in vitro (Mishra *et al.*, 2010).

As represented in Figure 8, cancer drug delivery approaches using nanoparticles as the delivery agents extends the principles of 'active' and 'passive' functioning. In this case, passive targeting exploits the enhanced permeability and retention (EPR) effect present in tumour vasculature (Maeda *et al.*, 2000), the impaired lymphatic drainage in the tumour tissue allowing for increased retention time of the drug-coated or conjugated nanoparticles. Active targeting involves the attachment of the drug, or encapsulating agent onto the nanoparticle, thus altering the chemical structure (Gullotti and Yeo, 2009). Studies go so far as to show that binding of a toxic anti-cancer protein (Tumour Necrosis Factor – TNF) to GNPs resulted in a decrease in cytotoxicity and effective tumour reduction when tested on a murine tumour model (Paciotti *et al.*, 2004).

The active mode of drug delivery is most commonly adopted in current research, as the potential surface functionalizations of GNPs offer an endless variety of medical applications. Cancer treatment is, by and large, the area in which GNPs have been most intensely evaluated as drug delivery vehicles thus far. However, targeted drug delivery using GNPs has opened up a number of possibilities in other medically-related areas, where such delivery vehicles would be highly beneficial.

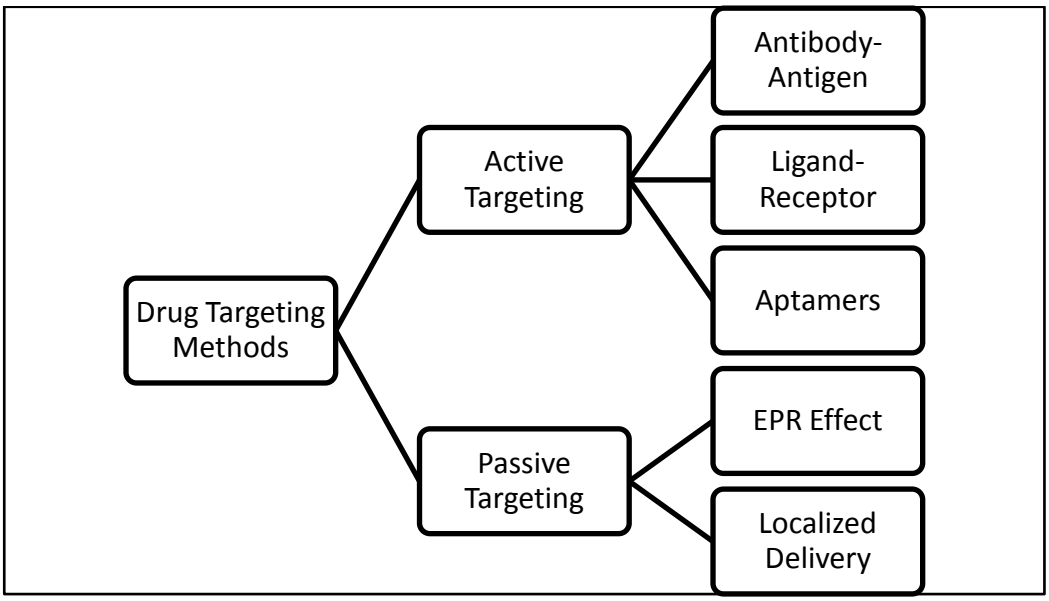

Figure 8: The various approaches to targeted drug delivery, including both active and passive modes of delivery.

The treatment of infections caused by bacterial pathogens is one such research area, with most of the focus aimed at the attachment of antibiotics to the surface of stabilized, biologically inert nanoparticles and subsequent targeted drug delivery to the bacterial cells, or, alternatively, the evaluation of the antimicrobial activity of the nanoparticles themselves. In the case of the former studies, antibiotics such as vancomycin, griseofulvin, various aminoglycosides and ciprofloxacin have been attached to the surface of the GNPs, in most cases, followed by extensive biological testing for investigation of the potential advantages they confer as drug delivery vehicles, as opposed to conventional methods of drug delivery. The nanoparticle route of delivery is also favourable as they are able to overcome drug resistance-related factors developed by bacteria, such as biofilm formation and cell envelopes that contribute to such resistance (Bolla *et al.*, 2011).

An alarming rise in the number of vancomycin-resistant organisms in recent years has led to an exploration of alternative methods for greater efficiency of treatment and drug delivery. Mohammed Fayaz *et al.* (2011) went the route of biologically synthesizing GNPs, using the fungus *Trichoderma viride*, and managed to restore antimicrobial activity of vancomycin against resistant *Staphylococcus aureus* by combining these GNPs with the antibiotic. Further work in this research area was conducted by Cui *et al.* (2012), in which bactericidal GNPs were found to function effectively in inhibiting

growth of *E. coli*. Attached to small, inactive inorganic molecules, such as 4, 6-diamino-2-pyramidinethiol, these GNPs were found to inhibit tRNA functions within the cell, as this compound is an analogue for a tRNA base. Thus, the functionalized GNPs were able to affect protein synthesis, through inhibition of tRNA activity, effectively killing the bacterial cells and preventing proliferation. Nirmala Grace and Pandian (2007) demonstrated that aminoglycoside antibiotics, streptomycin, gentamycin and neomycin, could all be physically attached to the surface of citrate-capped gold nanoparticles, further antimicrobial experiments showing that these antibiotic-coated GNPs were able to inhibit bacterial growth more effectively than the drugs in pure form. In addition to this, the modified GNPs functioned equally well against Gram positive and Gram negative bacterial strains tested.

Further insight into the mechanism of activity of the antibiotic-conjugated GNPs was provided by research performed by Saha *et al.* (2007) and Burygin *et al.* (2009). In the former study, GNPs were bound to the antibiotics ampicillin, streptomycin and kanamycin and a definite enhancement of antimicrobial action was observed in comparison to the free antibiotics. The results obtained were instrumental in demonstrating that the mode of action of the antibiotic plays a pivotal role in determining the extent of enhanced antimicrobial activity when conjugated to GNPs. The latter study contradicted the work of Saha *et al.* (2007), and earlier studies, in that the gentamycin-bound GNPs were found to exert no additional antimicrobial activity when tested on three bacterial strains, in comparison to the antibiotic in free form.

2.3.6. Mechanisms of drug delivery for treatment of infection

From studies performed thus far, it can be noted that the precise mechanism by which GNPs deliver their drug loads is not completely understood. From visual evidence obtained, researchers have been able to ascertain that the nanoparticles strongly adhere to and, in some cases, penetrate the cell membrane of the target cell. In this way, the GNPs act as delivery vehicles in the sense that they are able to convey a large number of drug molecules to a specific site (Nirmala Grace and Pandian, 2007; Saha *et al.*, 2007). It has been suggested that the nanoparticles mimic the glycoside cluster effect (Pissuwan *et al.*, 2010), a mechanism in which a multivalent entity (such as a

functionalized gold nanoparticle) would have a higher binding affinity to a glycosidic substrate (the bacterial cell wall) than many of the more common covalent linkages.

The conjugation of various antibiotics to gold nanomaterials and their subsequent testing on various bacterial species has had varied success in terms of bactericidal activity. Perni *et al.* (2009) was able to demonstrate that the presence of gold nanoparticles enhanced the oxidative effect of methylene blue, effectively killing both methicillin-resistant *Staphylococcus aureus* (MRSA) and *E. coli* species. The mechanism of activity displayed by the gold nanoparticles here appears to be related to increasing the production of reactive oxygen species and enhancement of the light-induced antimicrobial action of methylene blue itself. Other research has shown that gold nanoparticles are able to take a more active role in determination of antimicrobial effects, as demonstrated by Zhao *et al.* (2010), where gold nanoparticles were functionalized with amino-substituted pyrimidines. Neither substance acting alone possessed any antimicrobial effect against multidrug-resistant bacteria, however when combined, they displayed two significant bactericidal effects. The nanoparticle-substituted pyrimidine conjugates were able to both disrupt the bacterial cell membrane (by sequestration of calcium and magnesium ions), thus causing leakage of cellular contents, and furthermore, were internalized by the cells, causing inhibition of DNA and protein synthesis.

The gold nanoparticle-antibiotic conjugates synthesized and tested by Burygin *et al.* (2009) were found to display a contrast in antimicrobial activity when compared to the previous studies. Two conditions were identified as necessary in order for an enhanced effect to be produced, namely; the synthesis of stable, single particle, non-aggregated colloidal gold before attachment to the antibiotic and an adequate amount of the antibiotic attaching to the surface of the GNPs, taking full advantage of the larger surface area advantage conferred by nanomaterials when binding them to other molecules.

In the studies conducted by Saha *et al.* (2007) GNP-conjugated ampicillin showed a 10% decrease in the MIC value, whilst similarly conjugated streptomycin and kanamycin showed a 50% and 60% decrease in MIC values respectively, a significantly large margin of difference between the MIC values for the two groups of antibiotics.

Ampicillin functions by targeting and inhibiting cell wall biosynthesis, whilst streptomycin and kanamycin attach to bacterial ribosomes, blocking off sites that are essential to the translational process during protein synthesis. The binding affinity displayed by the GNP-coated antibiotics to their respective target molecule is the factor that seems to be enhanced by the conjugation effect, in turn, enhancing antimicrobial activity. The GNP-antibiotic conjugates have a specific property, absent in both the free GNPs and antibiotics that cause this phenomenon. This particular conclusion was further emphasized in the subsequent set of experiments, in which the bacterial species tested were exposed to both free GNPs and free antibiotics, however, separately and in turn, rather than in conjugated form. The results showed no significant enhancement of antimicrobial activity using this mode of treatment, as opposed to the defined decrease in MIC values obtained with the GNP-antibiotic conjugates.

2.4. Biocompatibility and safety of gold nanoparticles

Besides the highly promising potential applications in the field of drug delivery, GNPs have a variety of biological applications which can be subdivided into the categories of labeling, heating and sensing (Sperling *et al.*, 2008; Faraji and Wipf, 2009). GNPs have inert surface properties which are responsible for their lack of reactivity within biological systems. Various studies have indicated that there is no sign of acute cytotoxicity experienced by cell lines that have been cultured in the presence of GNPs. However, these results vary slightly depending on the cell line used, the stabilizing or coating molecules on the surface of the GNPs and the method of cytotoxicity testing (Sperling *et al.*, 2008; Uboldi *et al.*, 2009; Cui *et al.*, 2012; Freese *et al.*, 2012; Vijayakumar and Ganesan, 2012). Supporting the hypothesis that the degree of cytotoxic effect exerted by GNPs depends on the coating or stabilizing agent attached to the particle surface are studies conducted by (Uboldi *et al.*, 2009) and (Freese *et al.*, 2012) which focus, in particular, on GNPs that have been stabilized with sodium citrate. In the cases of both sets of research results, the citrate capping of the GNPs, effected by reduction of sodium citrate, was shown to reduce the viability and impair the proliferation of the cell lines tested (human ATII-like cell lines, A549 and NCIH441, and human endothelial cells from the vasculature and blood brain barrier). This slight cytotoxic effect could be due to the relative acidity of citrate (Vijayakumar and Ganesan, 2012).

Nanoparticle size is, of course, a major determinant in their effectiveness as drug delivery vehicles. Nano-scale delivery techniques are mainly successful due to the ability of these nanoparticles to be taken up by cells and deliver their drug payload within the cytoplasm. Once the nanoparticles have been subjected to cellular uptake, they are localized within the cell in vesicles or the nucleus (Shukla *et al.*, 2005). Larger nanoparticles are effectively cleared from the vasculature by phagocytosis. In contrast, very small nanoparticles (between 1 and 20 nm in size) exhibit slow extravasation from the circulatory system and have a much longer retention time. Particles with sizes of the order 30 to 100 nm are able to evade phagocytic mechanisms and reticuloendothelial clearance (Figure 9) (Faraji and Wipf, 2009).

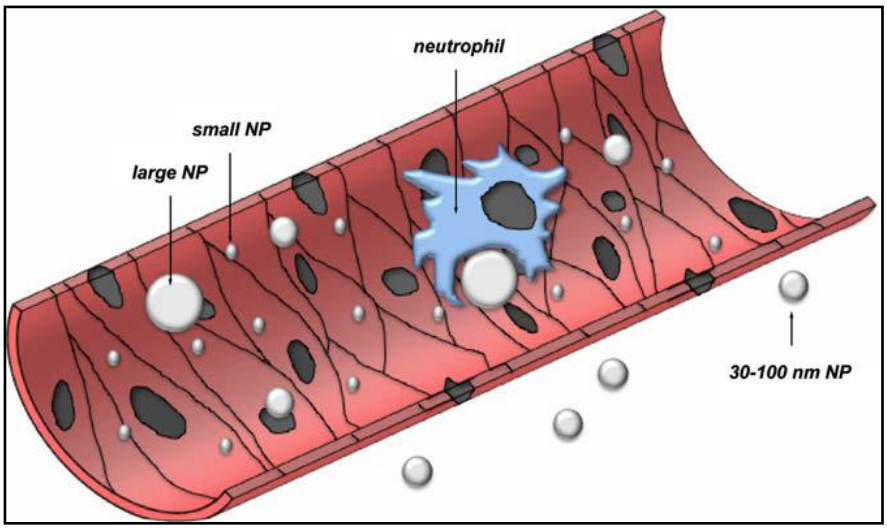

Figure 9: The fate of nanoparticles in vivo, indicating the results of exposure to small and large nanoparticles that have been introduced intravenously.

In addition, it was found that while slight impairment of growth and viability occurred in various cell lines tested, the rate of uptake and internalization of citrate-capped GNPs was unaffected by this parameter, appearing to be related to the interactions between the nanoparticle and the surface of the cell membrane (receptors present) (Freese *et al.*, 2012). Thus, the size of the nanoparticles involved in this treatment is thought to play a major role in determining the rate and degree of uptake by cells. By narrowing down size ranges and determining relative cytotoxicities, a conclusion can be made that GNPs of 13 nm and above are considered non-cytotoxic (Jahnen-Dechent and Simon, 2008), whereas those below 2 nm have been shown to possess active cytotoxic characteristics

(Schmid, 2008). A more detailed explanation for this size-dependant cytotoxic effect is partially revealed in research performed by Tsoli *et al.* (2005) in which the comparatively small size of the nanoparticles (1.4 nm) allowed them to have a specific interaction with the major grooves of the DNA double-helix structure, resulting in unprecedented levels of toxicity.

Although nanoparticle size ranges seem to contribute greatly to cytotoxic properties on tested cell lines, the toxic properties of the capping agent, sodium citrate, cannot be ignored in terms of their use in nanoparticle synthesis for biological applications (Freese *et al.*, 2012). If further methods of purification were employed, such as dialysis, and the overall presence or concentration of excess sodium citrate could be brought to a minimal level, this would be highly preferable before any further trials aimed at bringing these nanoparticles to a therapeutic level of action.

2.5. Ciprofloxacin: Mechanism of activity and conjugation

The antibiotic, ciprofloxacin, belongs to the flouroquinalone drug class, a range of broad-spectrum antibiotics that are orally absorbed and have favourable pharmacokinetic properties. The primary functional route of this class of antibiotic is the inhibition of the enzyme, DNA gyrase, in bacterial cells (bacterial topoisomerase II). This enzyme is responsible for negative supercoiling of DNA during the replication process. The inhibition of this enzyme's activity will, naturally, lead to a number of adverse and bactericidal effects as a result of inhibition of DNA replication. These effects include interfering with the DNA replication, transcription and the separation of the bacterial chromosomes, along with the damage of DNA and other cellular processes (Oates *et al.*, 1991).

Ciprofloxacin is recognized as one of the most effective antibiotics of the quinolone drug class (Oates *et al.*, 1991) and has been used for the treatment of urinary tract infections (Verbrugh *et al.*, 1992), sexually transmitted diseases (Wawer *et al.*, 1999), bacterial prostatitis (Bundrick *et al.*, 2003), and infections of the respiratory (Fass, 1987) and digestive tract (Enzensberger *et al.*, 1985). It has a zwitterionic structure (Figure 10), which accounts for its good solubility in acidic and basic solvents, while

experiencing poor solubility in water, ethanol, methanol and chloroform (Anacona and Toledo, 2001).

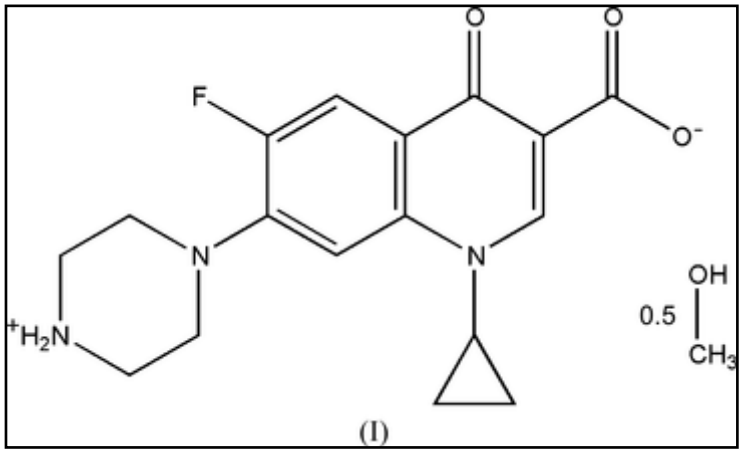

Figure 10: Structure of ciprofloxacin indicating the molecule's zwitterionic nature.

Ciprofloxacin displays presence of 7-piperazinyl and pyridone moieties as shown below, in Figure 11. Studies have shown that the amine (NH) group situated on the piperazine ring forming one of the essential components of ciprofloxacin's structure, binds strongly to the surface of the GNPs, while the pyridone moiety remains unchanged (Tom *et al.*, 2004; Kumar *et al.*, 2010). This attachment most probably occurs through bond formation between the nitrogen atom of the amide group and the citrate-capped GNPs (Tom *et al.*, 2004).

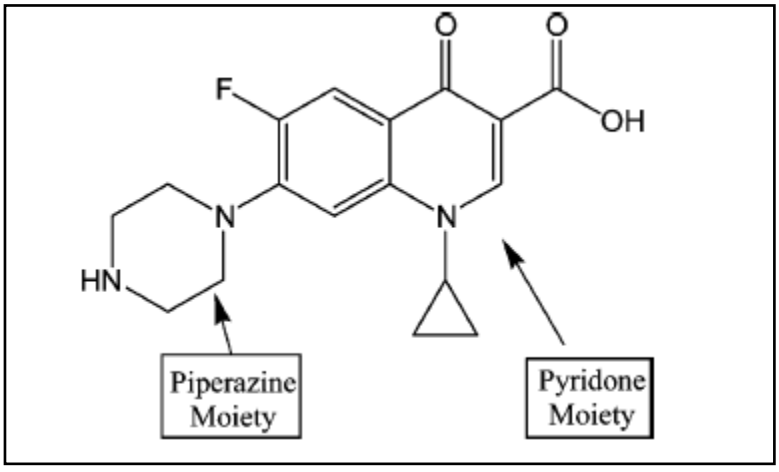

Figure 11: Structural representation of piperazine and pyridone moieties of ciprofloxacin (Tom *et al.*, 2004).

A number of studies have been conducted recently (Table 3) with regard to the conjugation of ciprofloxacin to nanomaterials and determination of the antimicrobial effects against various strains of bacteria. In most studies, an increase in antimicrobial activity was reported after conjugation of ciprofloxacin to the nanoparticles. However, no studies have been directed towards determining the antimicrobial effect of citrate-capped gold nanoparticles conjugated to ciprofloxacin, hence the undertaking of this study.

Table 3: Summary of studies performed involving ciprofloxacin conjugated to different nanoparticle types.

Nanoparticle type	Antimicrobial Activity	Reference
Polyisobutylcyanoacrylate (PIBCA)	• Enhanced antimicrobial activity against *Mycobacterium avium*	(Fawaz *et al.*, 1998)
Polyethylbutylcyanoacrylate (PEBCA)	• Have been linked to ciprofloxacin and the complex stabilized • Antimicrobial activity yet to be determined	(Page-Clisson *et al.*, 1998)
Poly(lactide-co-glycolide) (PLGA)	• Moderate enhanced antimicrobial effect on *Pseudomonas aeruginosa* and *Staphylococcus aureus*	(Dillen *et al.*, 2004)
Gold-silica core-shell	• Enhanced antimicrobial activity against *E.coli* and *Lactobacillus lactis* • Nanoparticles were shown to enter the bacterial cell to exert their antibacterial effect	(Rosemary *et al.*, 2006)

3. MATERIALS AND METHODS

3.1. Synthesis of citrate capped gold nanoparticles

Gold nanoparticles were synthesized by the Turkevich citrate reduction technique (Turkevich *et al.*, 1951) with modifications, and conjugation of ciprofloxacin to these synthesized nanoparticles was carried out as per (Tom *et al.*, 2004). All reagents were purchased from Sigma-Aldrich. Nanoparticles of diameters between 15 and 30 nm were synthesized by the reduction of choloroauric acid ($HAuCl_4$) with trisodium citrate ($Na_3C_6H_5O_7$). An aqueous stock of 0.01 M trisodium citrate was prepared by dissolving 0.030 g in 10 mL of distilled water, followed by vortexing. 0.1 M choloroauric acid solution was prepared by adding 0.034 g of the crystallized form to 10 mL of distilled water.

One mL of chloroauric acid was added to 9 mL of boiling distilled water in a 250 mL glass beaker on a heating plate. The solution was mechanically stirred to ensure even dispersion of reagents. Upon observation of a pale yellow colour, 1 mL of the trisodium citrate aqueous preparation was added to the beaker. The solution was further observed until formation of a deep, wine-red colour (indicating gold nanoparticle presence) and removed from the heating plate. Samples were transferred from the glass beaker to 2 mL Eppendorf tubes and refrigerated at 4 °C for subsequent ultra structural, stability and spectrophotometric analysis. The concentration of the gold nanoparticle suspension synthesized from the above procedure was 0.01 M.

3. 2. Synthesis of ciprofloxacin-coated gold nanoparticles

An aqueous stock of 0.0025 M ciprofloxacin was prepared by dissolving 0.0083 g of the antibiotic in 10 mL of distilled water. The antibiotic solution was filter sterilized and refrigerated at 4 °C overnight. To prepare the ciprofloxacin-coated nanoparticles, 5 mL of 0.0025 M ciprofloxacin was added to the nanoparticle dilution in a 250 mL glass beaker. The solution was stirred for 6 h, during which a characteristic indigo colour

formed. A 0.001 M dilution of gold nanoparticles was prepared by dissolving 2 mL of the 0.01 M nanoparticle solution in 18 mL of distilled water.

During this period, the samples for confirmation of antibiotic conjugation were removed every 30 min and analyzed by UV-Vis spectroscopy. The ciprofloxacin-conjugated nanoparticles were then transferred from the glass beaker to 2 mL Eppendorf tubes and refrigerated. The formation of the ciprofloxacin gold nanoparticles in solution was confirmed by UV-Vis spectroscopy, and TEM.

3.3. Colloidal stability of citrate-capped and ciprofloxacin-conjugated gold nanoparticles

The effect of storage temperature and time on colloidal stability of citrate-capped GNPs and ciprofloxacin-coated GNPs was determined by obtaining UV-visible spectra scans of the samples over a period of two weeks. The samples were stored at three different temperatures (4, 23 and 37 °C) in 2 mL Eppendorf tubes. To obtain UV-visible spectra, samples of citrate-capped GNPs and ciprofloxacin-coated GNPs, samples from the different temperature groups were removed and scanned at 48 h intervals for a 2 week period. All UV scans were within the wavelength range of 200 to 800 nm. Sterile distilled water was used as a reference for all samples. The cuvettes were rinsed thoroughly with distilled water after each sample analysis in order to prevent adherence of GNPs to the inner surface. Changes in absorbance were monitored for each sample over the two week period in order to determine how the experimental conditions (time and temperature) affected the stability of the nanoparticles in aqueous suspension.

3.4. Characterization of citrate capped gold nanoparticles and ciprofloxacin coated gold nanoparticles

3.4.1. Spectrophotometric analysis

The Fourier Transform Infrared (FTIR) spectra of the citrate-capped GNPs and ciprofloxacin-coated GNPs were obtained using a PerkinElmer Spectrum 100

spectrophotometer. A small quantity of the liquid sample was placed onto the detection plate, after which the probe was applied. The samples were scanned after which the spectra were analyzed in order to detect the types of chemical bonds present and changes in bonding between functional groups in the case of the ciprofloxacin-coated nanoparticles.

3.4.2. Ultrastructural analysis by TEM

Gold nanoparticle structure, size and morphology and the GNP-ciprofloxacin conjugate distribution and arrangement was observed using a JEOL JEM 1010 transmission electron microscope (UKZN- Westville) operating at an accelerated voltage of 120 kV. Samples were prepared for observation by placing a drop of the GNP and ciprofloxacin-coated GNP solution on formvar-coated copper grids, followed by a period of air-drying, after which the sample were viewed. Precise measurements of nanoparticle diameters were taken from different sectors on the copper grid.

3.5. Effect of citrate capped and ciprofloxacin coated nanoparticles on bacterial growth and on a Caco-2 cell line

3.5.1. Antimicrobial activity

3.5.1.1 Culture and maintenance of bacterial species

All bacterial strains used in this experiment were obtained from Lancet Laboratories (Durban) who had isolated the bacteria from infectious materials. The bacteria and their antibiograms were obtained with samples. All bacterial samples were identified by a code which specified the isolate and the sample from which it was obtained (Table 4). As these bacterial species were obtained from Lancet Laboratories and not directly from infectious material obtained from patients, Level 1 ethical clearance was provided by the Durban University of Technology Ethics and Biosafety Research Committee (attached under Appendix 3).

Bacterial species were selected for testing based on their classification as Gram negative or Gram positive, as it was essential to determine antimicrobial effect of

ciprofloxacin-coated gold nanoparticles against both bacterial types. The Gram positive strains of bacteria against which ciprofloxacin-coated GNPs were tested for antimicrobial activity include *Staphylococcus aureus* (S6158, P4256, S5878 and P4217) and *Enterococcus faecalis* (U11394 and U12318).

Table 4: Bacterial species used in this study.

Bacterial Species	Isolation code*
Staphylococcus aureus	S6158 P4256 S5878 P4217
Enterococcus faecalis	U11394 U12318
Pseudomonas spp.	S6125
Klebsiella pneumoniae	S5906 P3967 V258 U10705
Enterobacter spp.	P16743
Escherichia coli	B3578 P4055 U10948 U10804 P4299

***Key letters indicate the types of infectious material from which bacterial strains were isolated as follows: P (Pus swab), B (Blood sample), V (Vaginal swab), S (Skin swab) and U (Urine sample).**

Gram negative strains of bacteria included *Pseudomonas* spp. (S6125), *Klebsiella pneumoniae* (S5906, P3967, V258 and U10705), *Enterobacter* spp. (P16743) and *Escherichia coli* (B3578, P4055, U10948, U10804 and P4299).

Bacterial species were transported on dry ice on blood agar plates (Sigma). Upon receipt they were transferred to sterile 10 mL nutrient broth at room temperature and incubated at 37 °C for 24 h. Thereafter, the bacteria were transferred to nutrient agar plates and incubated at 37 °C for 36 h. The purity of the cultures was verified by Gram stain and they were stored into micro-banks as per manufacturers' instructions.

Ciprofloxacin-conjugated GNPs were tested for anti-bacterial activity against the 17 bacterial isolates. Concentrations of 0.3, 0.2 and 0.1 mM of the ciprofloxacin-nanoparticle conjugate solution were prepared. Where results showed an MIC of 0.1 mM, further tested at 0.05 and 0.025 mM of each compound were tested.

3.5.1.2. Antimicrobial effect of citrate capped gold nanoparticles and ciprofloxacin coated nanoparticles

Antibacterial activity of the ciprofloxacin-coated GNPs was determined by means of the MIC assay (Al-Bayati, 2009). The bacterial suspension was standardized by measuring the A_{600} = 0.5. If the absorbance was >0.5 or <05 the media was diluted as per formula (Appendix 2) or was further incubated until A_{600} = 0.5, respectively.

The experimental procedure for determining antimicrobial activity was carried out as outlined (Al-Bayati, 2009). The test was carried out in 96-well round bottom plates (Cellstar). 100 µL of sterile Mueller-Hinton broth was placed into all wells. This was followed by the addition of 100 µL of the 0.3, 0.2 and 0.1 mM solutions of citrate-capped GNPs and ciprofloxacin capped gold nanoparticles and ciprofloxacin to individual wells. Five µL of bacteria (at O.D. of 0.5, correlating to the MacFarlane standard) in Mueller Hinton broth was added to each well. A single bacterial species was tested per microtitre plate, in order to prevent cross-contamination.

The negative control was the bacterial culture grown in sterile Mueller Hinton broth, in the absence of any of the three substances tested (citrate-capped GNPs, ciprofloxacin, ciprofloxacin-conjugated GNPs). A sterility control, sterile Mueller Hinton broth, allowed for detection of any contamination which had occurred during the course of the experiment.

Antimicrobial activities of each concentration of the three substances tested were determined by the degree of bacterial growth after incubation in their presence for a period of 24 hrs. The growth indicator used for the assay was INT (p-iodonitrotetrazolium chloride). After 24 h of incubation, the 96-well microtitre plates were removed from the incubator and 50 µL of INT (0.2 mg/mL in sterile distilled water) was added to each well, including all controls. The plates were then incubated

for a further 30 min at 37 °C, after which they were removed and observations of colour change, indicating the degree of antimicrobial activity for each substance tested, was recorded. The INT indicates the degree of microbial growth through visualization of a colour change. A positive result (absence of bacterial growth and thus, confirmation of antimicrobial activity) is characterized by no colour change, whilst a negative result for antimicrobial activity is evidenced by a change in colour of the media within the well from light yellow/colourless to purplish-red after incubation. All assays were conducted in duplicate.

3.5.1.3. Statistical Analysis

Statistical analysis of the results of the MIC assay was conducted using the two-tailed *t*-test assuming equal variance in order to determine the significant difference between antibacterial activity of compounds tested. Comparison was made between the data sets representing duplicate MIC's of ciprofloxacin and ciprofloxacin-conjugated GNPs. Probability for rejecting the null hypothesis was set at p=0.05. The data was analyzed using GraphPad Prism©.

3.5.1.4. Determining the effect of ciprofloxacin conjugated GNPs on bacterial growth by TEM

To elucidate the mode of action of ciprofloxacin-conjugated GNPs' on bacterial cells, we compared the effect of ciprofloxacin, citrate-capped gold nanoparticles and ciprofloxacin-coated gold nanoparticles. Bacterial species, *Staphylococcus aureus*, *Enterobacter* spp., *Enterococcus faecalis*, *Klebsiella pneumoniae* and *Pseudomonas* spp., were all inoculated into 10 ml sterile Mueller Hinton broth under aseptic conditions. Selection of bacterial species for TEM observation was based on the effects noted on bacterial growth during the antimicrobial assay and to ensure an even distribution of Gram negative and Gram positive species.

Three colonies of each bacterial culture were transferred from nutrient agar plates into the broth. Citrate-capped GNPs and ciprofloxacin-conjugated GNPs were prepared to a concentration of 0.5 mM and added to separate test tubes of each bacterial suspension

(100 µL/ tube). The bacterial cultures were then incubated in the presence of the citrate-capped GNPs and the ciprofloxacin-coated GNPs for 24 h at 37°C.

Observation of the bacterial specimens was conducted at CSIR, the National Centre for Nano-structured Materials (NCNSM), in Pretoria. The cultures were stored on ice during transport and refrigerated at 4 °C at the facility. Samples were viewed with a JEOL model JEM-2100 transmission electron microscope. The bacterial specimens were prepared by placing a drop of the stored culture on a carbon-coated copper grid, followed by a period of air-drying. The grids, with the fixed sample present, were then loaded onto the microscope stage and viewed.

3.5.2. Anti-cancer activity of ciprofloxacin-coated gold nanoparticles on the Caco-2 cell line

3.5.2.1. Cell Line

The cell line utilized for determination of anti-cancer activity of the ciprofloxacin-conjugated GNPs was Caco-2 (cells derived from a human colon carcinoma), which are adherent, epithelial-like in nature and used in many studies as a model to mimic the effects of the tested compound on colon epithelium. The cell lines were obtained from MRC (Medical Research Council, Pretoria). They were transported on ice and stored according to the protocol outlined in 3.5.2.3.

3.5.2.2. Cell Maintenance

The cell line was maintained by culturing under aseptic conditions in a laminar flow cabinet. The cabinet was sterilized before each use by exposure to UV-light for 30 min, followed by swabbing with 70% ethanol. The cells were sub-cultured every 2 to 3 days until they were approximately 80% confluent. The medium employed for sub-culturing of the cells was Dulbecco's Modified Eagle Medium (DMEM) (Sigma) which was supplemented with both a 1% antibiotic-antimycotic solution (Sigma) and 10% heat-inactivated foetal calf serum (FCS). The medium itself consists of 1 mM L-glutamine, 1 mM sodium pyruvate and 4.5 g/L of glucose. The cells were grown in a monolayer on the inner surface of the flask.

For the sub-culturing process, the growth medium was removed from the flask in which the cells had been grown. The cells were washed with 5 mL of phosphate saline buffer (PBS). To detach the cells from the flask, 1 mL of trypsin was added, followed by incubation at 37°C with 5% CO_2 for three minutes in a humidified incubator. Once removed, the flasks were gently tapped on the side for 30 seconds. This is essential for detachment of the monolayer of cells. The detachment of the cells was followed by addition of 10 mL of DMEM. Five mL of this cell culture was transferred to another flask. The new flask containing the sub-cultured cells was then topped up with 20 mL of DMEM, followed by incubation at 37°C with 5% CO_2 in a humidified incubator. The cells were monitored on a daily basis under an inverted microscope for growth and possible contamination.

3.5.2.3. Storage of cells

For storage purposes, cell culture flasks that were 80% confluent were washed with PBS (5 mL). The cells were then trypsinized according to the protocol described in 3.5.2.2. Ten mL of DMEM was added to the flasks. The cells were then centrifuged (1500 rpm) for 10 min resulting in formation of a pellet. Cryo-protective medium was prepared (10% DMSO, 80% DMEM and 10 % FCS). The cells were re-suspended in 2 mL of this medium and 1 mL aliquots were placed in cryotubes which were then placed on ice for slow cooling. The cryotubes were then transferred to a thermos flask and stored overnight at – 20°C. After this process, the cells were transferred to an ultra-freezer and stored at – 85 °C.

3.5.2.4. Regeneration of cells

The cryotubes were removed from the ultra-freezer, swabbed with 70% ethanol and thawed rapidly. DMEM growth medium was pre-warmed and supplemented with 10% FCS and 1% antibiotic-antimycotic solution in 75 cm^2 tissue culture flasks. The cells were added to these flasks and incubated in a humidified incubator with 5% CO_2 atmosphere, at 37°C.

3.5.2.5. MTT Assay

The effect of the citrate-capped and ciprofloxacin-conjugated GNPs on the Caco-2 cell line was determined by means of the MTT assay. This is a simple, highly accurate method which yields results of a reproducible nature. The detection of viable cells is effected through detection of activity of mitochondrial dehydrogenases (such as succinate dehydrogenase) which are present in metabolically active cells. These enzymes have the ability to cleave the tetrazolium ring, reducing 3-(4,5-dimethylthiazol-2-yl)-2,5-diphenyltetrazolium bromide (MTT, which is yellow in colour) to formazan crystals (purple in colour). These formazan crystals can be dissolved in 100% DMSO or acidified isopropanol. The purple-coloured solution which results due to this reaction can be measured spectrophotometrically. The amount of formazan produced by these metabolically active cells can thus be quantified in order to give an indication of cell viability. An increase or decrease in cell viability would result in an according change in the amount of formazan produced, indicating the degree of cytotoxicity of the compound tested against the relative cell line (Mosmann, 1983).

The MTT assay was conducted according to the specifications of Mosmann (1983) with modifications to the technique. A volume of 200 µL (equivalent of 2×10^{-5} cells) of the Caco-2 cell line was seeded into 96-well microtitre plates. PBS (pH 7) was placed in the outer set of wells to prevent evaporation of the medium during the incubation period. These plates were incubated for 24 h in order to achieve confluence within the flasks. After the incubation period, the medium was removed and the monolayer of cells attached to the inner surface of the flask was washed with PBS. 100 µL of DMEM containing suspensions of citrate-capped GNPs and ciprofloxacin-conjugated GNPs (each at concentrations of 0.5 – 0.1 mM) were added to the wells. Gemcitabine, dissolved in DMEM at the relative concentrations, was added to individual wells as the positive control. DMEM was used as a negative control, in order to determine if DMSO had an effect on cell growth. All solutions tested (gemcitabine, citrate-capped GNPs and ciprofloxacin-conjugated GNPs) were tested in replicates of three. The microtitre plates containing the cells and GNPs were incubated for 24 hrs at 37°C in a humidified incubator with 5% CO_2. After this incubation period, the medium was replaced with 50 µL of MTT at a concentration of 5mg/mL. The plates were then incubated for a further four hours under the same incubation conditions. After the four hours, 100 µL of DMSO was added to all wells in order to dissolve the formazan crystals that were

formed in the metabolically active portion of the cells. Complete dissolution of the formazan crystals was effected through shaking the plates at room temperature for 2 min. The absorbance of all wells of the plate was detected and recorded on an ELISA reader (Biohit Plc, e-Lisa XL).

The Caco-2 cells, on which the assay was performed, belong to a colon cancer cell line. Gemcitabine, the chemotherapeutic drug used as a positive control, is one of the few anti-cancer drugs that is capable of a mode of action known as 'self-potentiation'. Gemcitabine, which is an analogue of deoxycytidine, attaches to the end of elongating DNA strands during the replication process and prevents further attachment and action of DNA polymerase III. Gemcitabine metabolites are also able to hinder cellular regulatory processes, causing further retardation of cancer cell proliferation (Plunkett *et al.*, 1995).

Gold nanoparticles have been shown to enhance anti-cancer activity in in vitro systems (Ghosh *et al.*, 2008). In this study the cytotoxic activity of citrate-capped GNPs on a Caco-2 cell line was evaluated using the MTT Assay. Individual absorbances obtained from the ELISA plate readings, for each concentration of compound tested, were determined. Percentage cell viability was calculated from the absorbance reading of each well. Percentage cytotoxicity was calculated for every percentage viability reading acquired. Thereafter, an average of percentage cytotoxicity for each concentration was determined (experiment performed in triplicate) (See Appendix B for relevant formulae).

For the assay, five concentrations of citrate-capped GNPs were tested for effect on the Caco-2 cell line, and the results were compared to the anti-cancer activity of gemcitabine (positive control – an anticancer drug) and the negative control, 2% DMSO.

3.5.2.6. Statistical Analysis

The percentage cytotoxicity for each concentration of citrate-capped GNPs and the anti-cancer drug, gemcitabine, was analyzed using a two-tailed *t*-test assuming equal variances in order to determine significant differences between treatments. Probability

for rejecting the null hypothesis was set at p=0.05 All data was analyzed using GraphPad Prism© version 5.0.

4. RESULTS

4.1. Synthesis of citrate-capped GNPs

The successful synthesis of citrate-capped gold nanoparticles was visually confirmed by means of the formation of an intense wine red colour (Figure 11, inset). This colour originates from coherent electron motion in the colloidal solution, giving rise to a characteristic absorption of light at a wavelength of 530 nm, as shown by peak 2 (Figure 12) Absorption peak 1, obtained at 290 nm (Figure 12) indicates the un-reacted sodium citrate in solution.

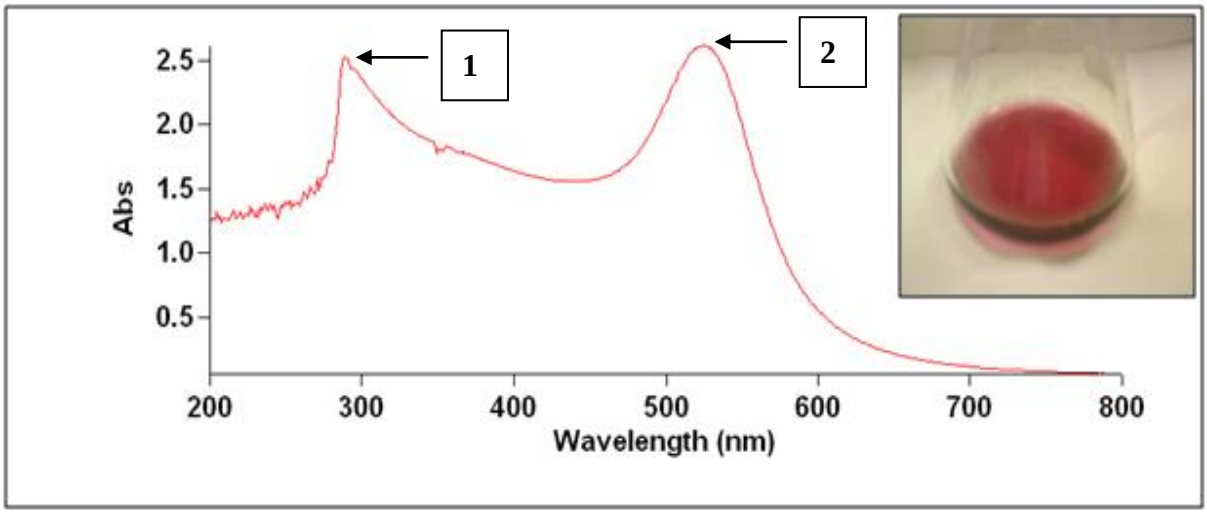

Figure 12: UV scan of citrate-capped GNPs in solution, with characteristic wine-red colour (inset), indicating excess sodium citrate (1) at 290 nm and the characteristic absorption maxima of GNPs (2) at 530 nm.

4.2. Colloidal stability of citrate-capped GNPs

4.2.1. Effect of time on colloidal stability

Stored at room temperature, the citrate-capped GNPs possess good colloidal stability over the 14 day storage period. The absorption maxima at 530 nm in Figure 13 (peak 1) appears defined throughout the time the nanoparticles were stored, indicating little to no loss of stability and maintenance of their colloidal suspension in aqueous medium.

Furthermore, the peak at 1 (Figure 13) appears narrow, with no subsequent broadening over time, indicating no aggregation of the nanoparticles.

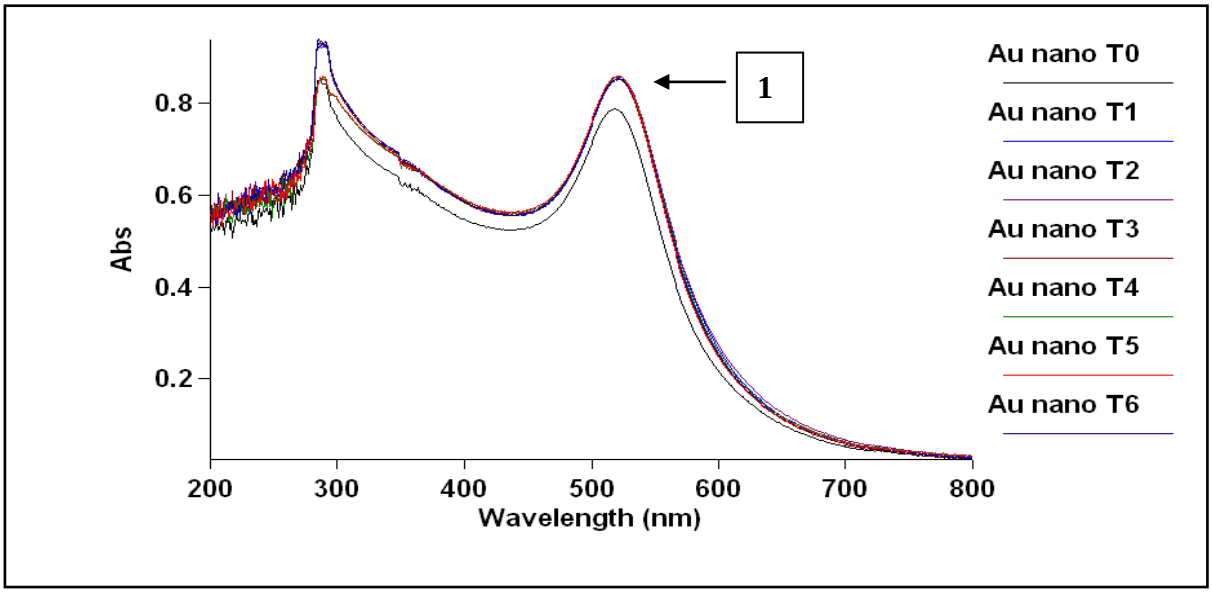

Figure 13: UV scan of citrate-capped GNPs in solution, with characteristic wine-red colour (inset), indicating excess sodium citrate (1) at 290 nm and the characteristic absorption maxima of GNPs (2) at 530 nm.

4.2.2. Effect of temperature on colloidal stability

Citrate-capped nanoparticles stored at room temperature (23°C) appear stable over the 14 day storage period, with no variation in broadness of the plasmon resonance peaks, as shown in Figure 15 (spectrum A, peak 1). The same maintenance of colloidal stability is observed when these nanoparticles are stored at 37°C (Figure 15, spectrum B). Here, there is even less variation in absorption over time (peak 2), indicating that the nanoparticles remained colloidally stable, to an even greater degree than when stored at room temperature. The citrate-capped GNPs stored at 4°C display a pronounced decrease in absorbance over time, with the plasmon resonance peak for the nanoparticles at an absorption maxima of 0.788 (T_0), decreasing after the 24 hour storage period to 0.342 (T_1). For the remaining 14 day storage term at 4°C, this absorbance maxima is more or less maintained, with an increase observed at T_5 to 0.859, followed by a subsequent decrease in the absorption maxima to 0.470, still significantly higher than that obtained at T_1. Furthermore, the plasmon resonance peak

appears to broaden as time passed (Figure 15, spectrum C, peak 3), reflecting aggregation of the nanoparticles over time and subsequent precipitation out of solution.

4.3. Synthesis of ciprofloxacin-conjugated GNPs

After 6 h of stirring, the conjugated nanoparticles were characterized by a new absorption peak (Figure 14, peak 1) forming at a wavelength of 667 nm on the absorption spectrum. Ciprofloxacin has characteristic absorption peaks at 284, 323 and 334 nm (Figure 14, peak 2, 3 and 4, respectively).

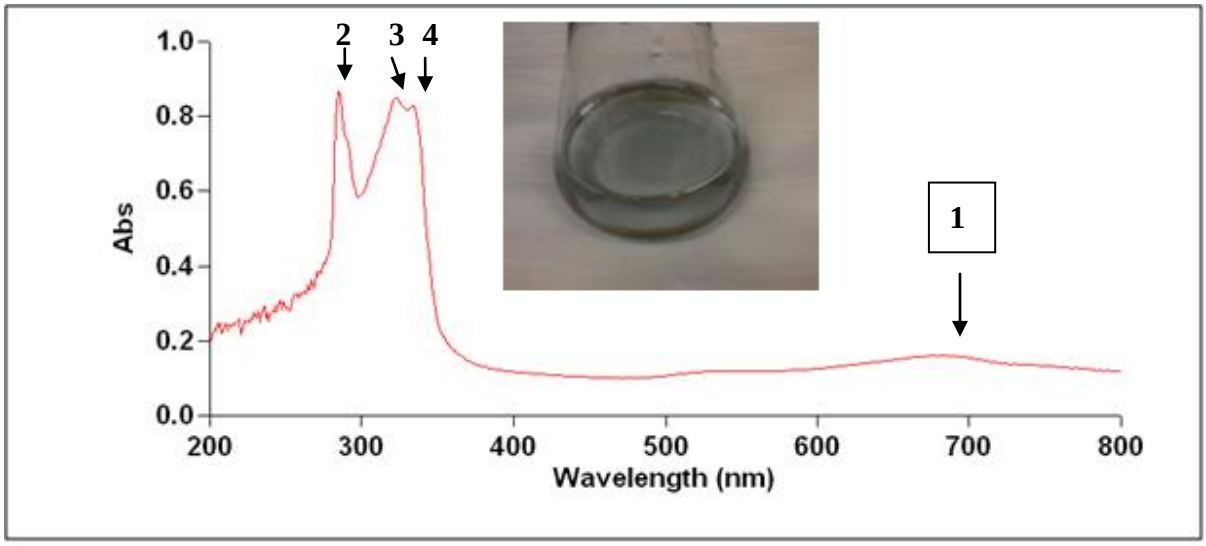

Figure 14: UV scan of ciprofloxacin conjugated GNPs, characterized by a dark blue/indigo colour (inset) indicating relative aggregation of nanoparticles. Ciprofloxacin-conjugated GNPs are detected (1) at 667nm as well as unbound ciprofloxacin (2, 3 and 4) at 284, 323 and 334 nm.

Successful conjugation of ciprofloxacin to the citrate-capped GNPs was effected by the 6 h process of mechanical stirring. The UV-absorption spectra obtained for the samples removed from the conjugate solution every 30 min reflect the attachment process (Figures 16-19). At a sampling time of 30 min a decrease in the free ciprofloxacin absorption can be seen, with absorption decreasing from 0.922 to 0.811 at 284 nm (Figure 16, spectrum B, peak 1). Furthermore, the plasmon resonance peak for the citrate-capped GNPs is no longer present at 530 nm.

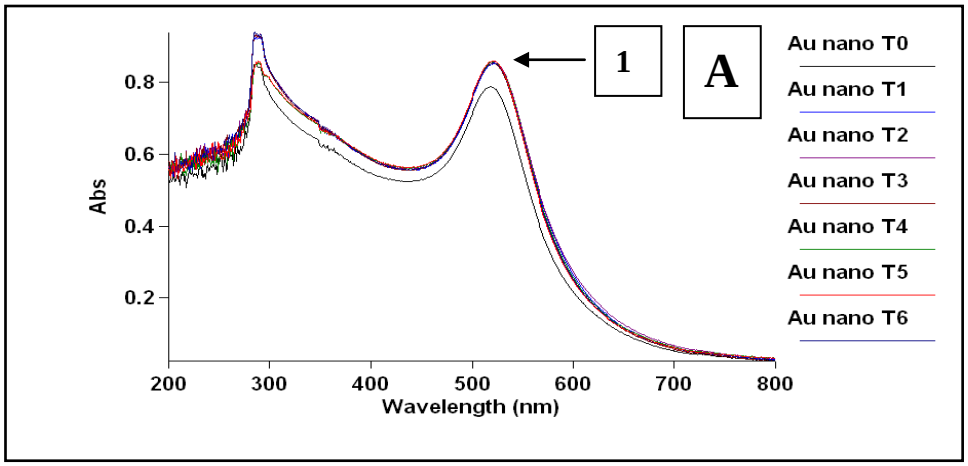

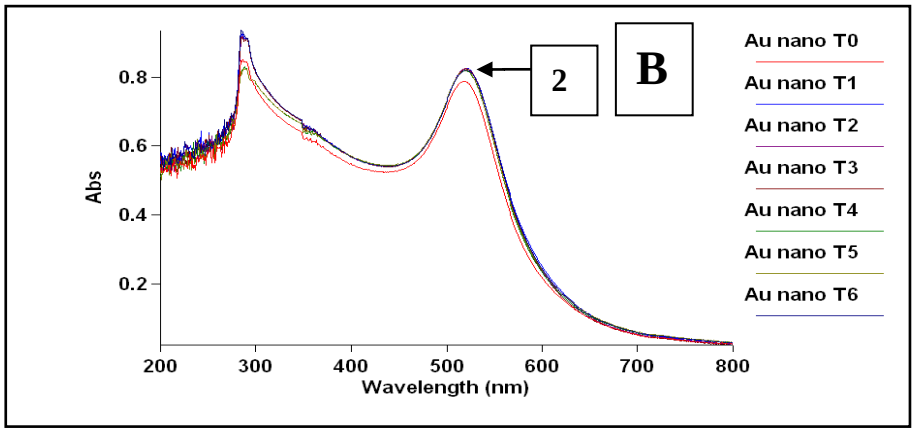

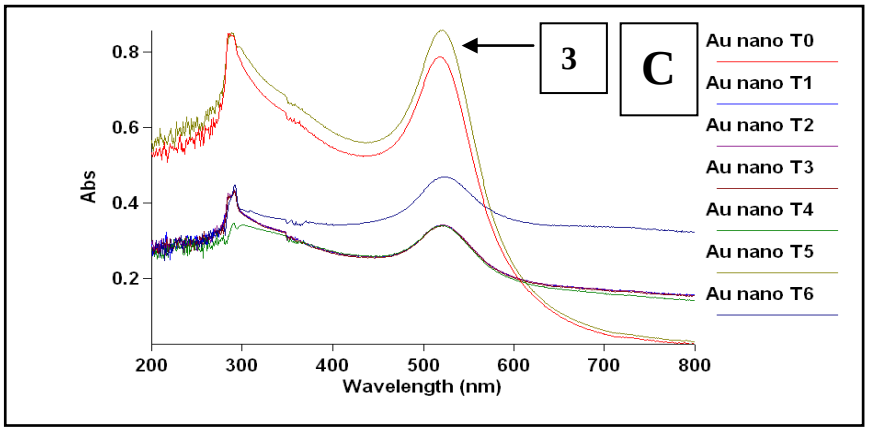

Figure 15: UV scan of citrate capped GNPs at 23°C (A); 37°C(B) and 4°C (C) with the characteristic absorption maxima of the GNPs at 530 nm indicated by A1, B2 and C3.

The decrease in absorption of, for both the free ciprofloxacin and citrate-capped GNPs, is indicative of a reduction in the concentration of both substances. In accompaniment to this decrease in absorption of the antibiotic and nanoparticles, is a simultaneous increase in absorption at a wavelength of 667 nm (Figure 16, spectrum B, peak 2) indicating the emergence of an entirely new species of nanoparticle within the mixture. This absorption reflects the shift in surface plasmon resonance of the citrate-capped GNPs to a longer wavelength once they become a conjugated species. At the sampling time of 30 min, these conjugates displayed an absorption value of 0.214. Although the absorption peak at 667 nm (with small variation over time) persisted throughout the time that samples were taken (6 h), the concentration of the newly formed nanoparticles decreases over time. This is shown by the decrease in absorption, from 0.214 at a sampling time of 30 min (Figure 18, spectrum B, peak 2) to 0.160 at a sampling time of 360 min (Figure 19, peak 1).

The peaks on the absorption spectrum at wavelengths 334, 323 and 284 nm indicate the presence of the un-reacted antibiotic, ciprofloxacin. Evidence for the conjugation of ciprofloxacin to the citrate-capped GNPs is shown in figures 16-19 (spectra A – M).

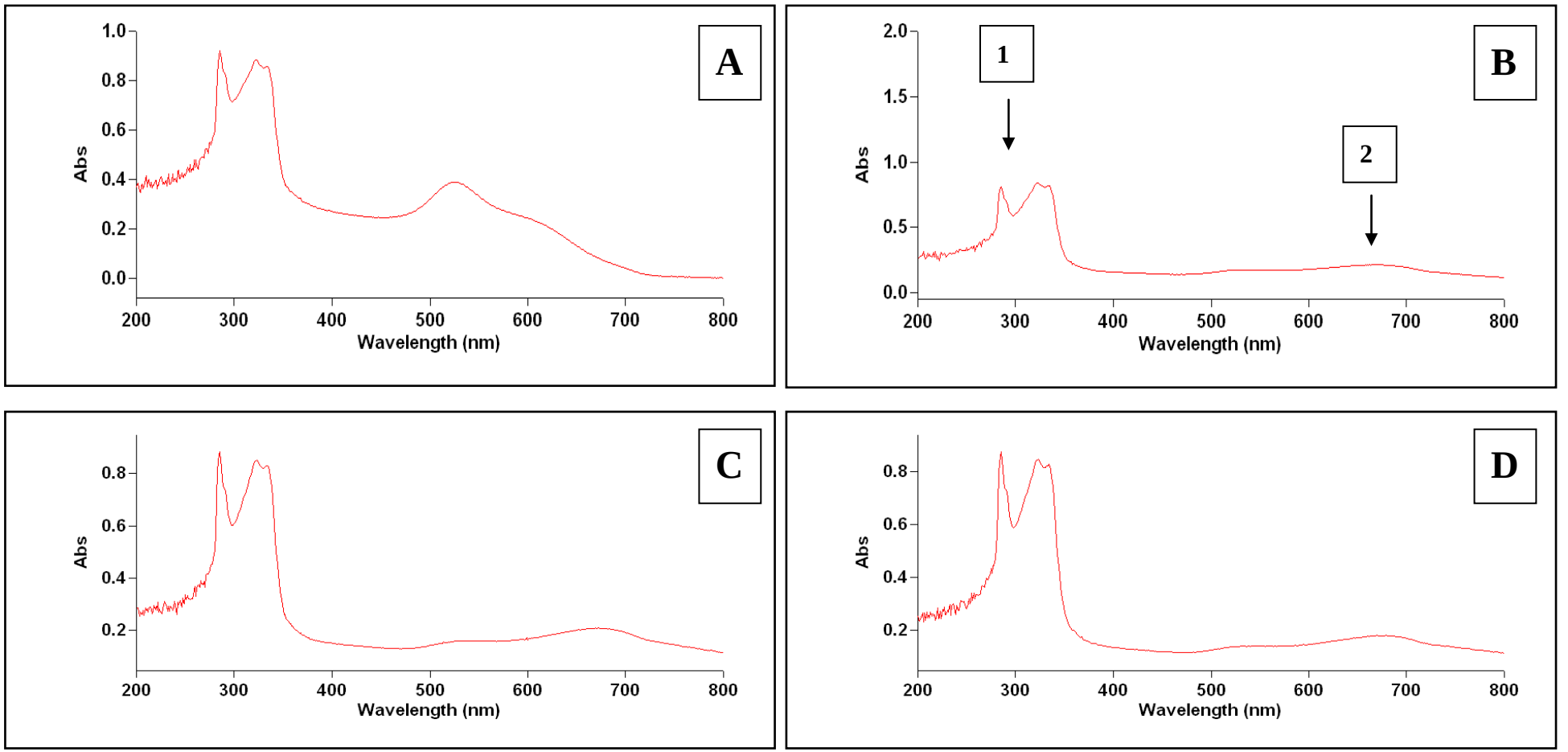

Figure 16: UV scans of conjugation of GNPs to ciprofloxacin. Successful formation of the conjugate is shown by peak formation at 667 nm (B2, C2 and D2), after 0 min (A), 30 min (B), 60 min (C) and 90 min (D).

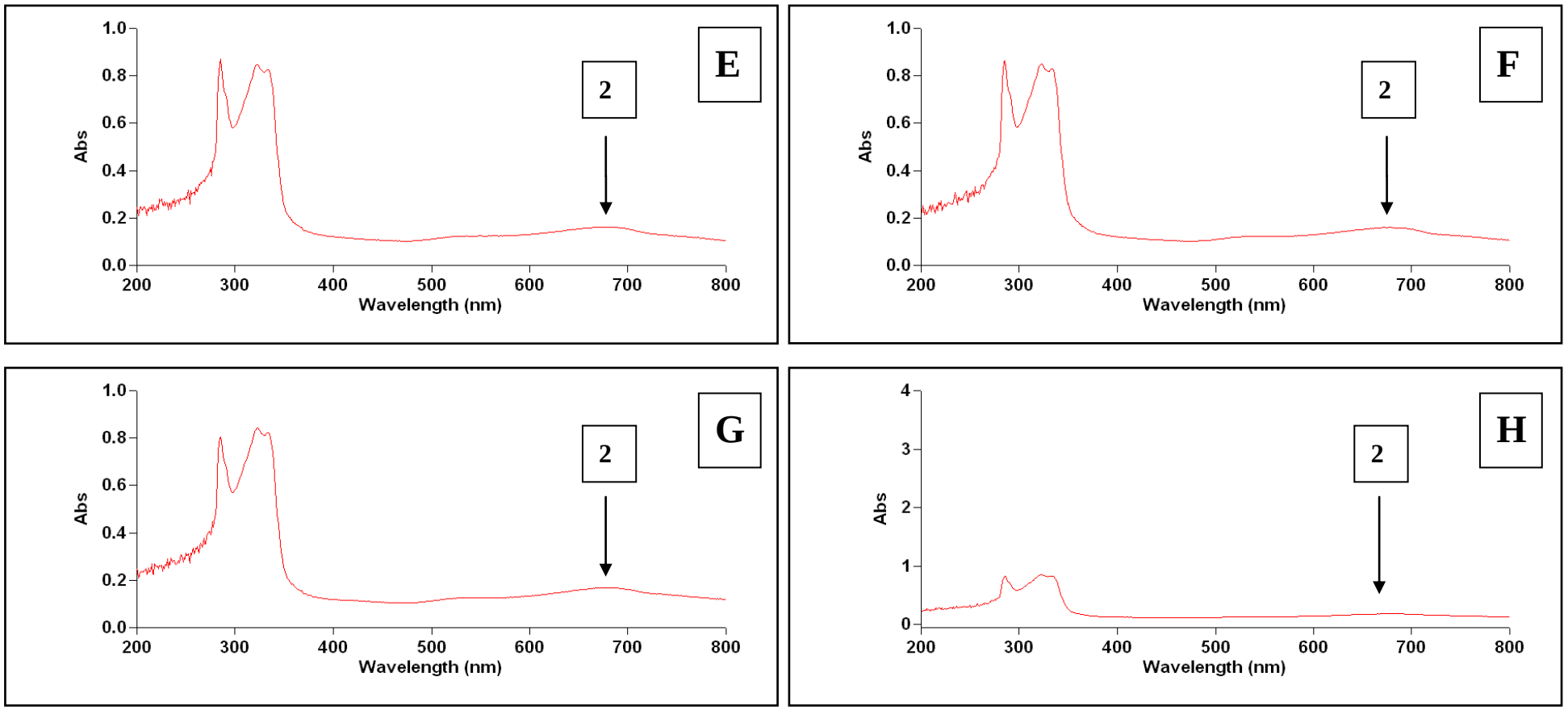

Figure 17: UV scans of conjugation of GNPs to ciprofloxacin. Successful formation of the conjugate is shown by peak formation at 667 nm (E2, F2, G2 and H2), after 120 min (E), 150 min (F), 180 min (G) and 210 min (H).

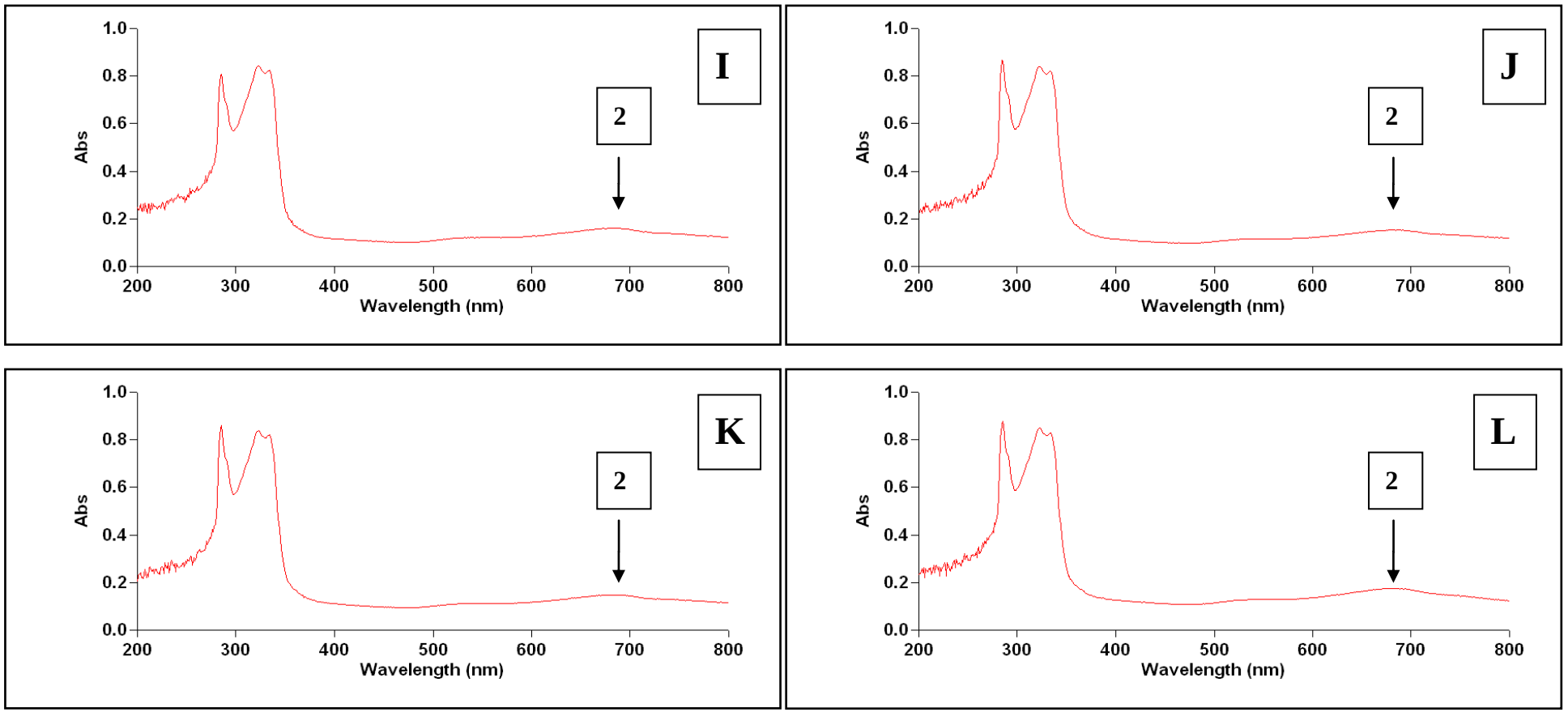

Figure 18: UV scans of conjugation of GNPs to ciprofloxacin. Successful formation of the conjugate is shown by peak formation at 667 nm (I2, J2, K2 and L2), after 240 min (I), 270 min (J), 300 min (K) and 330 min (L).

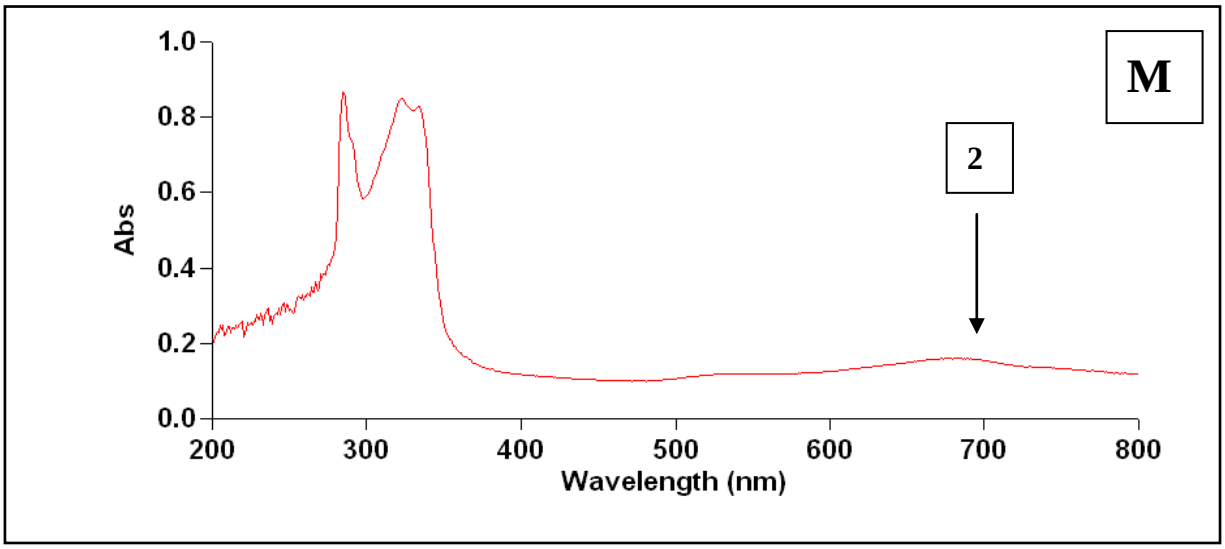

Figure 19: UV scan of conjugation of ciprofloxacin to GNPs. Successful formation of the conjugate is shown by peak formation at 667 nm (M2) after 360 min (6 h).

4.4. Colloidal stability of ciprofloxacin-conjugated GNPs

4.4.1. Effect of time on colloidal stability

The UV spectrum below (Figure 20) indicates the spectrum analysis of ciprofloxacin-conjugated GNPs over the 14 day storage period at 23°C. The ciprofloxacin-coated GNPs display good stability for the duration of the first 8 days (T_0 to T_4), after which (T_5 – T_6) the plasmon resonance peak at 667 nm (Figure 19, peak 1) broadens, indicating aggregation of the nanoparticles. Visual inspection showed that the nanoparticles had precipitated out of solution, further evidence for the loss of colloidal stability. Thus, over time, there is a loss of colloidal stability of the ciprofloxacin-nanoparticles. This is in direct contrast to the citrate-capped GNPs (Figure 13), which remained stable over the 14 day storage period.

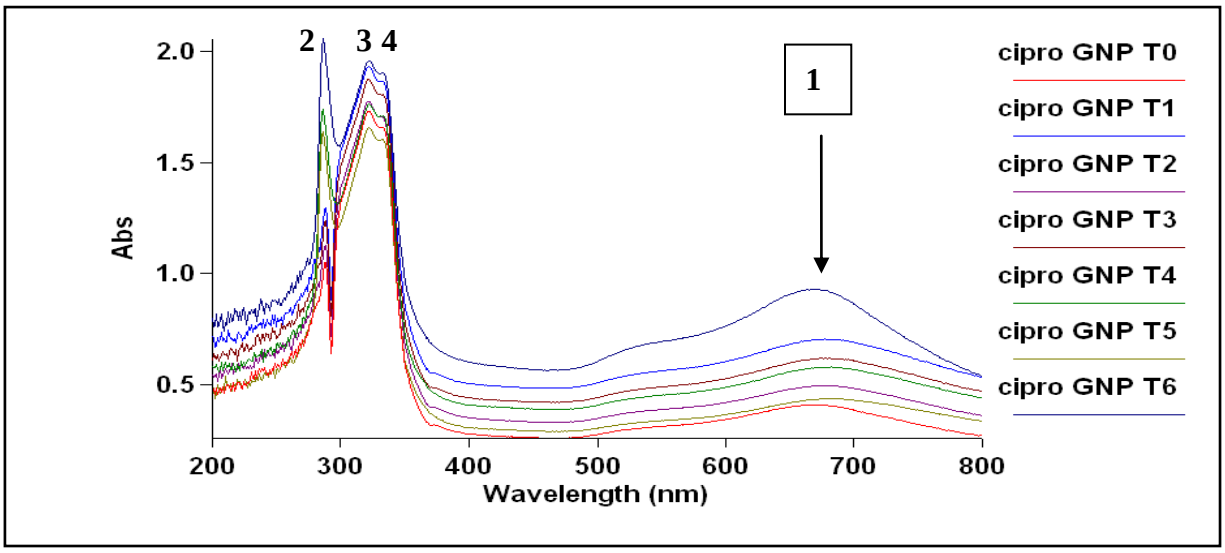

Figure 20: UV scan of the stability of ciprofloxacin-coated GNPs over a 14 day period (T0 – T6) at 23°C. The ciproflaxocin coated gold nanoparticles (Cipro GNP) is shown by a peak at 667nm (1). Excess ciproflaxacin (2, 3 and 4) is also indicated.

4.4.2. Effect of temperature on colloidal stability

Ciprofloxacin-conjugated GNPs show different colloidal stability characteristics under different storage conditions. Those stored at 23°C remain stable over 8 days of storage, after which their colloidal stability rapidly degenerates due to the formation of nanoparticle-antibiotic aggregates (Figure 21A, peak 1). Those ciprofloxacin-conjugated GNPs stored at 37 °C display a similar loss of colloidal stability, with a decrease in overall absorbance by the nanoparticles from 0.548 (T_1) to 0.308 (T_6) (Figure 21B, peak 2). This was accompanied by a broadening of the surface plasmon resonance peak, indicating aggregation of the conjugate GNPs.

Storage at 4°C seems to result in the best maintenance of colloidal stability for these nanoparticles. Under these storage conditions, there is an improvement in colloidal stability over time (Figure 21C, peak 3). From an absorbance of 0.494 at T_1, there is a gradual increase in this absorbance at T_3 (0.661), followed by a slight decrease at T_6 (0.621). This indicates an increase in detectable concentrations of ciprofloxacin-coated nanoparticles within the desired size range (at a wavelength of 667 nm). Furthermore, the plasmon maxima grows more defined as time passes, pointing to an improvement in colloidal stability at 4 °C.

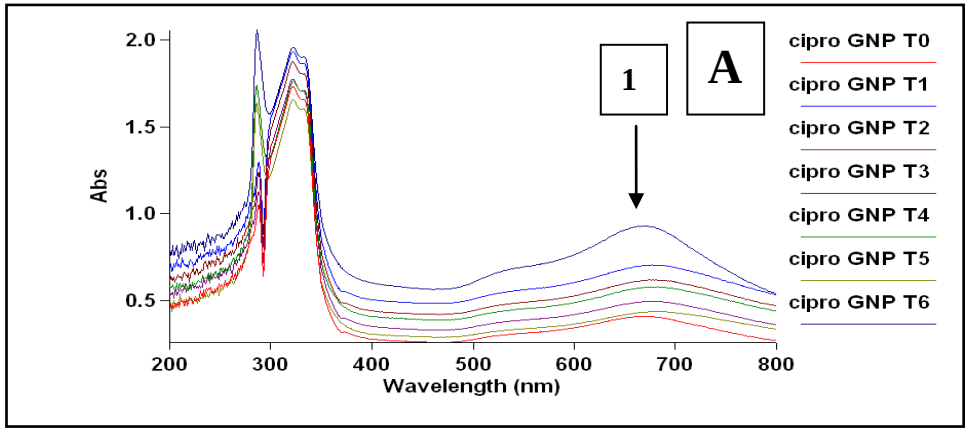

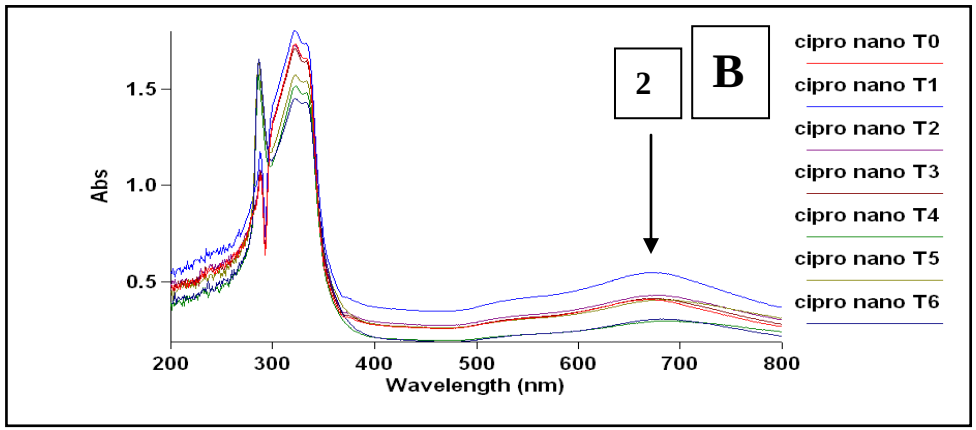

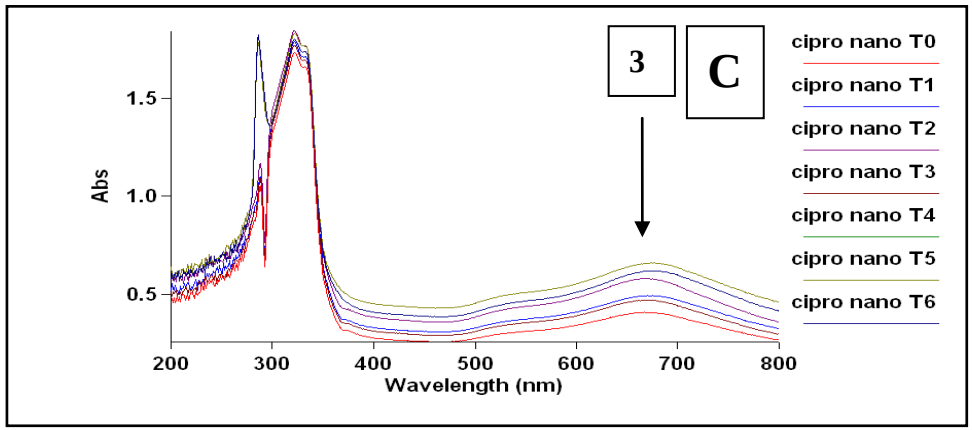

Figure 21: UV scan of the stability of ciprofloxacin-coated GNPs over a 14 day period (T1 – T6) at 23 °C (A); at 37 °C (B); and 4 °C with characteristic absorption peak of the conjugated nanoparticles at 667 nm shown by A1, B2 and C3 respectively.

4.5. Characterization of citrate-capped and ciprofloxacin-conjugated GNPs

4.5.1. Spectrophotometric analysis

Fourier transform infrared (FT-IR) spectrum analysis was carried out on free ciprofloxacin and ciprofloxacin-conjugated GNPs in order to determine the functional groups present on both antibiotic and nanoparticles, and characterization of bonding between the two. The FT-IR spectrum of ciprofloxacin in aqueous medium is shown in Figure 22. The absorption peaks that remain clear are at 3361 cm^{-1} (Figure 22A), 1643 cm^{-1} (Figure 22B) and 1082 cm^{-1} (Figure 22C), corresponding to the vibrational frequency of stretching of the N-H bond of the imino moiety on the piperazinyl group of ciprofloxacin, a primary amine (N-H) bend of the pyridone moiety and the C-F functional group, respectively. Due to the presence of water in the sample, partial obscuring of the N-H group on the piperazinyl moiety has occurred.

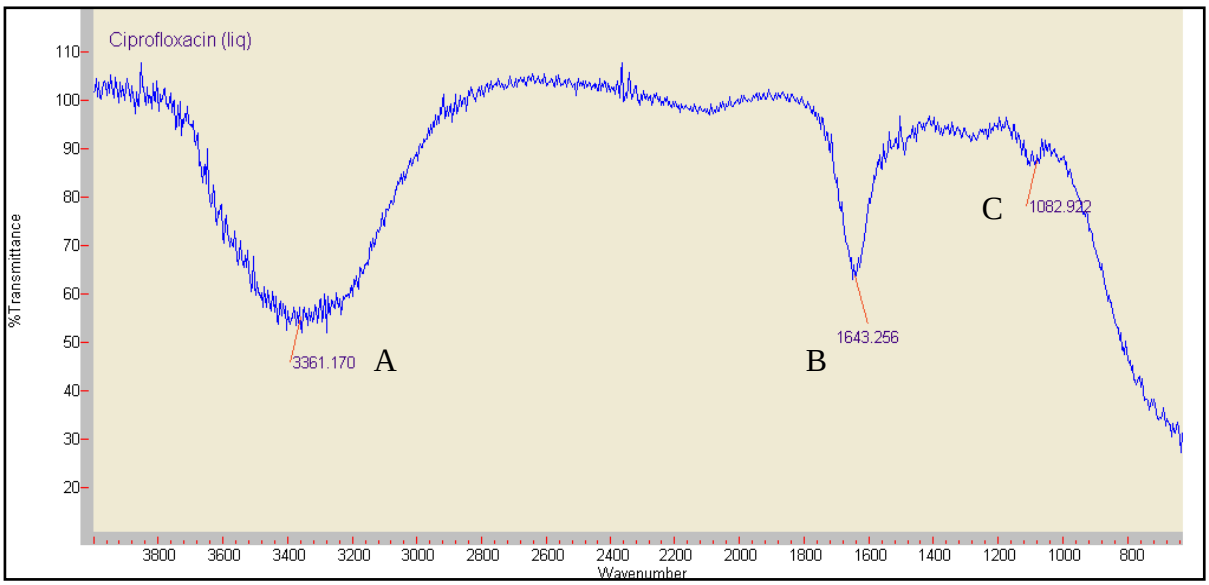

Figure 22: FTIR scan of ciprofloxacin in aqueous medium, with N-H bond of the piperazinyl group (A), primary amine bend (B) and C-F bond (C).

The FT-IR spectrum of the ciprofloxacin-conjugated GNPs shows that the primary C-F bond remain unchanged, as well as the primary amine bend of the pyridone group (Figure 23B). The C-N bond stretching present on the ciprofloxacin molecule also remains unchanged, though more visible on the FTIR spectrum of the ciprofloxacin-

conjugated GNPs (Figure 23C). The band at 3361 cm^{-1} appears broader in the case of the ciprofloxacin-conjugated GNPs, indicating a change in the N-H bond formation of the imino group of the piperazinyl moiety (Figure 23A).

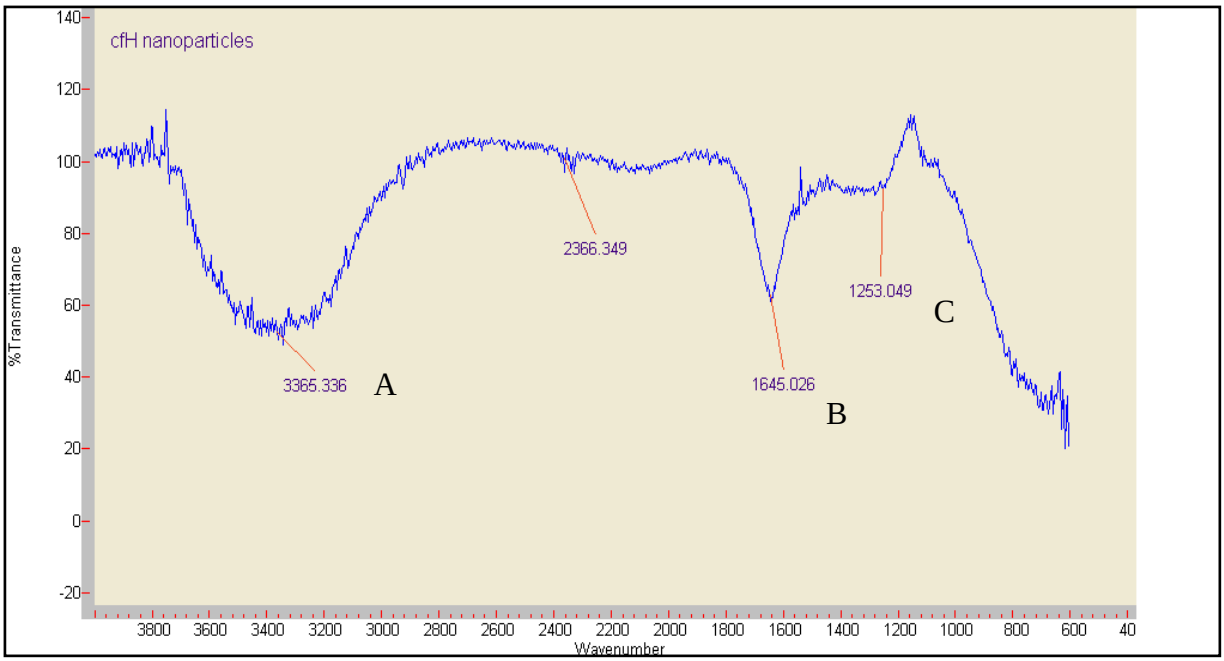

Figure 23: FTIR scan of ciprofloxacin-conjugated GNPs, with N-H bond of the piperazinyl group (A), primary amine bend (B) and C-N stretching (C).

4.5.2. Ultrastructural analysis by TEM

It was found that the citrate-reduction technique generated GNPs that were predominantly spherical in shape, with the presence of few multi-faceted nanoparticles (Figure 24, A1) and triangular shapes (Figure 24, C2 and C3). Measurement of nanoparticle diameters in selected areas of the copper grid showed that the GNPs synthesized were all in the range of 15 to 30 nm (Figure 24, C). This size distribution corresponds with the diameter range of GNPs formed that were synthesized by Tom *et al.* (2004), Nirmala Grace and Pandian (2007) and Thanh and Green (2010).

Ciprofloxacin-coated GNPs display a high level of aggregation (Figure 24, B). Size ranges and morphologies are identical to those of citrate-capped GNPs, with the hybrid nanoparticles ranging between 15 and 30 nm in size and appearing spherical in shape. Ciprofloxacin can be distinguished forming a coating on the surface of the

nanoparticles and aiding in the formation of nanoparticle aggregates. This aggregation phenomenon corresponds to the shift to a longer absorbance wavelength of the ciprofloxacin-coated GNPs.

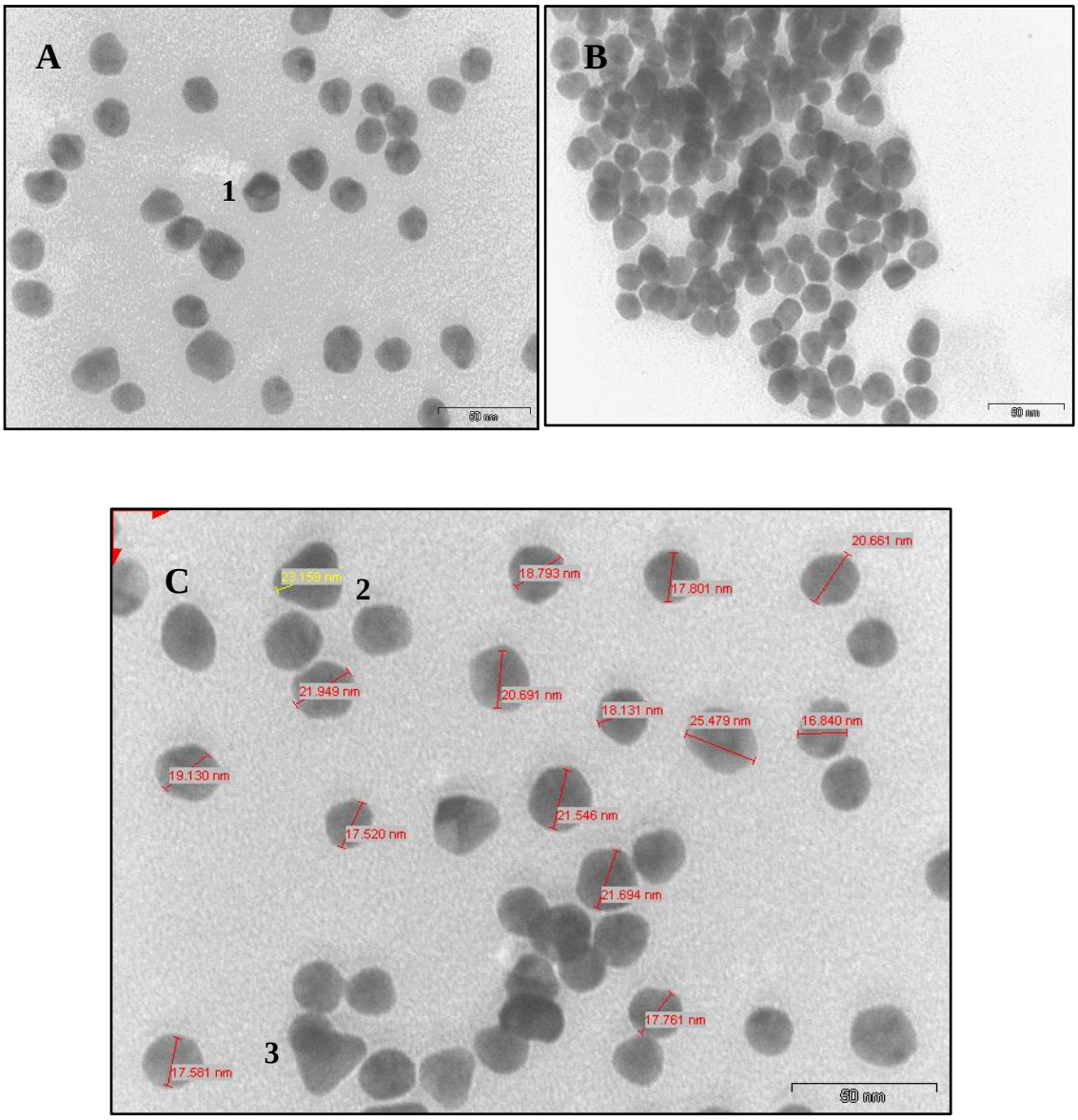

Figure 24: TEM of citrate-capped GNPs, with multifaceted nanoparticle type (A1), ciprofloxacin conjugated GNPs (B) and citrate-capped GNPs measuring between 15 and 30 nm in diameter, with triangular nanoparticles (C2 and C3).

4.6. Antimicrobial activity of ciprofloxacin-conjugated GNPs

The effects of ciprofloxacin, citrate-capped GNPs and ciprofloxacin-conjugated GNPs were tested on 6 Gram positive and 11 Gram negative strains. All the tests were conducted in duplicate. The MIC values obtained for ciprofloxacin, ciprofloxacin-conjugated GNPs and citrate capped gold nanoparticles for the bacteria tested is shown in Table 5 and illustrated in Figure 25. The MICs of ciprofloxacin coated GNP compared to ciprofloxacin show increased antibacterial activity of the conjugated nanoparticles, except in the cases of bacterial species *Klebsiella pneumoniae* (S5906), *E. coli* (B3578), *E. coli* (U10948), *E. coli* (U10804), *Enterococcus faecalis* (U12318) and *S. aureus* (P4256).

The MICs of ciprofloxacin conjugated GNPs for the *Staphylococcus aureus* isolates S6158, S5878 and P4217 were 0.05, 0.2 and 0.2 mM, respectively and for ciprofloxacin were 0.25, 0.3 and 0.3 mM, respectively. A comparison of the MIC's of ciprofloxacin conjugated GNP to ciprofloxacin showed that the MIC were lower for the ciprofloxacin conjugated GNP. This was observed for all replicates except for *S. aureus* (P4256), which showed complete resistance to both ciprofloxacin and ciprofloxacin-conjugated GNPs. The MICs of the ciprofloxacin conjugated GNPs for *Enterococcus faecalis* showed a greater antibacterial effect on isolate U11394, as opposed to free ciprofloxacin, with MIC values of 0.2 and 0.3 mM for the conjugate GNPs and ciprofloxacin respectively. *Enterococcus faecalis* (U12318) was resistant to both ciprofloxacin and ciprofloxacin-conjugated GNPs.

Amongst the Gram negative bacteria, the single *Pseudomonas* spp. (isolate S6125), three of the four *Klebsiella pneumoniae* isolates (P3967, V258 and U10705), the single *Enterobacter* spp. (P16743) and two of the five *E. coli* isolates (P4055 and P4299), a better antimicrobial effect was observed after treatment with ciprofloxacin-conjugated GNPs (MIC values of 0.1 mM, 0.1 mM, 0.05 mM. 0.05 mM, 0.05 mM, 0.05 mM and 0.1 mM respectively, in contrast to the citrate-capped GNPs' MIC values of 0.3 mM, 0.3 mM, 0.1 mM, 0.2 mM, 0.1 mM, 0.3 mM and 0.25 mM, for the same species.

Table 5: MICs of citrate capped GNPs, ciprofloxacin-conjugated GNPs, and ciprofloxacin on pathogenic bacterial strains.

Bacterial Species	Average MIC (mM) for citrate-capped GNPs	Average MIC (mM) for ciprofloxacin-conjugated GNPs	Average MIC (mM) for ciprofloxacin
Pseudomonas spp. (S6125)	None	0.1	0.3
Klebsiella pneumoniae (S5906)	None	None	0.25 ± 0.07
Klebsiella pneumoniae (P3967)	None	0.1	0.3
Klebsiella pneumoniae (V258)	None	0.05	0.1
Klebsiella pneumoniae (U10705)	None	0.05	0.2
Enterobacter spp. (P16743)	None	0.05	0.1
Escherichia coli (B3578)	None	None	None
Escherichia coli (P4055)	None	0.05	0.3
Escherichia coli (U10948)	None	0.25 ± 0.07	0.2
Escherichia coli (U10804)	None	0.3	0.25 ± 0.07
Enterococcus faecalis (U12318)	None	None	None
Esherichia coli (P4299)	None	0.1	0.25 ± 0.07
Enterococcus faecalis (U11394)	None	0.2	0.3
Staphylococcus aureus (S6158)	None	0.05	0.25 ± 0.07
Staphylococcus aureus (P4256)	None	None	None
Staphylococcus aureus (S5878)	None	0.2	0.3
Staphylococcus aureus (P4217)	None	0.2	0.3

*Shaded rows indicate cases of ciprofloxacin-conjugated GNPs exerting greater antimicrobial effects (lower MIC values) in comparison to ciprofloxacin on the specified bacterial isolates.

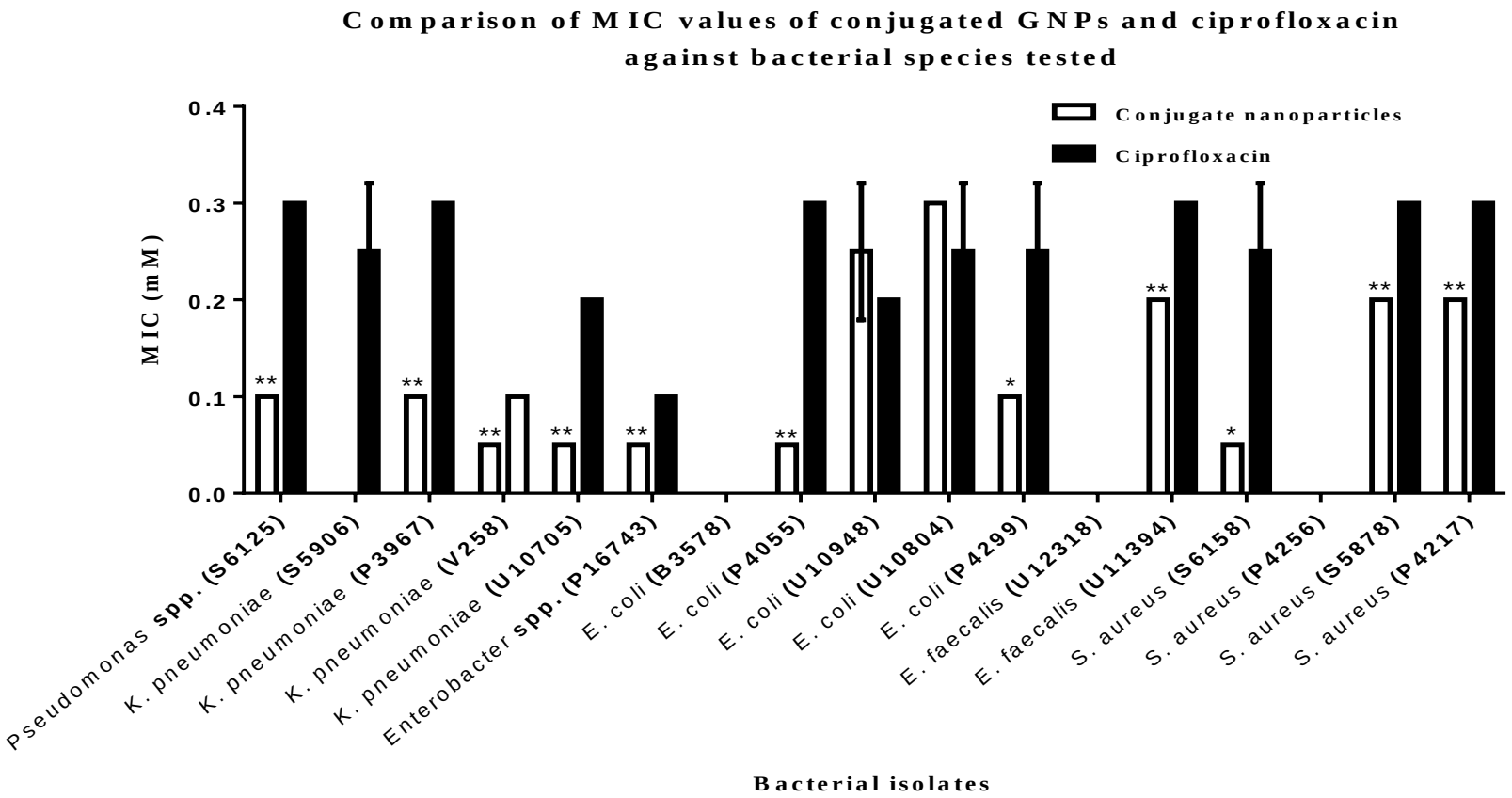

Figure 25: MICs of ciprofloxacin conjugated nanoparticles and ciprofloxacin against isolates of *Pseudomonas* spp., *Klebsiella pneumoniae, Enterobacter* spp., *Escherichia coli, Enterococcus faecalis* and *Staphylococcus aureus*. Comparison between the two are indicated by ** (highly significant,) and * (significant) (n = 2).

4.6.1. Effect of ciprofloxacin conjugated GNPs on bacterial growth by transmission electron microscopy

The images obtained by TEM indicate the mode of drug delivery by ciprofloxacin-conjugated GNPs. Ultra structural observation of the effect of ciprofloxacin-conjugated GNPs on *Staphylococcus aureus*, *Enterococcus faecalis*, *Pseudomonas* spp. and *Klebsiella pneumoniae* is shown in Figures 26-29. These show that the nanoparticles concentrate ciprofloxacin on the surface of the bacterial cell. Single samples of all bacterial species tested against were examined by transmission electron microscopy.

In micrograph A (Figure 26), the ciprofloxacin-conjugated GNPs aggregate at the surface of the *S. aureus* cell, as indicated by the arrows. The nanoparticles' presence and position is evidenced by the darker spots surrounding the bacterial cell (1). Micrograph B shows a magnified view of the bacterial cell, with the cell wall clearly visible and indicated (1). Here, a more detailed view of this particle aggregation on the cell surface can be seen (2). Micrograph C (Figure 27) shows the cell of the bacterial species, *Enterococcus faecalis*, surrounded by ciprofloxacin-conjugated GNPs (1), which appear to adhere closely to the surface of the bacterial cells (2 and 3). Micrograph D shows a magnified image of the interaction between the cell wall of the bacteria (4) and the nanoparticle aggregates (5). As with *S. aureus*, the conjugated nanoparticles appear to exert an effect which involves the concentration of the antibiotic at the cell wall surface.

Micrographs obtained detailing the interaction of ciprofloxacin-conjugated GNPs on the cells of *Pseudomonas aeruginosa* shows a similar concentration effect through aggregation at the cell wall surface in Figure 28 (1). These nanoparticle aggregations can be seen more clearly in Micrograph F, as indicated in positions 2, 3 and 4. For the species *Klebsiella pneumoniae*, images were obtained for bacterial cultures treated with both citrate-capped and ciprofloxacin-conjugated GNPs. For *Klebsiella pneumoniae*, the TEM image showed attachment and aggregation of these nanoparticles at the surface of the cell (Figure 29, micrograph G, 1 and 2), much the same as the phenomenon as that observed for all ciprofloxacin-conjugated GNPs. Micrograph H shows the attachment of large aggregates of ciprofloxacin-conjugated GNPs to biofilm

components surrounding the cell (1), with the biofilm components themselves represented by 2.

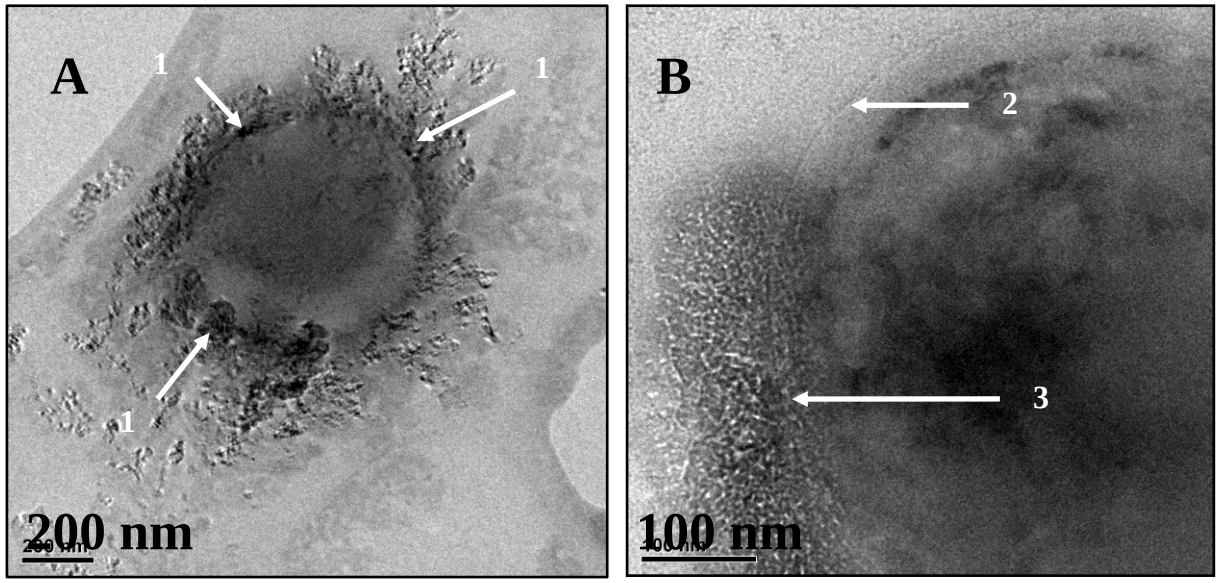

Figure 26: TEM of ciprofloxacin conjugated GNPs and S. aureus (A) with aggregation of the GNPs at the cell surface (1) and at a higher magnification (B) indicating the cell wall (2) and nanoparticle aggregation (3).

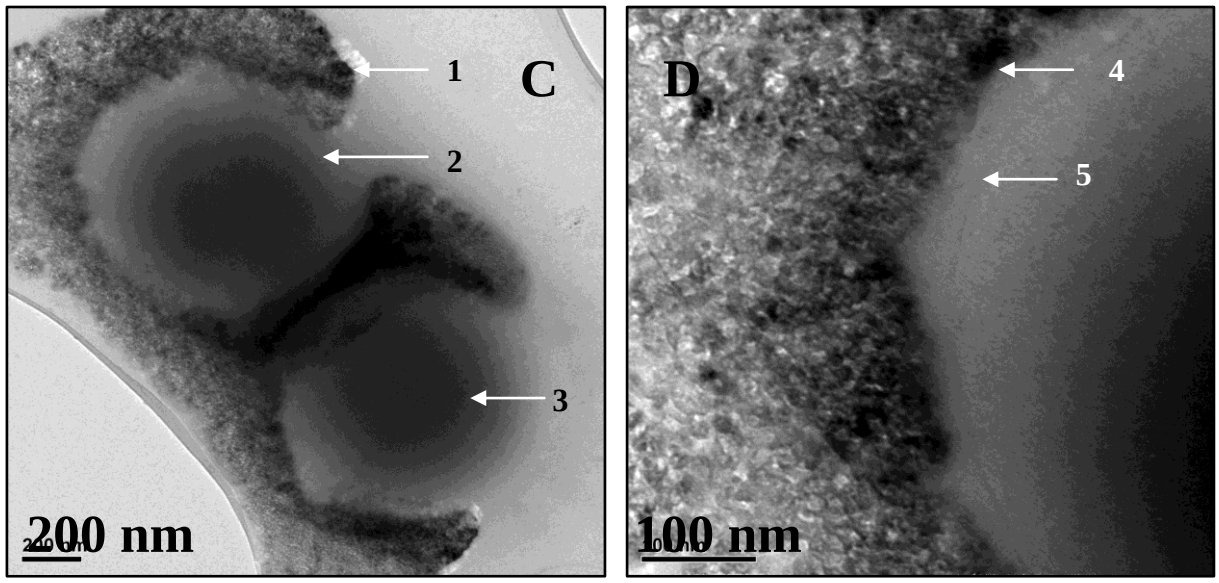

Figure 27: TEM of ciprofloxacin conjugated GNPs and *Enterococcus faecalis* (C), showing the bacterial cell (2 and 3) with GNP aggregation (1), as well as at higher magnification (D) indicating the cell wall (5) and GNP aggregation (4).

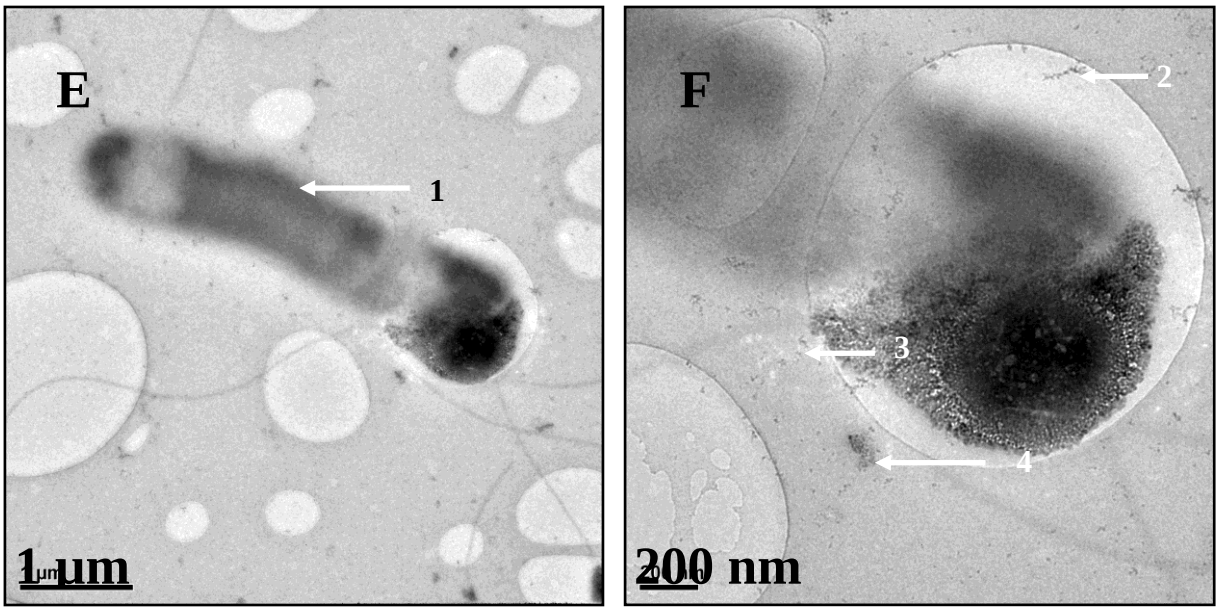

Figure 28: TEM of ciprofloxacin conjugated GNPs and *Pseudomonas* spp. (E) showing the bacterial cell (1) and at higher magnification (F) showing interaction of ciprofloxacin conjugated GNPs (2, 3 and 4) with the cell surface.

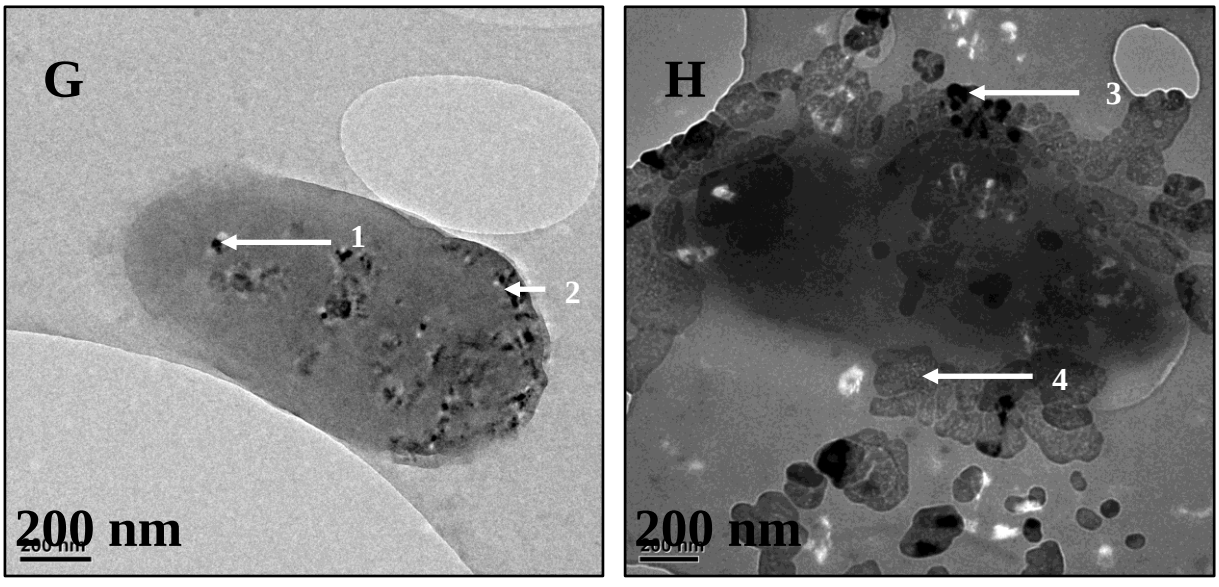

Figure 29: TEM of ciprofloxacin conjugated GNPs and *Klebsiella pneumoniae* (G) showing interaction of GNPs at the cell surface (1 and 2) and at higher magnification (H) showing aggregation of ciprofloxacin conjugated GNPs (3) on an extracellular polymer (4).

4.7. Anti-cancer activity of citrate-capped GNPs on the Caco-2 cell line

Anti-cancer activity of citrate-capped GNPs was determined from cell viability of Caco-2 cells after treatment with the nanoparticles at varying concentrations in the MTT assay. The cytotoxicity of the GNPs was calculated from cell viability. The percentage cytotoxicity of citrate-capped GNPs was compared to that of gemcitabine, a chemotherapeutic drug used as a positive control in the MTT assay.

At the highest concentration tested, 0.5 mM, the cytotoxicity of the citrate-capped GNPs was similar to that of gemcitabine, showing slight elevation in cytotoxic activity ($p = 0.04$). For all other concentrations tested (0.1, 0.2, 0.3 and 0.4 mM) no significant comparisons could be made between the cytotoxic activities of citrate-capped GNPs and gemcitabine due to the large variance amongst the triplicate cytotoxicity values calculated from the MTT assay ($p > 0.05$ for all concentration comparisons other than 0.5 mM). The results show, however, that citrate-capped GNPs do exert cytotoxic activity against the Caco-2 cells, with average percentage cytotoxicity levels of 44.44%, 45.33%, 40.78%, 49.37% and 50.63% at concentrations of 0.1 mM, 0.2 mM, 0.3 mM, 0.4 mM and 0.5 mM respectively (Figure 30).

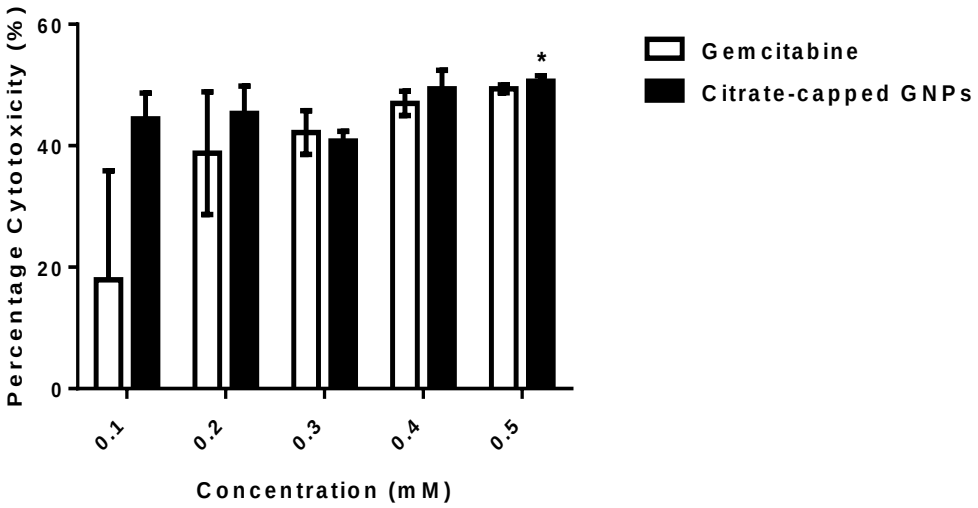

Figure 30: Cytotoxicity of gemcitabine and citrate-capped GNPs at concentrations ranging from 0.1 to 0.5 mM on the Caco-2 cell line. Significant difference in cytotoxic activity is indicated by * ($p = 0.04$).

The effect of citrate-capped GNPs and gemcitabine on the Caco-2 cells is shown in Figure 31 (B) and (C), respectively. Untreated Caco-2 cell are shown in Figure 33A. The cells are pyriform in shape and are translucent. Cells treated with gemcitabine (Figure 33C) show granulated and rounded cells, whereas cells treated with citrate-capped GNPs (Figure 33B) showed a complete loss of cellular morphology and granulation.

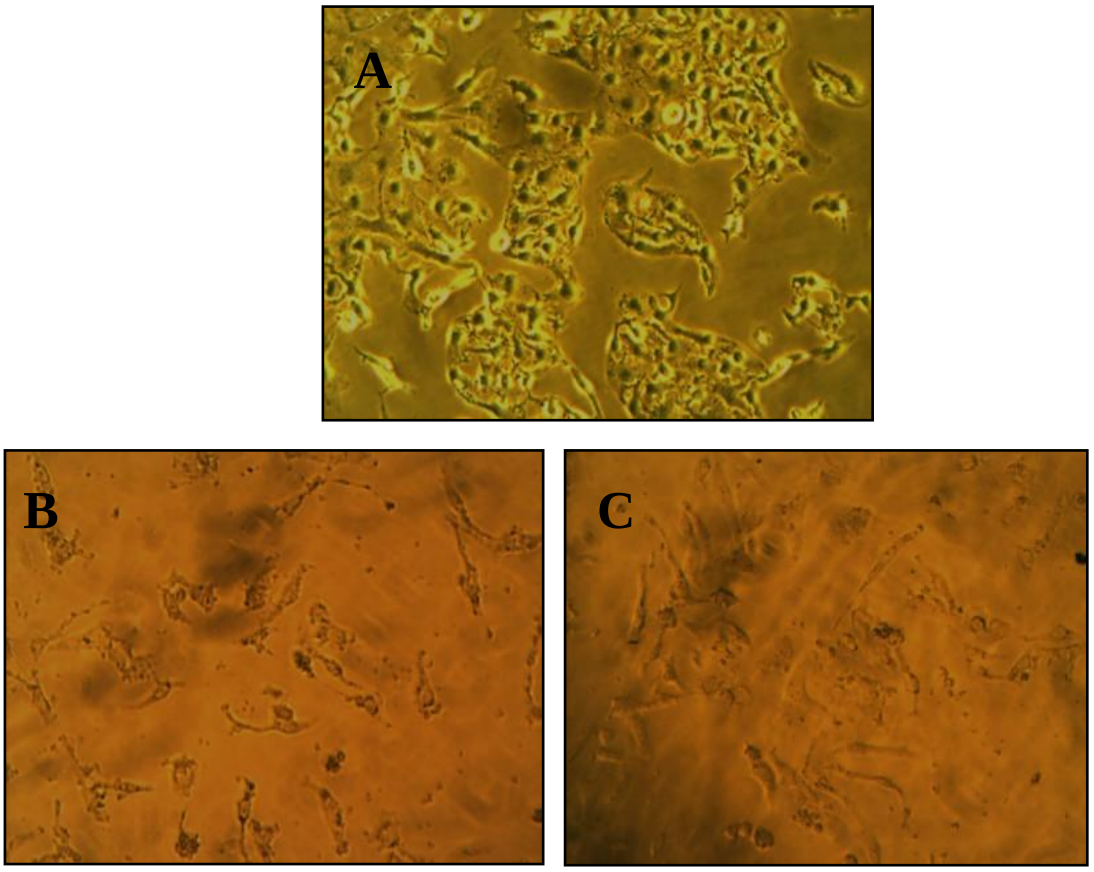

Figure 31: Effect of citrate-capped GNPs (B) and gemcitabine (C) on Caco-2 cells. Untreated Caco-2 cells are shown in A (X 100).

5. DISCUSSION

5.1. Characterization of citrate-capped gold nanoparticles by UV Vis Spectroscopy

In order to verify the presence of GNPs in aqueous medium after citrate reduction has been carried out, UV spectrum analysis was conducted on the sample to indicate the absorption. Various studies involving characterization of GNPs have shown that these nanoparticles have a distinctive absorption peak within a wavelength range of 518 – 530 nm (Tom *et al.*, 2004; Nirmala Grace and Pandian, 2007). Furthermore, once the nanoparticles have been conjugated with the desired antibiotic, in the present case, ciprofloxacin, a shift in the spectrum allows one to verify the bond formation through a shift in the peak to a longer wavelength on the spectrum (Tom *et al.*, 2004; Pissuwan *et al.*, 2010).

In the case of this study, the citrate-capped GNPs absorbed light at a characteristic wavelength of 530 nm. Free electrons in the conduction band of the metal oscillate in unison, thus resulting in this intense absorption of light. These oscillations, are in turn, caused by the source of electromagnetic radiation, in this case, the light with which the nanoparticles are bombarded. The wine-red colour of the nanoparticle solution is a physical manifestation of the localized surface plasmon resonance (Vujačić *et al.*, 2012). Upon conjugation to ciprofloxacin, the colour of the nanoparticle solution changed from wine red to light purple/blue. This phenomenon was reflected in the UV-spectra obtained for ciprofloxacin-conjugated GNPs which corresponds to the phenomena observed by Tom *et al.* (2004) and Pissuwan *et al.* (2010) in terms of aggregation of nanoparticles and the shift in absorbance to a longer wavelength.

5.2. Synthesis of ciprofloxacin-conjugated GNPs

Tom *et al.* (2004) showed that there is a marked colour change in the citrate-capped GNP suspension once conjugation to ciprofloxacin occurs. This visible alteration in colour from wine-red to light blue is a direct result of aggregation of the nanoparticles with the addition of ciprofloxacin. The formation of these conjugate nanoparticle

aggregates leads to the shifting of the maximum plasmon peak position to a longer wavelength, physically manifesting as a colour change from red (shorter wavelength) to purplish blue (Vujačić *et al.*, 2012).

According to results of this study, ciprofloxacin has characteristic absorption in the 250 – 350 nm range, with the peaks at 334, 323 and 284 nm indicating the presence of the molecule, as confirmed in research conducted by Tom *et al.* (2004). At a sampling time of T_0, the surface plasmon maxima for the gold nanoparticles is highly evident at 530 nm, indicating their presence along with that of ciprofloxacin. Thus, both nanoparticles and antibiotic are present as separate and detectable entities. At a sampling time of T_1 (30 min), there is a decrease in absorption by the free antibiotic in the suspension, from an absorbance of 0.922 to 0.811. This indicates a decrease in concentration of free ciprofloxacin over the 30 min period. Simultaneously, there is a significant decrease in the absorption by the gold nanoparticles present, with the emergence of a new surface plasmon maxima at 667 nm. This is indicative of formation of a new species of gold nanoparticle, one that has been surface functionalized by the antibiotic. The antibiotic serves to have an aggregation effect on the nanoparticles once it has formed a visible coating on their surface. This causes a wavelength shift from a shorter reading (530 nm) to a longer (667 nm) (Vujačić *et al.*, 2012). Furthermore, the plasmon maxima peak is shorter and broader (indicative of aggregation of the nanoparticles) in comparison to the initial peak at T_0 which appears defined and narrow. This is further evidence of the aggregation phenomenon, as the variation in size of nanoparticles present, as opposed to the narrow size range present in the sample at T_0, creates a broadening of the peak (Chen *et al.*, 2008).

The decrease in absorption of the ciprofloxacin molecule over time, along with the formation of the new nanoparticle species leads to the conclusion that formation of ciprofloxacin-conjugated GNPs has occurred. Over time, as evidenced at T_1 (30 min), there is a maximum absorbance for the conjugated nanoparticles at 0.214, followed by a decrease in absorption to 0.148 at T_{11} (330 min). This indicates a decrease in concentration of detectable ciprofloxacin-conjugated GNPs. This may simply be due to experimental conditions (adherence of the aggregated ciprofloxacin-coated GNPs to the inner surface of the conical flask and to the surface of the stirrer bar, thus reducing their detectable concentration) or due to these nanoparticles aggregating to an extent that

there is loss of colloidal stability which causes them to precipitate out of solution. Thus the mixing time needed to create these conjugate nanoparticles should be reduced, as a period of 6 hrs seems to cause such an effect. From the experimental data, a mixing time of an hour should be ideal for creating colloidally stable conjugate nanoparticles.

5.3. Colloidal stability of citrate-capped and ciprofloxacin-coated GNPs

Stability of GNPs in aqueous medium is accounted for by the addition of trisodium citrate, which acts as both a reducing and stabilizing agent (Tom *et al.*, 2004). This stability allows the GNPs to retain their colloidal stability in solution through the positive charges on their surface which repel other nanoparticles with like charges, thus maintaining their distribution in solution. Over time, and under different storage conditions, however, the colloidal stability alters, rendering the GNPs unfit for use as drug delivery vehicles. Furthermore, studies have shown that upon attachment to antibiotics and other drugs, GNPs display a characteristic aggregation phenomenon (Nirmala Grace and Pandian, 2007). In order to determine whether the time and temperature have an effect on the colloidal stability of the GNPs, this study determined the stability of the nanoparticles by looking at absorbance readings produced over 14 days of storage at three different temperatures.

5.3.1. Effect of time on colloidal stability

The effect of storage time, at 23°C, showed retention of colloidal stability for the citrate-capped GNPs. For the duration of the 14 day storage period, the plasmon resonance peak remains defined, with no broadening to indicate aggregation. Ciprofloxacin-conjugated GNPs show loss of colloidal stability over 14 days. This is caused by formation of nanoparticle aggregates (as shown by the broadening in width of the plasmon resonance peaks) and visual evidence of the precipitation of the GNPs out of solution over time.

The forces of attraction between citrate-capped gold nanoparticles take the form of ionic interactions. The like charges present on the GNP surfaces cause repulsion between nanoparticles, allowing them to remain as discrete entities in solution and retain their colloidal stability. This study shows that the colloidal stability imparted by

trisodium citrate (the surfactant) is retained for the storage period of 14 days at 23°C. Ciprofloxacin on the surface of the conjugated GNPs exists in zwitterionic form in aqueous medium. Once attached to the surface of the GNPs, they will, to an extent, negate the stabilizing effect of the citrate molecule. This de-stabilizing effect is caused by hydrogen bond formation between the zwitterionic ciprofloxacin molecules (Turel and Golobic, 2003) thus causing the formation of antibiotic-nanoparticle aggregates. This aggregation effect is evident over the 14 day storage period at 23°C, as the ciprofloxacin-conjugated GNPs show stability for 8 days (T_4) after which colloidal stability is lost.

If citrate-capped GNPs are to be used in medical applications, storage for this time period is suitable, since colloidal stability of the nanoparticles is retained. However, the ciprofloxacin-conjugated GNPs do not remain stable under the same storage conditions. If these nanoparticles are to be stored in health-care facilities and employed in treatment of infection in intravenous form, which requires administration of solutions, the appropriate storage conditions, with the object of retaining colloidal stability and thus biological activity, required further investigation.

5.3.2. Effect of temperature on colloidal stability

The colloidal stability (the dispersion of nanoparticles in solution) over different temperature ranges was measured by observing any changes that may occur in the UV spectrum of the pre-formed GNPs. The citrate-capped and ciprofloxacin-coated GNPs were stored at 4°C, 23°C and 37°C. Ciprofloxacin and ciprofloxacin-conjugated GNPs have distinct and specific peaks on the UV spectrum and any changes in absorbance would be recognized. A widening in peak breadth indicates aggregation of nanoparticles, thus, loss of colloidal stability.

Our results showed that citrate-capped GNPs stored at 4°C showed loss of colloidal stability over 14 days, due to the formation of nanoparticle aggregates (Figure. 13, spectrum C). The nanoparticles stored at 23°C retained colloidal stability over 14 days, whilst those stored at 37°C remained colloidally stable to an even greater degree. In this case, the colloidal stability appears to be directly proportional to an increase in

temperature. The capping agent for these nanoparticles, trisodium citrate, is an ionic compound. Increases in temperature result in improved solubility of these compounds, and vice versa. At a low storage temperature (4°C), solubility would be decreased to the extent that the GNPs coated with trisodium citrate would precipitate out of solution, thus losing their colloidal stability. Ionic bonds are characterized by high melting points. Thus, while the citrate-capped GNPs show good colloidal stability at 23°C and 37°C, at storage temperatures of 50°C and higher, the GNPs would most probably not remain stable in solution.

In contrast, ciprofloxacin-conjugated GNPs stored at 4°C showed the highest degree of colloidal stability, with minimal change in absorbance over time and no broadening of the plasmon resonance peak. Work performed by (Eisenhart and Disso, 2012) has shown that ciprofloxacin and other compounds belonging to the quinolone drug class undergo degradation at higher storage temperatures. A specific temperature range responsible for this effect was found to lie between 32 and 93°C. Thermal degradation of the drug leads to precipitation out of solution, accounting for a similar effect observed in the ciprofloxacin-conjugated GNPs under storage conditions of moderate and high temperatures. In accordance with most storage instructions for the antibiotic, the greatest colloidal stability of ciprofloxacin-conjugated GNPs was observed at 4°C, where minimal denaturation occurred.

This has implications for using these conjugate nanoparticles in treatment of infection, given that the appropriate temperature conditions are needed for maintenance of colloidal stability. In rural areas, where there is no ready access to refrigerated storage areas, the transport and storage of such nanoparticle solutions would be rendered unviable. There would be additional costs involved in installing the appropriate facilities, as well as a decrease in effectiveness of the drug without regular replenishment of supplies. Such treatments are more suitable for employment in established and large-scale hospitals and clinics with ready access to cold storage, the necessary infrastructure and logistics.

This finding corresponds to work done by Wang *et al.* (2009) and Chang *et al.* (2008) where synthesized GNPs were stored at room temperature and found to retain stability. Antibiotic-bound GNPs were found to retain colloidal stability under refrigeration

conditions, as found in our study as well that performed by Mohammed Fayaz *et al.* (2011). Furthermore, Saha *et al.* (2007) demonstrated decreasing stability and bactericidal activity with increase in temperature, of gold nanoparticles conjugated to streptomycin and kanamycin. This correlates to the findings of this study, where the greatest stability of the conjugate nanoparticles was found at the lowest storage temperature tested, 4°C.

5.4. Ultrastructural analysis of citrate-capped and ciprofloxacin-coated GNPs by TEM

Transmission electron microscopy serves as a further means to establish GNP formation, indicating size, distribution and morphology of the GNPs formed. In order for effective drug delivery to occur to bacterial cells and to ensure that there will be adequate attachment of ciprofloxacin molecules to the drug surface, the nanoparticles should ideally be between 10 and 30 nm in size and spherical in shape, as smaller sizes have been shown to have better antibacterial activity (Arshi *et al.*, 2011).

The citrate-capped and ciprofloxacin-conjugated GNPs were all found, from measurements taken, to be between 15 and 30 nm in diameter. This is a direct result of the presence of the citrate salt in solution, which is responsible for influencing the size of the nanoparticles as well as the relative size distribution. Monodispersed GNPs with variations in size from 20 to 40 nm have been produced by altering the pH of the solution, through control of the added proportion of sodium citrate (Zhao *et al.*, 2012). Sodium citrate is, itself, a very weak reducing agent, thus this technique relied on the high temperatures (boiling temperature of 100 °C) and vigorous stirring to generate nanoparticles within this particular size range.

By this means, the formation of citrate-capped and ciprofloxacin-conjugated GNPs were confirmed visually. This monodispersity of GNPs formed is a desired attribute in terms of surface functionalization and subsequent application. The equivalent surface areas of the GNPs allows for greater equilibrium in the ligand exchange reaction, allowing us to better establish protocols for the binding of specific compounds to the nanoparticle surface (Hiramatsu and Osterloh, 2004).

5.5. Spectrophotometric analysis of ciprofloxacin-coated GNPs

In order to investigate bond formation between the functional groups present on the surface of the GNPs and ciprofloxacin, it is necessary to analyze the infra-red (FT-IR) spectrum of the samples. This will indicate whether ciprofloxacin has bound to the surface of the GNPs and between which functional groups this bond has formed.

Previous studies have indicated that neither the keto nor the carboxyl groups present on the ciprofloxacin molecule are involved in binding to the surface of the GNPs. Thus, bond formation with the GNPs occurs through a nitrogen atom, of either the pyridine moiety or the imino group of the piperazinyl moiety. The results of this study show that there is no change in bond formation on the pyridine moiety of the ciprofloxacin molecule. Rather, a change in the N-H bond on the piperazinyl group suggests that this is the region in which bond formation between the ciprofloxacin molecule and the citrate-capped GNPs occurs.

The fluoroquinolone ring of the ciprofloxacin molecule causes delocalization of electrons from the quinolone ring, where the pyridone moiety is situated, decreasing the chances of binding to GNPs in this region. Furthermore, steric hindrance by the cyclopropyl and pyridone groups would obstruct bond formation. The only remaining atom available for bond formation, is the nitrogen atom of the piperazinyl moiety of ciprofloxacin, a conclusion supported by work done by Tom *et al.* (2004).

This result gives us a further demonstration of bonding between the antibiotic, ciprofloxacin and the GNP surface and the functional groups involved in formation of the bond. If future studies are conducted with different species of nanoparticle, the appropriate surface functionalization could be carried out, with the knowledge of which atoms on the antibiotic structure interact with the nanoparticle surface. The nitrogen atom of the piperazinyl moiety of the ciprofloxacin molecule is capable of forming bonds with hydrogen and carbon atoms and metal ions in particular (Drevenšek *et al.*, 2006), allowing for a variety of organic and inorganic carrier molecules to be conjugated to the antibiotic.

5.6. Antimicrobial activity of ciprofloxacin-coated GNPs

Studies have shown that when coupled with laser therapy and bombarded with light at specific frequency, power and fluence, GNPs are able to vibrate at a frequency which raises the temperature of and effectively kills target cells with minimal damage to surrounding healthy tissue. This phenomenon is known as hyperthermal therapy and is generally used in treatment of cancer, however, the selective killing of cells of *S. aureus* has been reported using a similar technique (Khlebtsov *et al.*, 2006). GNPs also have use in photodynamic therapy, where they can be employed as stabilizers of photodynamic drugs which target specific infections (Embleton *et al.*, 2004). However, besides these laser-activated and functionalized forms of therapy, there has been no record of GNPs, particularly the citrate-stabilized species, exerting any antimicrobial effects as a sole agent. All other cases in which antimicrobial activity has been related to the use of GNPs involves these nanoparticles acting as adjuvants to the therapeutic process or as drug delivery vehicles for established antibiotics and other antimicrobial compounds (Huh and Kwon, 2011).

This study clearly shows that the citrate-capped GNPs have no inhibitory effect on bacterial growth of any of the strains tested. This lack of bacterial growth inhibition points to the fact that unlike human cells, in which cytotoxicity from citrate-capped GNPs has been reported, bacterial cells are characterized by the presence of a pronounced cell wall. This applies to both Gram negative and positive species, with variations in composition between the two (Starr *et al.*, 2008). Exposure to citrate-capped GNPs over a prolonged period of time, and in specific doses, as shown in section 2.6.5., would result in an increase in acidity as the citrate molecules eventually detach from the surface of the GNPs and form citric acid upon reaction with water (Freese *et al.*, 2012). This would explain the lack of sensitivity to the presence of citrate-capped GNPs in the case of all bacterial species tested.

The results of this study showed lower MIC's amongst certain bacterial populations treated with conjugated GNPs, as compared to the MIC's of those bacteria treated with ciprofloxacin. This indicates improvement of antimicrobial activity by conjugation of

ciprofloxacin to citrate-capped GNPs against both Gram positive and Gram negative bacterial isolates tested. The citrate-capped GNPs exerted no effect on bacterial growth. Thus, the null hypothesis is rejected (p = 0.0008) and it can be concluded that ciprofloxacin-conjugated gold nanoparticles effectively enhance antimicrobial activity of ciprofloxacin.

Various studies concerned with this particular type of nano-conjugate testing have revealed that equal enhancements of antimicrobial activity against Gram positive and Gram negative bacteria have been effected with GNPs, using a variety of antibiotics, including streptomycin, gentamycin, neomycin (Nirmala Grace and Pandian, 2007; Saha *et al.*, 2007) and ferrous oxide (Huang *et al.*, 2009). This study demonstrates the same patterns of antimicrobial activity amongst the Gram positive and Gram negative strains tested. It can be concluded that the mode of activity of the ciprofloxacin-conjugated GNPs lies not in their specific activity against components of the Gram positive and Gram negative cell wall, but rather, that there is a general and all-encompassing effect. This enhancement reflects the action of the drug itself, a broad spectrum fluoroquinalone, which functions equally well against Gram negative and Gram positive strains of bacteria in nosocomial environments and amongst the community (Class *et al.*, 2002).

It should also be noted that within certain species of bacteria, there are isolates which do not conform to the results obtained for inhibition of growth by ciprofloxacin-conjugated GNPs amongst other isolates of the same species. This can be observed with the isolates *Klebsiella pneumoniae* (S5906), *E. coli* (B3578), *Enterococcus faecalis* (U12318) and *Staphylococcus aureus* (P4256), in which no antimicrobial activity of ciprofloxacin-conjugated GNPs was recorded, along with *E. coli* (U10948) and *E. coli* (U10804), in which the antimicrobial activity of free ciprofloxacin was either greater than or the same as that of the conjugated form of the antibiotic (Table 5). Certain species display resistance to ciprofloxacin, along with the conjugated antibiotic, growing uninhibited in the presence of both substances. This enforces the conclusion that the GNPs themselves merely act as drug carriers, without influencing bacterial resistance to the antibiotic in any way.

Furthermore, within the species tested, where an enhancement of antimicrobial activity was effected by conjugation to GNPs, there were variations in the MIC values obtained for different isolates, as observed in the *Klebsiella pneumoniae* and *Staphylococcus aureus* isolates. This result could be explained by the same phenomenon mentioned above, but in a more specific manner. Within a species, the separate isolates may have lost antibiotic resistance in varying degrees. In simpler terms, certain bacterial cells within each isolate population may have retained the resistance genes, whilst others had not. The proportion of resistant to non-resistant bacterial cells would vary drastically within each isolate population, thus accounting for this phenomenon.

5.7. Determining the effect of ciprofloxacin conjugated GNPs on bacterial growth by TEM

The precise mechanism by which GNPs exert their enhancement of antimicrobial activity of ciprofloxacin is clearly indicated in the micrographs obtained. Both the GNPs and ciprofloxacin-conjugated GNPs appear to aggregate at the bacterial cell wall surface, as indicated by the arrows in the diagram. The high density and conductive capabilities of the GNPs, normally make them an excellent contrast agent for diagnosis of cancer (Sperling *et al.*, 2008) serves the same function in this case. The GNPs appear darker in comparison to the bacterial cell components, thus allowing for clear visualization of their position relative to the cell.

As mentioned previously, the antimicrobial enhancement effected by the conjugated GNPs does not appear to be specific to the classification of the bacterial cells (that is, Gram negative or positive). The conjugated GNPs and citrate-capped GNPs adhere to the cell surface non-specifically. In the case of the citrate-capped GNPs, even though aggregation at the cell wall occurs, no antimicrobial effect is observed, as the increase in acidity resulting from the release of citrate over time is too negligible to have a drastic effect on bacterial growth. In the case of the ciprofloxacin-conjugated GNPs, however, the clustering behaviour of the nanoparticles serves to concentrate the antibiotic (ciprofloxacin) at the surface of the cell, increasing the number of molecules of ciprofloxacin available to the cell by an exponential degree. This is due to the large collective surface area of the GNPs, directly impacting on the total number of molecules that can bind to their surface (Sperling *et al.*, 2008).

The adherence of both the citrate-capped and ciprofloxacin-ligated GNPs to the cell walls of bacteria, irrespective of whether Gram negative or positive, appears to be charge related. The use of sodium citrate as a capping and stabilizing agent for GNPs results in the formation of cationic (positively charged) nanoparticles, which are thus attracted to the negatively charged cell walls of the bacteria. The negative charges on bacterial cell walls arise due to the negative charges of the phosphate groups comprising the phospholipids, a major component of the cell wall (Costerton and Cheng, 1975) as indicated (Figure 32).

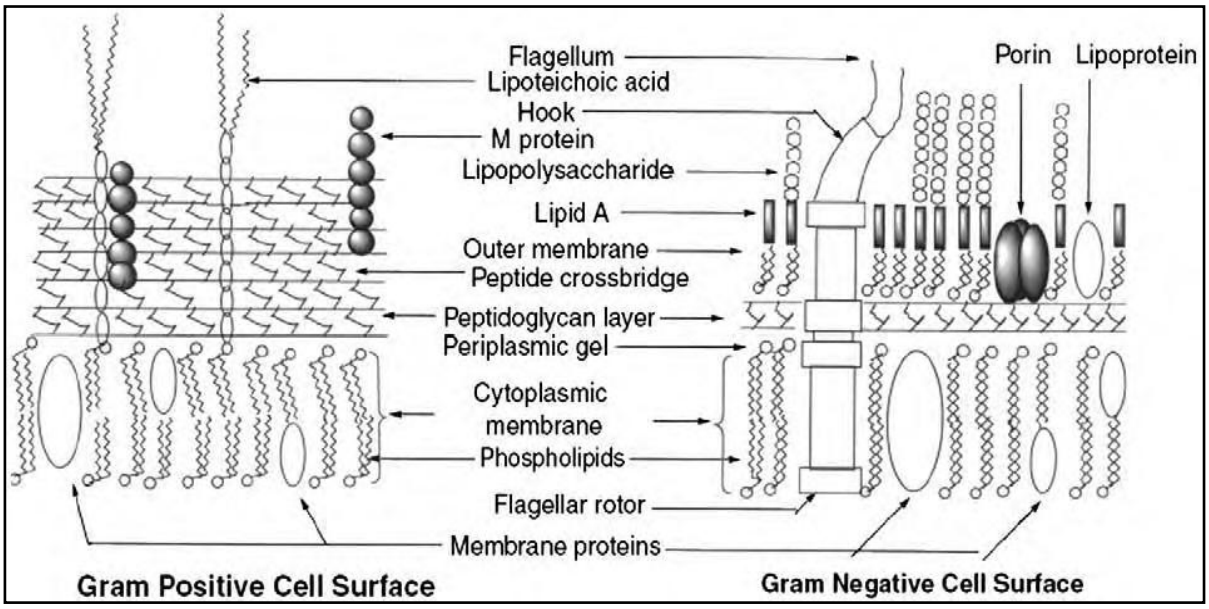

Figure 32: Diagram of structural components of Gram positive and Gram negative cell wall with phospholipid layers indicated.

An interesting phenomenon was observed in the case of *Klebsiella pneumoniae* (P3967) treated with ciprofloxacin-conjugated GNPs. With reference to Figure 33, it can be observed that an extracellular polymer has formed on the surface of the cell. The conjugated GNPs have attached to both the bacterial cell and this compound. We hypothesize that the compound produced by the *Klebsiella pneumoniae* bacterial cell may be exo-polysaccharide (EPS), in combination with other elements of biofilms. The presence of ciprofloxacin may contribute to the bacteria producing this biofilm element, as a form of resistance. In many cases, antibiotic agents are retarded in their motion and diffusion through the cell membrane, thus allowing the bacteria to remain unharmed. Some antibiotics are de-activated within the biofilm matrix, while others are able to

diffuse through freely (Stewart and William Costerton, 2001). As shown in Figure 33, the ciprofloxacin-conjugated GNPs attach to the EPS on the bacterial surface. However, the growth of the bacteria is still inhibited to a great degree, in comparison to free ciprofloxacin. Thus the GNPs still act as effective drug carriers, despite the presence of the biofilm components and EPS formation.

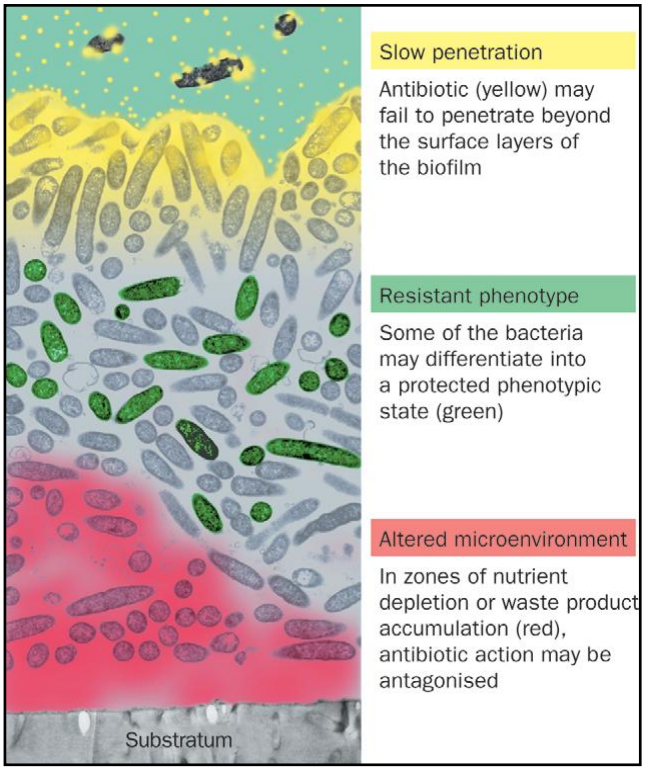

Figure 33: Illustration showing three hypotheses for the mechanisms of antimicrobial action in biofilms. The aqueous phase of the surrounding environment is represented at the top, whilst the attachment surface for the bacterial cells appears at the bottom (Stewart and William Costerton, 2001).

In this study, this defense response and production of EPS to immobilize the GNPs on the surface of *Klebsiella pneumoniae* cell is further exacerbated by the presence of ciprofloxacin. The enhancement of inhibition of bacterial growth in the presence of the ciprofloxacin-conjugated GNPs for this species is a clear indication that the nanoparticles are able to overcome this resistance mechanism to an extent. This has great implications for the use of GNP-antibiotic conjugates for combating bacterial resistance caused by biofilm formation.

This has significant implications for the incorporation of antibiotic conjugated GNPs into wound dressings, as biofilms are a major obstacle to clean healing and disinfection in cases of open wounds. Pressure ulcers located on the leg and foot were found to be particularly susceptible to biofilm formation in hospital environments and often lead to the need for amputation due to inability to overcome such infections through regular treatments and drugs (Hetrick *et al.*, 2009). The killing of bacterial cells in a biofilm may also require up to a 1000 fold increase in drug concentration in comparison to the dosage required to kill bacterial cells in regular culture suspension (Smith, 2005). As the results of this study show that the GNPs serve to concentrate the dose of antibiotic available to the bacterial cells, this mode of action could present an additional benefit when treating infections caused by biofilms.

5.8. Anti-cancer activity of citrate-capped GNPs

The citrate-capped GNPs showed anti-cancer activity against the Caco-2 cell line at all concentrations tested. However, due to variance of results within concentrations tested, comparisons between the cytotoxic activity of citrate-capped GNPs and gemcitabine, at all concentrations besides 0.5 mM, was rendered unviable. At a concentration of 0.5 mM, a comparable equivalence was shown to that of the chemotherapeutic compound, gemcitabine at Research by Malugin and Ghandehari (2010) has shown that plain gold, spherical nanoparticles have no effect on growth of the human prostate cancer cell line, PC-3. Our study shows death of Caco-2 cells, which may be due the functionalization of the GNP surface.

The citrate capping of the GNPs lead to cell death of the Caco-2 cells. This effect is due to the citrate capping agent dissolving in the aqueous component of the growth medium, thus decreasing the pH and creating an environment acidic enough to ensure cell death (Freese *et al.*, 2012). This anti-cancer effect is a constant feature through all concentrations tested. At a concentration of 0.5 mM, the anti-cancer effect on the Caco-2 cells is very similar and slightly greater than that exerted by gemcitabine ($p = 0.04$). Functioning in the absence of any anti-cancer compound, this study showed that the citrate-capped GNPs acted as anti-cancer agents against the Caco-2 cells. Microscopic observation of the treated Caco-2 cells showed loss of cellular contents and granulation.

This effect is consistent with studies performed by Moore *et al.* (1955) and Gerweck (1977).

Thus, citrate-capped GNPs have potential application for cancer treatment. Chemotherapeutic compounds employed in cancer treatment on a general basis have a number of detrimental side-effects that greatly impact on the patient's quality of life (Burstein, 2000). Introducing means by which cancer can be effectively treated with avoidance of side effects is a highly desirable research goal. The results obtained show potential for such treatment with citrate-capped GNPs. It must be taken into account, however, that further studies need to be conducted in order to verify a more specific effect on cancer cells, with minimal damage to surrounding healthy tissue. Biocompatibility of any novel treatment technique needs to be extensively investigated before integration into mainstream therapy.

6. CONCLUSIONS AND FUTURE WORK

In this study, the formation of citrate-capped GNPs was confirmed by identifying their characteristic surface plasmon resonance on the UV visible spectrum. These nanoparticles were found to be colloidally stable over a storage period of two weeks, with a storage temperature of 37°C being the most favourable in terms of retaining this stability. This optimum storage temperature is greatly significant, as these nanoparticles would remain stable when used in human clinical trials for cancer treatment. The formation of antibiotic-conjugated GNPs, identified by the shift in plasmon resonance caused by binding to ciprofloxacin, was also confirmed. These nanoparticles were found to have the greatest degree of colloidal stability at 4°C, losing this stability when stored at higher temperatures. This is in accordance with storage instructions of ciprofloxacin suspensions used for medical treatment.

Ultra structural observations of the citrate-capped GNPs showed an even size distribution (between 15 and 30 nm) and a predominance of spherical nanoparticles. Further observation of the ciprofloxacin-conjugated GNPs showed an aggregation phenomenon which is reflected in the plasmon resonance maxima. Spectrophotometrical analysis of the ciprofloxacin-conjugated GNPs indicated that chemical bonding most likely occurs between the piperazinyl moiety of ciprofloxacin and the citrate-capped GNP surfaces.

Ciprofloxacin-conjugated GNPs were shown to have greater antimicrobial effect on certain pathogens tested, in comparison to free ciprofloxacin. Species against which this enhanced effect was observed included *S. aureus*, *Klebsiella pneumoniae*, *Pseudomonas* spp., *Enterobacter* spp. and *Enterococcus faecalis*. From these results, the conjugate nanoparticles were found to be equally effective against Gram positive and Gram negative bacteria. Looking further into the mechanism of this antimicrobial enhancement, the nanoparticles effectively concentrate the ciprofloxacin at the surface of the bacterial cell wall. Due to the large collective surface area of the nanoparticles and the bound ciprofloxacin on their surface, they would serve to supply a higher concentration of the antibiotic to the bacterial cell, as opposed to exposure to free ciprofloxacin. TEM results show this concentration effect at the surface of the bacterial

cell. Thus, the ciprofloxacin-conjugated GNPs were found to be a highly effective drug delivery vehicle for the antibiotic ciprofloxacin to selected bacterial pathogens.

In summary, citrate-capped GNPs can be easily synthesized and stabilized by the citrate reduction technique and their physical and chemical properties characterized by TEM and FTIR. These nanoparticles are spherical, have diameters ranging in size between 15 and 30 nm, their size advantageous to drug delivery applications due to their monodispersity and even distribution of the delivered molecule. These nanoparticles can be conjugated to the antibiotic, ciprofloxacin. Ciprofloxacin-conjugated GNPs show improved antibiotic activity in comparison to ciprofloxacin.

The significance of our results regarding the conjugation of ciprofloxacin to GNPs is the enhancement of the antibacterial activity of ciprofloxacin. This increase in activity is due to the concentration of ciprofloxacin at the bacterial cell wall caused by the ionic interaction between the nanoparticles and the bacterial cell wall. This phenomena could be the basis of using nanoparticle conjugated antibiotics incorporated into wound dressings, for example, in leg and foot ulcers where biofilms develop and are resistant to disinfection, hence requiring a higher concentration of antibiotic at the site of infection.

The MTT assay showed that the citrate capped GNPs had a cytotoxic effect on colorectal cancer cells (Caco-2 cells). This implies that citrate capped GNP may be able to kill cancer cells. However, this would require further research into the mechanism of the cell death by apoptotic studies.

Ciprofloxacin conjugated GNP improve the antibacterial activity of ciprofloxacin against both Gram positive and Gram negative bacteria. With regard to the differential activity of ciprofloxacin conjugated GNPs against Gram positive and Gram negative bacteria, a greater number and variety of bacterial species, including a higher number of drug resistant species, would have to be tested. The work described in this thesis covers the effect of the conjugate GNPs on common pathogens encountered in most environments and nosocomial settings. In order to determine the anti-cancer potential to a greater degree, a variety of cancer cell lines should be tested and the precise mechanism of anti-cancer effect determined by apoptotic studies.

Future studies in this research area would span the conjugation of different antibiotics to the surface of gold nanoparticles. Antibiotics which are currently used in hospitals with greater impact on drug resistant strains of bacteria, such as fluoroquinalones (the family of drug to which ciprofloxacin and other broad spectrum antibiotics belong) as well as aminoglycosides, could be ligated to varying sizes of gold nanoparticles and their antimicrobial activity determined. Depending on the chemical composition and structure of these drugs, surface functionalization of the gold nanoparticles may be required in order to provide the suitable ligands for specific attachment of the antibiotics. It is also essential that focus be placed on determining the mechanism of antimicrobial activity (or enhancement of antimicrobial activity, if present) in order to gain better insight into how nanomaterials can be engineered to possess certain desirable properties for such application.

As is the case of research into any biomedical application, the relative biocompatibility of the materials tested is an important determinant of applicability in treatment programmes. Cytotoxic evaluation of any newly developed or adapted nanoparticles is therefore a requirement in view of the potential risks. Further research into such possible effects would have to be conducted in order to eliminate the possibility of undesirable long term side effects, with the aim of eventually establishing a protocol for testing of nanomaterials in biomedical applications.

Our studies show that gold nanoparticles enhance the delivery of ciprofloxacin to bacterial cells thus increasing the antibiotic effectiveness. Citrate capped GNPs can also have cytotoxic activity against colon cancer cells.

7. REFERENCES

AL-BAYATI, F. A. 2009. Isolation and identification of antimicrobial compound from Mentha longifolia L. leaves grown wild in Iraq. *Annals of clinical microbiology and antimicrobials,* 8**,** 20.

ALANAZI, F. K., RADWAN, A. A. & ALSARRA, I. A. 2010. Biopharmaceutical applications of nanogold. *Saudi Pharmaceutical Journal,* 18**,** 179-193.

ALBRECHT-BUEHLER, G. 1979. The angular distribution of directional changes of guided 3T3 cells. *The Journal of cell biology,* 80**,** 53-60.

ALI, S. H. 2004. A socio-ecological autopsy of the *E. coli* O157: H7 outbreak in Walkerton, Ontario, Canada. *Social science & medicine,* 58**,** 2601-2612.

ALLAKER, R. P. & REN, G. 2008. Potential impact of nanotechnology on the control of infectious diseases. *Transactions of the Royal Society of Tropical Medicine and Hygiene,* 102**,** 1-2.

ANACONA, J. R. & TOLEDO, C. 2001. Synthesis and antibacterial activity of metal complexes of ciprofloxacin. *Transition Metal Chemistry,* 26**,** 228-231.

ARSHI, N., AHMED, F., KUMAR, S., ANWAR, M., LU, J., KOO, B. H. & LEE, C. G. 2011. Microwave assisted synthesis of gold nanoparticles and their antibacterial activity against *Escherichia coli* (*E. coli*). *Current Applied Physics,* 11**,** S360-S363.

BACH, L. G., ISLAM, M. R., JEONG, Y. T., GAL, Y. S. & LIM, K. T. 2012. Synthesis and characterization of chemically anchored adenosine with PHEMA grafted gold nanoparticles. *Applied Surface Science,* 258**,** 2816-2822.

BASTÚS, N. G., SÁNCHEZ-TILLÓ, E., PUJALS, S., FARRERA, C., KOGAN, M. J., GIRALT, E., CELADA, A., LLOBERAS, J. & PUNTES, V. 2009. Peptides conjugated to gold nanoparticles induce macrophage activation. *Molecular immunology,* 46**,** 743-748.

BLECHER, K., NASIR, A. & FRIEDMAN, A. 2011. The growing role of nanotechnology in combating infectious disease. *Virulence,* 2**,** 395-401.

BOLLA, J.-M., ALIBERT-FRANCO, S., HANDZLIK, J., CHEVALIER, J., MAHAMOUD, A., BOYER, G., KIEĆ-KONONOWICZ, K. & PAGÈS, J.-M. 2011. Strategies for bypassing the membrane barrier in multidrug resistant Gram-negative bacteria. *FEBS letters,* 585**,** 1682-1690.

BOUCHER, H. W., TALBOT, G. H., BRADLEY, J. S., EDWARDS, J. E., GILBERT, D., RICE, L. B., SCHELD, M., SPELLBERG, B. & BARTLETT, J. 2009. Bad bugs, no drugs: no ESKAPE! An update from the Infectious Diseases Society of America. *Clinical Infectious Diseases,* 48**,** 1-12.

BOZDOGAN, B., ESEL, D., WHITENER, C., BROWNE, F. A. & APPELBAUM, P. C. 2003. Antibacterial susceptibility of a vancomycin-resistant *Staphylococcus aureus* strain isolated at the Hershey Medical Center. *Journal of Antimicrobial Chemotherapy,* 52**,** 864-868.

BROWN, A. N., SMITH, K., SAMUELS, T. A., LU, J., OBARE, S. O. & SCOTT, M. E. 2012. Nanoparticles Functionalized with Ampicillin Destroy Multiple-Antibiotic-Resistant Isolates of *Pseudomonas aeruginosa* and *Enterobacter aerogenes* and Methicillin-Resistant *Staphylococcus aureus*. *Applied and environmental microbiology,* 78**,** 2768-2774.

BUNDRICK, W., HERON, S. P., RAY, P., SCHIFF, W. M., TENNENBERG, A. M., WIESINGER, B. A., WRIGHT, P. A., WU, S.-C., ZADEIKIS, N. & KAHN, J. B. 2003. Levofloxacin versus ciprofloxacin in the treatment of chronic bacterial prostatitis: a randomized double-blind multicenter study. *Urology,* 62**,** 537-541.

BURSTEIN, H. J. 2000. Side effects of chemotherapy. *Journal of Clinical Oncology,* 18**,** 693-693.

BURYGIN, G., KHLEBTSOV, B., SHANTROKHA, A., DYKMAN, L., BOGATYREV, V. & KHLEBTSOV, N. 2009. On the enhanced antibacterial activity of antibiotics mixed with gold nanoparticles. *Nanoscale research letters,* 4**,** 794-801.

BUSBEE, B. D., OBARE, S. O. & MURPHY, C. J. 2003. An Improved Synthesis of High-Aspect-Ratio Gold Nanorods. *Advanced Materials,* 15**,** 414-416.

BYRNE, J. D., BETANCOURT, T. & BRANNON-PEPPAS, L. 2008. Active targeting schemes for nanoparticle systems in cancer therapeutics. *Advanced drug delivery reviews,* 60**,** 1615-1626.

CADEMARTIRI, L. & OZIN, G. A. 2009. *Concepts of nanochemistry*, Wiley-VCH.

CAI, W., GAO, T., HONG, H. & SUN, J. 2008. Applications of gold nanoparticles in cancer nanotechnology. *Nanotechnol Sci Appl,* 1**,** 17-32.

CAWTHORN, D.-M., BOTHA, S. & WITTHUHN, R. C. 2008. Evaluation of different methods for the detection and identification of *Enterobacter sakazakii* isolated from South African infant formula milks and the processing environment. *International journal of food microbiology,* 127**,** 129-138.

CHAMUNDEESWARI, M., SOBHANA, S., JACOB, J. P., KUMAR, M. G., DEVI, M. P., SASTRY, T. P. & MANDAL, A. B. 2010. Preparation, characterization and evaluation of a biopolymeric gold nanocomposite with antimicrobial activity. *Biotechnology and applied biochemistry,* 55**,** 29-35.

CHANG, M. Y., SHIAU, A. L., CHEN, Y. H., CHANG, C. J., CHEN, H. H. W. & WU, C. L. 2008. Increased apoptotic potential and dose-enhancing effect of gold nanoparticles in combination with single-dose clinical electron beams on tumor-bearing mice. *Cancer science,* 99**,** 1479-1484.

CHEN, H., KOU, X., YANG, Z., NI, W. & WANG, J. 2008. Shape-and size-dependent refractive index sensitivity of gold nanoparticles. *Langmuir,* 24**,** 5233-5237.

CHEN, J., YANG, M., ZHANG, Q., CHO, E. C., COBLEY, C. M., KIM, C., GLAUS, C., WANG, L. V., WELCH, M. J. & XIA, Y. 2010. Gold nanocages: a novel class of multifunctional nanomaterials for theranostic applications. *Advanced Functional Materials,* 20**,** 3684-3694.

CLASS, I., CIPROFLOXACIN, O. F., SPARFLOXACIN, L. L. & MOXIFLOXACIN, G. T. 2002. Quinolones: a comprehensive review. *Am Fam Physician,* 65**,** 455-465.

COHEN, M. L. 2000. Changing patterns of infectious disease. *Nature,* 406**,** 762-767.

COSTERTON, J. & CHENG, K.-J. 1975. The role of the bacterial cell envelope in antibiotic resistance. *Journal of Antimicrobial Chemotherapy,* 1**,** 363-377.

COUVREUR, P. & VAUTHIER, C. 2006. Nanotechnology: intelligent design to treat complex disease. *Pharmaceutical research,* 23**,** 1417-1450.

CUI, Y., ZHAO, Y., TIAN, Y., ZHANG, W., LÜ, X. & JIANG, X. 2012. The molecular mechanism of action of bactericidal gold nanoparticles on *Escherichia coli*. *Biomaterials,* 33**,** 2327-2333.

CUNNINGHAM, D., HUMBLET, Y., SIENA, S., KHAYAT, D., BLEIBERG, H., SANTORO, A., BETS, D., MUESER, M., HARSTRICK, A. & VERSLYPE, C. 2004. Cetuximab monotherapy and cetuximab plus irinotecan in irinotecan-refractory metastatic colorectal cancer. *New England Journal of Medicine,* 351**,** 337-345.

DASTJERDI, R. & MONTAZER, M. 2010. A review on the application of inorganic nano-structured materials in the modification of textiles: focus on anti-microbial properties. *Colloids and Surfaces B: Biointerfaces,* 79**,** 5-18.

DE LA ESCOSURA-MUÑIZ, A. & MERKOÇI, A. 2011. A Nanochannel/Nanoparticle-Based Filtering and Sensing Platform for Direct Detection of a Cancer Biomarker in Blood. *Small,* 7**,** 675-682.

DEMERS, L. M., MIRKIN, C. A., MUCIC, R. C., REYNOLDS, R. A., LETSINGER, R. L., ELGHANIAN, R. & VISWANADHAM, G. 2000. A fluorescence-based method for determining the surface coverage and hybridization efficiency of thiol-capped oligonucleotides bound to gold thin films and nanoparticles. *Analytical Chemistry,* 72**,** 5535-5541.

DILLEN, K., VANDERVOORT, J., VAN DEN MOOTER, G., VERHEYDEN, L. & LUDWIG, A. 2004. Factorial design, physicochemical characterisation and activity of ciprofloxacin-PLGA nanoparticles. *International journal of pharmaceutics,* 275**,** 171-187.

DREVENŠEK, P., ULRIH, N. P., MAJERLE, A. & TUREL, I. 2006. Synthesis, characterization and DNA binding of magnesium–ciprofloxacin (cfH) complex [Mg $(cf)_2]\cdot$ 2.5 H_2O. *Journal of inorganic biochemistry,* 100**,** 1705-1713.

EISENHART, A. E. & DISSO, N. M. 2012. Thermostability Determination of Antibiotics at High Temperatures by Liquid Chromatography-Mass Spectrometry. *2012 NCUR.*

EL-SAYED, I. H., HUANG, X. & EL-SAYED, M. A. 2005. Surface plasmon resonance scattering and absorption of anti-EGFR antibody conjugated gold nanoparticles in cancer diagnostics: applications in oral cancer. *Nano letters,* 5**,** 829-834.

EMBLETON, M. L., NAIR, S. P., COOKSON, B. D. & WILSON, M. 2004. Antibody-directed photodynamic therapy of methicillinresistant *Staphylococcus aureus*. *Microbial Drug Resistance,* 10**,** 92-97.

ENZENSBERGER, R., SHAH, P. & KNOTHE, H. 1985. Impact of Oral Ciprofloxacin on the. *Infection,* 13.

FARAJI, A. H. & WIPF, P. 2009. Nanoparticles in cellular drug delivery. *Bioorganic & medicinal chemistry,* 17**,** 2950-2962.

FASS, R. 1987. Efficacy and safety of oral ciprofloxacin in the treatment of serious respiratory infections. *The American journal of medicine,* 82**,** 202.

FAWAZ, F., BONINI, F., MAUGEIN, J. & LAGUENY, A. 1998. Ciprofloxacin-loaded polyisobutylcyanoacrylate nanoparticles: pharmacokinetics and in vitro antimicrobial activity. *International journal of pharmaceutics,* 168**,** 255-259.

FAYAZ, A. M., BALAJI, K., GIRILAL, M., YADAV, R., KALAICHELVAN, P. T. & VENKETESAN, R. 2010. Biogenic synthesis of silver nanoparticles and their synergistic effect with antibiotics: a study against gram-positive and gram-negative bacteria. *Nanomedicine,* 6**,** e103.

FORTINA, P., KRICKA, L. J., GRAVES, D. J., PARK, J., HYSLOP, T., TAM, F., HALAS, N., SURREY, S. & WALDMAN, S. A. 2007. Applications of nanoparticles to diagnostics and therapeutics in colorectal cancer. *Trends in biotechnology,* 25**,** 145-152.

FRANGIONI, J. V. 2003. *In vivo* near-infrared fluorescence imaging. *Current opinion in chemical biology,* 7**,** 626-634.

FREESE, C., UBOLDI, C., GIBSON, M. I., UNGER, R. E., WEKSLER, B. B., ROMERO, I. A., COURAUD, P.-O. & KIRKPATRICK, C. J. 2012. Uptake and cytotoxicity of citrate-coated gold nanospheres: Comparative studies on human endothelial and epithelial cells. *Particle and Fibre Toxicology,* 9**,** 1-11.

FREIRE-MORAN, L., ARONSSON, B., MANZ, C., GYSSENS, I. C., SO, A. D., MONNET, D. L. & CARS, O. 2011. Critical shortage of new antibiotics in development against multidrug-resistant bacteria—time to react is now. *Drug resistance updates,* 14**,** 118-124.

FRENS, G. 1973. Controlled nucleation for the regulation of the particle size in monodisperse gold suspensions. *Nature,* 241**,** 20-22.

GERWECK, L. E. 1977. Modification of cell lethality at elevated temperatures the pH effect. *Radiation Research,* 70**,** 224-235.

GHOSH, P., HAN, G., DE, M., KIM, C. K. & ROTELLO, V. M. 2008. Gold nanoparticles in delivery applications. *Advanced drug delivery reviews,* 60**,** 1307-1315.

GINDY, M. E. & PRUD'HOMME, R. K. 2009. Multifunctional nanoparticles for imaging, delivery and targeting in cancer therapy.

GOODMAN, C. M., MCCUSKER, C. D., YILMAZ, T. & ROTELLO, V. M. 2004. Toxicity of gold nanoparticles functionalized with cationic and anionic side chains. *Bioconjugate chemistry,* 15**,** 897-900.

GOVOROV, A. O., ZHANG, W., SKEINI, T., RICHARDSON, H., LEE, J. & KOTOV, N. A. 2006. Gold nanoparticle ensembles as heaters and actuators: melting and collective plasmon resonances. *Nanoscale Research Letters,* 1**,** 84-90.

GULLOTTI, E. & YEO, Y. 2009. Extracellularly activated nanocarriers: a new paradigm of tumor targeted drug delivery. *Molecular pharmaceutics,* 6**,** 1041-1051.

HAMOUDA, T., HAYES, M. M., CAO, Z., TONDA, R., JOHNSON, K., WRIGHT, D. C., BRISKER, J. & BAKER, J. R. 1999. A novel surfactant nanoemulsion with broad-spectrum sporicidal activity against Bacillus species. *Journal of Infectious Diseases,* 180**,** 1939-1949.

HAYAT, M. A. 1989. Colloidal gold. Principles, methods, and applications. *San Diego, etc,* 2.

HEATH, J. R. & DAVIS, M. E. 2008. Nanotechnology and cancer. *Annu. Rev. Med.,* 59**,** 251-265.

HETRICK, E. M., SHIN, J. H., PAUL, H. S. & SCHOENFISCH, M. H. 2009. Anti-biofilm efficacy of nitric oxide-releasing silica nanoparticles. *Biomaterials,* 30**,** 2782-2789.

HIRAMATSU, H. & OSTERLOH, F. E. 2004. A simple large-scale synthesis of nearly monodisperse gold and silver nanoparticles with adjustable sizes and with exchangeable surfactants. *Chemistry of materials,* 16**,** 2509-2511.

HIRSCH, L. R., STAFFORD, R., BANKSON, J., SERSHEN, S., RIVERA, B., PRICE, R., HAZLE, J., HALAS, N. & WEST, J. 2003. Nanoshell-mediated near-infrared thermal therapy of tumors under magnetic resonance guidance. *Proceedings of the National Academy of Sciences,* 100**,** 13549-13554.

HUANG, W. C., TSAI, P. J. & CHEN, Y. C. 2009. Multifunctional Fe3O4@ Au Nanoeggs as Photothermal Agents for Selective Killing of Nosocomial and Antibiotic-Resistant Bacteria. *Small,* 5**,** 51-56.

HUANG, Z., ZHENG, X., YAN, D., YIN, G., LIAO, X., KANG, Y., YAO, Y., HUANG, D. & HAO, B. 2008. Toxicological effect of ZnO nanoparticles based on bacteria. *Langmuir,* 24**,** 4140-4144.

HUFF, T. B., TONG, L., ZHAO, Y., HANSEN, M. N., CHENG, J.-X. & WEI, A. 2007. Hyperthermic effects of gold nanorods on tumor cells. *Nanomedicine,* 2**,** 125-132.

HUH, A. J. & KWON, Y. J. 2011. "Nanoantibiotics": A new paradigm for treating infectious diseases using nanomaterials in the antibiotics resistant era. *Journal of Controlled Release,* 156**,** 128-145.

JAHNEN-DECHENT, W. & SIMON, U. 2008. Function follows form: shape complementarity and nanoparticle toxicity. *Nanomedicine (London, England),* 3**,** 601.

JAIN, K. K. 2005. The role of nanobiotechnology in drug discovery. *Drug discovery today,* 10**,** 1435-1442.

JANA, N. R., GEARHEART, L. & MURPHY, C. J. 2001. Seed-mediated growth approach for shape-controlled synthesis of spheroidal and rod-like gold nanoparticles using a surfactant template. *Advanced Materials,* 13**,** 1389.

JIANG, Z.-H. & KOGANTY, R. 2003. Synthetic vaccines: the role of adjuvants in immune targeting. *Current medicinal chemistry,* 10**,** 1423-1439.

JOHNSTON, H. J., HUTCHISON, G., CHRISTENSEN, F. M., PETERS, S., HANKIN, S. & STONE, V. 2010. A review of the in vivo and in vitro toxicity of silver and gold particulates: particle attributes and biological mechanisms responsible for the observed toxicity. *Critical reviews in toxicology,* 40**,** 328-346.

KANG, S., PINAULT, M., PFEFFERLE, L. D. & ELIMELECH, M. 2007. Single-walled carbon nanotubes exhibit strong antimicrobial activity. *Langmuir,* 23**,** 8670-8673.

KELLY, K. A. & JONES, D. A. 2003. Isolation of a colon tumor specific binding peptide using phage display selection. *Neoplasia (New York, NY),* 5**,** 437.

KEREN, S., ZAVALETA, C., CHENG, Z., DE LA ZERDA, A., GHEYSENS, O. & GAMBHIR, S. 2008. Noninvasive molecular imaging of small living subjects using Raman spectroscopy. *Proceedings of the National Academy of Sciences,* 105**,** 5844-5849.

KEYNAN, Y. & RUBINSTEIN, E. 2007. The changing face of *Klebsiella pneumoniae* infections in the community. *International journal of antimicrobial agents,* 30**,** 385-389.

KHLEBTSOV, B., ZHAROV, V., MELNIKOV, A., TUCHIN, V. & KHLEBTSOV, N. 2006. Optical amplification of photothermal therapy with gold nanoparticles and nanoclusters. *Nanotechnology,* 17**,** 5167.

KIM, D.-J. & KIM, K.-S. 2011. Controlled synthesis and biomolecular probe application of gold nanoparticles. *Micron,* 42**,** 207-227.

KIMLING, J., MAIER, M., OKENVE, B., KOTAIDIS, V., BALLOT, H. & PLECH, A. 2006. Turkevich method for gold nanoparticle synthesis revisited. *The Journal of Physical Chemistry B,* 110**,** 15700-15707.

KLASEN, H. 2000. Historical review of the use of silver in the treatment of burns. I. Early uses. *Burns,* 26**,** 117-130.

KREUTER, J. 1995. Nanoparticles as adjuvants for vaccines. *Vaccine Design.* Springer.

KUMAR, S., HARRISON, N., RICHARDS-KORTUM, R. & SOKOLOV, K. 2007. Plasmonic nanosensors for imaging intracellular biomarkers in live cells. *Nano letters,* 7**,** 1338-1343.

KUMAR, S. A., CHANG, Y.-T., WANG, S.-F. & LU, H.-C. 2010. Synthetic antibacterial agent assisted synthesis of gold nanoparticles: Characterization and application studies. *Journal of Physics and Chemistry of Solids,* 71**,** 1484-1490.

LEVY, S. B. 2005. Antibiotic resistance—the problem intensifies. *Advanced drug delivery reviews,* 57**,** 1446-1450.

LI, Q., MAHENDRA, S., LYON, D. Y., BRUNET, L., LIGA, M. V., LI, D. & ALVAREZ, P. J. 2008. Antimicrobial nanomaterials for water disinfection and microbial control: potential applications and implications. *water research,* 42**,** 4591-4602.

LIU, Y., HE, L., MUSTAPHA, A., LI, H., HU, Z. & LIN, M. 2009. Antibacterial activities of zinc oxide nanoparticles against *Escherichia coli* O157: H7. *Journal of Applied Microbiology,* 107**,** 1193-1201.

LIVERMORE, D. M. 2003. Bacterial resistance: origins, epidemiology, and impact. *Clinical Infectious Diseases,* 36**,** S11-S23.

LOOK, M., BANDYOPADHYAY, A., BLUM, J. S. & FAHMY, T. M. 2010. Application of nanotechnologies for improved immune response against infectious diseases in the developing world. *Advanced drug delivery reviews,* 62**,** 378-393.

LYON, D. Y., FORTNER, J. D., SAYES, C. M., COLVIN, V. L. & HUGHES, J. B. 2005. Bacterial cell association and antimicrobial activity of a C60 water suspension. *Environmental toxicology and chemistry,* 24**,** 2757-2762.

MAEDA, H., WU, J., SAWA, T., MATSUMURA, Y. & HORI, K. 2000. Tumor vascular permeability and the EPR effect in macromolecular therapeutics: a review. *Journal of Controlled Release,* 65**,** 271-284.

MALUGIN, A. & GHANDEHARI, H. 2010. Cellular uptake and toxicity of gold nanoparticles in prostate cancer cells: a comparative study of rods and spheres. *Journal of Applied Toxicology,* 30**,** 212-217.

MANESS, P.-C., SMOLINSKI, S., BLAKE, D. M., HUANG, Z., WOLFRUM, E. J. & JACOBY, W. A. 1999. Bactericidal activity of photocatalytic TiO_2 reaction: toward an understanding of its killing mechanism. *Applied and environmental microbiology,* 65**,** 4094-4098.

MANI, G., JOHNSON, D. M., MARTON, D., FELDMAN, M. D., PATEL, D., AYON, A. A. & AGRAWAL, C. 2008. Drug delivery from gold and titanium surfaces using self-assembled monolayers. *Biomaterials,* 29**,** 4561-4573.

MEDINA, C., SANTOS-MARTINEZ, M., RADOMSKI, A., CORRIGAN, O. & RADOMSKI, M. 2007. Nanoparticles: pharmacological and toxicological significance. *British journal of pharmacology,* 150**,** 552-558.

MICHAEL, Y. S., XU, H., PENN, S. G. & CROMER, R. 2007. SERS nanoparticles: a new optical detection modality for cancer diagnosis. *Nanomedicine,* 2**,** 725-734.

MISHRA, B., PATEL, B. B. & TIWARI, S. 2010. Colloidal nanocarriers: a review on formulation technology, types and applications toward targeted drug delivery. *Nanomedicine: Nanotechnology, biology and medicine,* 6**,** 9-24.

MOGHIMI, S. M., HUNTER, A. C. & MURRAY, J. C. 2005. Nanomedicine: current status and future prospects. *The FASEB Journal,* 19**,** 311-330.

MOHAMMED FAYAZ, A., GIRILAL, M., VENKATESAN, R. & KALAICHELVAN, P. 2011. Biosynthesis of anisotropic gold nanoparticles using *Maduca longifolia* extract and their potential in infrared absorption. *Colloids and Surfaces B: Biointerfaces,* 88**,** 287-291.

MOORE, A. E., SABACHEWSKY, L. & TOOLAN, H. W. 1955. Culture characteristics of four permanent lines of human cancer cells. *Cancer Research,* 15**,** 598-602.

MOSMANN, T. 1983. Rapid colorimetric assay for cellular growth and survival: application to proliferation and cytotoxicity assays. *Journal of immunological methods,* 65**,** 55-63.

MUDSHINGE, S. R., DEORE, A. B., PATIL, S. & BHALGAT, C. M. 2011. Nanoparticles: emerging carriers for drug delivery. *Saudi Pharmaceutical Journal,* 19**,** 129-141.

NIRMALA GRACE, A. & PANDIAN, K. 2007. Antibacterial efficacy of aminoglycosidic antibiotics protected gold nanoparticles—A brief study. *Colloids and Surfaces A: Physicochemical and Engineering Aspects,* 297**,** 63-70.

OATES, J. A., WOOD, A. J., HOOPER, D. C. & WOLFSON, J. S. 1991. Fluoroquinolone antimicrobial agents. *New England Journal of Medicine,* 324**,** 384-394.

OBERDÖRSTER, G., OBERDÖRSTER, E. & OBERDÖRSTER, J. 2005. Nanotoxicology: an emerging discipline evolving from studies of ultrafine particles. *Environmental health perspectives,* 113**,** 823.

OLDENBURG, S. J., WESTCOTT, S. L., AVERITT, R. D. & HALAS, N. J. 1999. Surface enhanced Raman scattering in the near infrared using metal nanoshell substrates. *The Journal of chemical physics,* 111**,** 4729.

PACIOTTI, G. F., MYER, L., WEINREICH, D., GOIA, D., PAVEL, N., MCLAUGHLIN, R. E. & TAMARKIN, L. 2004. Colloidal gold: a novel nanoparticle vector for tumor directed drug delivery. *Drug delivery,* 11**,** 169-183.

PAGE-CLISSON, M.-E., PINTO-ALPHANDARY, H., OUREVITCH, M., ANDREMONT, A. & COUVREUR, P. 1998. Development of ciprofloxacin-loaded nanoparticles: physicochemical study of the drug carrier. *Journal of controlled release,* 56**,** 23-32.

PAL, S., TAK, Y. K. & SONG, J. M. 2007. Does the antibacterial activity of silver nanoparticles depend on the shape of the nanoparticle? A study of the gram-negative bacterium *Escherichia coli*. *Applied and environmental microbiology,* 73**,** 1712-1720.

PANYAM, J. & LABHASETWAR, V. 2003. Biodegradable nanoparticles for drug and gene delivery to cells and tissue. *Advanced drug delivery reviews,* 55**,** 329-347.

PAPAZOGLOU, E. S. & PARTHASARATHY, A. 2007. Bionanotechnology. *Synthesis Lectures On Biomedical Engineering,* 2**,** 1-139.

PARKIN, D. M., BRAY, F., FERLAY, J. & PISANI, P. 2005. Global cancer statistics, 2002. *CA: a cancer journal for clinicians,* 55**,** 74-108.

PARVEEN, S., MISRA, R. & SAHOO, S. K. 2012. Nanoparticles: a boon to drug delivery, therapeutics, diagnostics and imaging. *Nanomedicine: Nanotechnology, Biology and Medicine,* 8**,** 147-166.

PELLEGRINO, T., SPERLING, R., ALIVISATOS, A. & PARAK, W. 2008. Gel electrophoresis of gold-DNA nanoconjugates. *BioMed Research International,* 2007.

PEREIRA, V., LOPES, C., CASTRO, A., SILVA, J., GIBBS, P. & TEIXEIRA, P. 2009. Characterization for enterotoxin production, virulence factors, and antibiotic

susceptibility of *Staphylococcus aureus* isolates from various foods in Portugal. *Food Microbiology,* 26**,** 278-282.

PERES, A. G. & MADRENAS, J. 2013. The broad landscape of immune interactions with *Staphylococcus aureus*: From commensalism to lethal infections. *Burns*.

PERNI, S., PICCIRILLO, C., PRATTEN, J., PROKOPOVICH, P., CHRZANOWSKI, W., PARKIN, I. P. & WILSON, M. 2009. The antimicrobial properties of light-activated polymers containing methylene blue and gold nanoparticles. *Biomaterials,* 30**,** 89-93.

PETRENKO, V. A. & SOROKULOVA, I. B. 2004. Detection of biological threats. A challenge for directed molecular evolution. *Journal of microbiological methods,* 58**,** 147-168.

PICOT, L., CHEVALIER, S., MEZGHANI-ABDELMOULA, S., MERIEAU, A., LESOUHAITIER, O., LEROUX, P., CAZIN, L., ORANGE, N. & FEUILLOLEY, M. G. 2003. Cytotoxic effects of the lipopolysaccharide from *Pseudomonas fluorescens* on neurons and glial cells. *Microbial pathogenesis,* 35**,** 95-106.

PIDDOCK, L. J. 1999. Mechanisms of fluoroquinolone resistance: an update 1994–1998. *Drugs,* 58**,** 11-18.

PINGARRÓN, J. M., YÁÑEZ-SEDEÑO, P. & GONZÁLEZ-CORTÉS, A. 2008. Gold nanoparticle-based electrochemical biosensors. *Electrochimica Acta,* 53**,** 5848-5866.

PISSUWAN, D., CORTIE, C. H., VALENZUELA, S. M. & CORTIE, M. B. 2010. Functionalised gold nanoparticles for controlling pathogenic bacteria. *Trends in biotechnology,* 28**,** 207-213.

PISSUWAN, D., VALENZUELA, S. M. & CORTIE, M. B. 2006. Therapeutic possibilities of plasmonically heated gold nanoparticles. *TRENDS in Biotechnology,* 24**,** 62-67.

PLUNKETT, W., HUANG, P., XU, Y.-Z., HEINEMANN, V., GRUNEWALD, R. & GANDHI, V. Gemcitabine: metabolism, mechanisms of action, and self-potentiation. Seminars in oncology, 1995. 3-10.

POPE, J. V., TEICH, D. L., CLARDY, P. & MCGILLICUDDY, D. C. 2011. *Klebsiella pneumoniae* Liver Abscess: An Emerging Problem in North America. *The Journal of Emergency Medicine,* 41**,** e103-e105.

PRAGER, R., FRUTH, A., SIEWERT, U., STRUTZ, U. & TSCHÄPE, H. 2009. *Escherichia coli* encoding Shiga toxin 2f as an emerging human pathogen. *International Journal of Medical Microbiology,* 299**,** 343-353.

PRATAP REDDY, M., VENUGOPAL, A. & SUBRAHMANYAM, M. 2007. Hydroxyapatite-supported Ag–TiO_2 as *Escherichia coli* disinfection photocatalyst. *Water research,* 41**,** 379-386.

PROJAN, S. J. 2003. Why is big Pharma getting out of antibacterial drug discovery? *Current opinion in microbiology,* 6**,** 427-430.

RABEA, E. I., BADAWY, M. E.-T., STEVENS, C. V., SMAGGHE, G. & STEURBAUT, W. 2003. Chitosan as antimicrobial agent: applications and mode of action. *Biomacromolecules,* 4**,** 1457-1465.

RAI, M., YADAV, A. & GADE, A. 2009. Silver nanoparticles as a new generation of antimicrobials. *Biotechnology advances,* 27**,** 76-83.

RASTOGI, L., KORA, A. J. & ARUNACHALAM, J. 2012. Highly stable, protein capped gold nanoparticles as effective drug delivery vehicles for amino-glycosidic antibiotics. *Materials Science and Engineering: C.*

RICE, L. B. 2009. The clinical consequences of antimicrobial resistance. *Current opinion in microbiology,* 12**,** 476-481.

ROSEMARY, M., MACLAREN, I. & PRADEEP, T. 2006. Investigations of the antibacterial properties of ciprofloxacin@ SiO2. *Langmuir,* 22**,** 10125-10129.

ROUHANA, L. L., JABER, J. A. & SCHLENOFF, J. B. 2007. Aggregation-resistant water-soluble gold nanoparticles. *Langmuir,* 23**,** 12799-12801.

SAHA, B., BHATTACHARYA, J., MUKHERJEE, A., GHOSH, A. K., SANTRA, C. R., DASGUPTA, A. K. & KARMAKAR, P. 2007. In vitro structural and functional evaluation of gold nanoparticles conjugated antibiotics. *Nanoscale Research Letters,* 2**,** 614-622.

SALTZ, L. B., COX, J. V., BLANKE, C., ROSEN, L. S., FEHRENBACHER, L., MOORE, M. J., MAROUN, J. A., ACKLAND, S. P., LOCKER, P. K. & PIROTTA, N. 2000.

Irinotecan plus fluorouracil and leucovorin for metastatic colorectal cancer. *New England Journal of Medicine,* 343**,** 905-914.

SCHALLER, M., LAUDE, J., BODEWALDT, H., HAMM, G. & KORTING, H. 2003. Toxicity and antimicrobial activity of a hydrocolloid dressing containing silver particles in an ex vivo model of cutaneous infection. *Skin Pharmacology and Physiology,* 17**,** 31-36.

SCHMID, G. 2008. The relevance of shape and size of Au55 clusters. *Chemical Society Reviews,* 37**,** 1909-1930.

SCHMID, G. & HORNYAK, G. L. 1997. Metal clusters-new perspectives in future nanoelectronics. *Current Opinion in Solid State and Materials Science,* 2**,** 204-212.

SHAHVERDI, A. R., FAKHIMI, A., SHAHVERDI, H. R. & MINAIAN, S. 2007. Synthesis and effect of silver nanoparticles on the antibacterial activity of different antibiotics against *Staphylococcus aureus* and *Escherichia coli*. *Nanomedicine: Nanotechnology, Biology and Medicine,* 3**,** 168-171.

SHARON, M. 2012. *Bio-nanotechnology: concepts and applications*, Ane Books.

SHATKIN, J. A. 2012. *Nanotechnology: health and environmental risks*, CRC PressI Llc.

SHRIVASTAVA, S., BERA, T., ROY, A., SINGH, G., RAMACHANDRARAO, P. & DASH, D. 2007. Characterization of enhanced antibacterial effects of novel silver nanoparticles. *Nanotechnology,* 18**,** 225103.

SHUKLA, R., BANSAL, V., CHAUDHARY, M., BASU, A., BHONDE, R. R. & SASTRY, M. 2005. Biocompatibility of gold nanoparticles and their endocytotic fate inside the cellular compartment: a microscopic overview. *Langmuir,* 21**,** 10644-10654.

SHVEDOVA, A., KISIN, E., PORTER, D., SCHULTE, P., KAGAN, V., FADEEL, B. & CASTRANOVA, V. 2009. Mechanisms of pulmonary toxicity and medical applications of carbon nanotubes: two faces of Janus? *Pharmacology & therapeutics,* 121**,** 192-204.

SINGH, S. K., SHRIVASTAVA, S. & DASH, D. 2011. Metallic Nanoparticles: Biological Perspective. *Metal Nanoparticles in Microbiology.* Springer.

SKRABALAK, S. E., AU, L., LU, X., LI, X. & XIA, Y. 2007. Gold nanocages for cancer detection and treatment. *Nanomedicine,* 2**,** 657-668.

SMITH, A. M., DAVE, S., NIE, S., TRUE, L. & GAO, X. 2006. Multicolor quantum dots for molecular diagnostics of cancer. *Expert Review of Molecular Diagnostics,* 6**,** 231-244.

SMITH, A. W. 2005. Biofilms and antibiotic therapy: is there a role for combating bacterial resistance by the use of novel drug delivery systems? *Advanced drug delivery reviews,* 57**,** 1539-1550.

SPERLING, R. A., GIL, P. R., ZHANG, F., ZANELLA, M. & PARAK, W. J. 2008. Biological applications of gold nanoparticles. *Chemical Society Reviews,* 37**,** 1896-1908.

STARR, C., TAGGART, R. & STARR, L. 2008. *Biology: The unity and diversity of life*, Thomson Brooks/Cole.

STEWART, P. S. & WILLIAM COSTERTON, J. 2001. Antibiotic resistance of bacteria in biofilms. *The Lancet,* 358**,** 135-138.

SUZUKI, D. & KAWAGUCHI, H. 2005. Gold nanoparticle localization at the core surface by using thermosensitive core-shell particles as a template. *Langmuir,* 21**,** 12016-12024.

TALLURY, P., MALHOTRA, A., BYRNE, L. M. & SANTRA, S. 2010. Nanobioimaging and sensing of infectious diseases. *Advanced drug delivery reviews,* 62**,** 424-437.

TALON, D., MENGET, P., THOUVEREZ, M., THIRIEZ, G., GBAGUIDI HAORE, H., FROMENTIN, C., MULLER, A. & BERTRAND, X. 2004. Emergence of *Enterobacter cloacae* as a common pathogen in neonatal units: pulsed-field gel electrophoresis analysis. *Journal of Hospital Infection,* 57**,** 119-125.

TAUBES, G. 2008. The bacteria fight back. *Science,* 321**,** 356-361.

TAYLOR, P. W., STAPLETON, P. D. & PAUL LUZIO, J. 2002. New ways to treat bacterial infections. *Drug Discovery Today,* 7**,** 1086-1091.

THANH, N. T. & GREEN, L. A. 2010. Functionalisation of nanoparticles for biomedical applications. *Nano Today,* 5**,** 213-230.

TIAN, F., CUI, D., SCHWARZ, H., ESTRADA, G. G. & KOBAYASHI, H. 2006. Cytotoxicity of single-wall carbon nanotubes on human fibroblasts. *Toxicology in vitro,* 20**,** 1202-1212.

TOM, R. T., SURYANARAYANAN, V., REDDY, P. G., BASKARAN, S. & PRADEEP, T. 2004. Ciprofloxacin-protected gold nanoparticles. *Langmuir,* 20**,** 1909-1914.

TORCHILIN, V. P. 2005. Recent advances with liposomes as pharmaceutical carriers. *Nature Reviews Drug Discovery,* 4**,** 145-160.

TSOLI, M., KUHN, H., BRANDAU, W., ESCHE, H. & SCHMID, G. 2005. Cellular uptake and toxicity of Au55 clusters. *Small,* 1**,** 841-844.

TUREL, I. & GOLOBIC, A. 2003. Crystal Structure of Ciprofloxacin Hydrochloride 1.34-Hydrate. *Analytical sciences,* 19**,** 329-330.

TURKEVICH, J., STEVENSON, P. C. & HILLIER, J. 1951. A study of the nucleation and growth processes in the synthesis of colloidal gold. *Discussions of the Faraday Society,* 11**,** 55-75.

TUROS, E., REDDY, G., GREENHALGH, K., RAMARAJU, P., ABEYLATH, S. C., JANG, S., DICKEY, S. & LIM, D. V. 2007a. Penicillin-bound polyacrylate nanoparticles: Restoring the activity of β-lactam antibiotics against MRSA. *Bioorganic & medicinal chemistry letters,* 17**,** 3468-3472.

TUROS, E., SHIM, J.-Y., WANG, Y., GREENHALGH, K., REDDY, G., DICKEY, S. & LIM, D. V. 2007b. Antibiotic-conjugated polyacrylate nanoparticles: New opportunities for development of anti-MRSA agents. *Bioorganic & medicinal chemistry letters,* 17**,** 53-56.

UBOLDI, C., BONACCHI, D., LORENZI, G., HERMANNS, M. I., POHL, C., BALDI, G., UNGER, R. E. & KIRKPATRICK, C. J. 2009. Gold nanoparticles induce cytotoxicity in the alveolar type-II cell lines A549 and NCIH441. *Part Fibre Toxicol,* 6**,** 18.

UĞUR, Ş. S., SARıIŞıK, M., AKTAŞ, A. H., UÇAR, M. Ç. & ERDEN, E. 2010. Modifying of cotton fabric surface with nano-ZnO multilayer films by layer-by-layer deposition method. *Nanoscale research letters,* 5**,** 1204-1210.

VAN CUTSEM, E., KÖHNE, C.-H., HITRE, E., ZALUSKI, J., CHANG CHIEN, C.-R., MAKHSON, A., D'HAENS, G., PINTÉR, T., LIM, R. & BODOKY, G. 2009. Cetuximab and chemotherapy as initial treatment for metastatic colorectal cancer. *New England Journal of Medicine,* 360**,** 1408-1417.

VAN DER ZANDE, B. M., BÖHMER, M. R., FOKKINK, L. G. & SCHÖNENBERGER, C. 1997. Aqueous gold sols of rod-shaped particles. *The Journal of Physical Chemistry B,* 101**,** 852-854.

VERBRUGH, H., VERKOOYEN BSC, R., VAN DER WALL, E., HUSTINX, W., OOSTINGA, J., MINTJES-DE GROOT, J. & VAN DIJK, A. 1992. Prophylactic ciprofloxacin for catheter-associated urinary-tract infection. *The Lancet,* 339**,** 946-951.

VIJAYAKUMAR, S. & GANESAN, S. 2012. In vitro cytotoxicity assay on gold nanoparticles with different stabilizing agents. *Journal of Nanomaterials,* 2012**,** 14.

VUJAČIĆ, A., VASIĆ, V., DRAMIĆANIN, M., SOVILJ, S. P., BIBIĆ, N. A., HRANISAVLJEVIC, J. & WIEDERRECHT, G. P. 2012. Kinetics of J-aggregate formation on the surface of Au nanoparticle colloids. *The Journal of Physical Chemistry C,* 116**,** 4655-4661.

WALSH, C. 2000. Molecular mechanisms that confer antibacterial drug resistance. *Nature,* 406**,** 775-781.

WANG, Y., WEI, W., LIU, X. & ZENG, X. 2009. Carbon nanotube/chitosan/gold nanoparticles-based glucose biosensor prepared by a layer-by-layer technique. *Materials Science and Engineering: C,* 29**,** 50-54.

WAWER, M. J., SEWANKAMBO, N. K., SERWADDA, D., QUINN, T. C., PAXTON, L. A., KIWANUKA, N., WABWIRE-MANGEN, F., LI, C., LUTALO, T. & NALUGODA, F. 1999. Control of sexually transmitted diseases for AIDS prevention in Uganda: a randomised community trial. *The lancet,* 353**,** 525-535.

WEARE, W. W., REED, S. M., WARNER, M. G. & HUTCHISON, J. E. 2000. Improved synthesis of small (d core≈ 1.5 nm) phosphine-stabilized gold nanoparticles. *Journal of the American Chemical Society,* 122**,** 12890-12891.

WEIR, E., LAWLOR, A., WHELAN, A. & REGAN, F. 2008. The use of nanoparticles in anti-microbial materials and their characterization. *Analyst,* 133**,** 835-845.

WELLER, R. B. 2009. Nitric Oxide–Containing Nanoparticles as an Antimicrobial Agent and Enhancer of Wound Healing. *Journal of Investigative Dermatology,* 129**,** 2335-2337.

WILLNER, B., KATZ, E. & WILLNER, I. 2006. Electrical contacting of redox proteins by nanotechnological means. *Current opinion in biotechnology,* 17**,** 589-596.

WOOD, A. J., GOLD, H. S. & MOELLERING JR, R. C. 1996. Antimicrobial-drug resistance. *New England Journal of Medicine,* 335**,** 1445-1453.

ZETOLA, N., FRANCIS, J. S., NUERMBERGER, E. L. & BISHAI, W. R. 2005. Community-acquired meticillin-resistant *Staphylococcus aureus*: an emerging threat. *The Lancet infectious diseases,* 5**,** 275-286.

ZHAO, P., LI, N. & ASTRUC, D. 2012. State of the Art in Gold Nanoparticle Synthesis. *Coordination Chemistry Reviews***,** 1-77.

ZHAO, Y., TIAN, Y., CUI, Y., LIU, W., MA, W. & JIANG, X. 2010. Small molecule-capped gold nanoparticles as potent antibacterial agents that target gram-negative bacteria. *Journal of the American Chemical Society,* 132**,** 12349-12356.

Materials, Suppliers and Equipment

1. Synthesis of ciprofloxacin-conjugated Gold nanoparticles

Reagent	**Empirical Formulae**	**Supplier**	**Catalogue number**
Choroauric acid	$HAuCl_4.3H_2O$	Sigma-Aldrich	254169-5G
Trisodium citrate dihydrate	$HOC(COONa)CH_2COONa)_2.2H_2O$	Sigma-Aldrich	S1804-1KG
Ciprofloxacin	$C_{17}H_{18}FN_3O_3$	Sigma-Aldrich	17850-5G-F

2. Culture and Maintenance of Bacterial Cultures

Media/Equipment	**Supplier**	**Catalogue Number**
Nutrient broth	Sigma-Aldrich	70122-100G
Nutrient Agar	Sigma-Aldrich	N9405-500G

3. MIC Assay

Media/Equipment	**Supplier**	**Catalogue number**
Mueller-Hinton broth	Sigma-Aldrich	70192-100G
GREINER Cellstar 96-well, round-bottomed microtitre plates	Sigma-Aldrich	M9436-100EA
p-iodonitrotetrazolium chloride	Sigma-Aldrich	I8377-5G

4. MTT Assay

Media/Equipment	**Supplier**	**Catalogue number**
Ethanol	Sigma-Aldrich	
Dulbecco's Modified Eagle Medium (DMEM)	Sigma-Aldrich	D6429-500ML
1% antibiotic-antimycotic solution	Sigma-Aldrich	A5955-20ML
10% heat-inactivated foetal calf serum (FCS)	Sigma-Aldrich	F0685-3G
Phosphate buffered saline (PBS)	Sigma-Aldrich	P5493-1L
Trypsin	Sigma-Aldrich	T1763-25UN
100% dimethyl sulfoxide (DMSO)	Sigma-Aldrich	D8418-100ML
3-(4,5-dimethylthiazol-2-yl)-2,5-diphenyltetrazolium bromide (MTT reagent)	Sigma-Aldrich	M2003-1G
Cell culture flasks	Sigma-Aldrich	CLS3920

5. Equipment

Experimental use	**Equipment**
UV-spectrum generation and analysis	Cary 100 UV-Vis spectrophotometer
FT-IR analysis and generation of spectrum	PerkinElmer Spectrum 100 spectrophotometer
TEM (nanoparticle synthesis)	JEOL JEM-1010 transmission electron microscope
TEM (antibacterial activity of conjugated GNPs)	JEOL JEM-2100 transmission electron microscope
MTT assay (plate reader)	Biohit Plc, e-Lisa XL
MTT assay (cell culture incubation)	Snijders Scientific CO190IR CO_2 incubator
MIC assay (incubation of bacterial cultures)	INFORS-HT Ecotron incubator

APPENDIX B

Equations and Formulae

1. Standardization of bacterial cultures

Bacterial cultures for the MIC assay were standardized by absorbance readings in accordance with the Macfarlane standard. The desired absorbance was 0.5 at a wavelength of 600 nm on the UV-visible spectrum. If absorbance of bacterial culture suspensions were over 0.5, the following equations were used to dilute the suspension appropriately, such that the inoculum for the MIC assay correlated to the MacFarlane standard of 0.5.

The dilution factor (Eq. 1) was determined, followed by calculation of the required volumes of both culture suspension and sterile media diluent (Eq. 2 and 3). The 5 ml culture suspension that serves as the MIC assay inoculums was calculated in the final step (Eq. 4).

$$\textbf{DF (}\text{Dilution Factor}) = \frac{0.5}{\text{Absorbance of bacterial suspension}} \quad \text{(Eq. 1)}$$

$$\textbf{CV}\ (\text{Volume of culture required for diluton}) = \text{DF} * 5\ \text{mL} \quad \text{(Eq. 2)}$$

$$\textbf{DV}\ (\text{Volume of sterile Mueller Hinton broth required for dilution}) = 5\ \text{mL} \quad \text{(Eq. 3)}$$

$$\text{Inoculum for MIC Assay} = \textbf{CV} + \textbf{DV} \quad \text{(Eq. 4)}$$

2. MTT Assay

From the absorbance readings obtained after scanning MTT assay plates via ELISA reader, the percentage cell viability was calculated by the following equation:

$$\text{Percentage viability (\%)} = \frac{\text{Absorbance of treated cell}}{\text{Absorbance of untreated cells (negative control)}} \times 100 \quad \text{(Eq. 5)}$$

The percentage cytotoxicity of the tested compound was then calculated from the percentage viability by the following equation:

Percentage cytotoxicity (%) = 100 – (Percentage viability) (Eq. 6)

Since the assay was performed in triplicate, an average of the three percentage cytotoxicity readings for each concentration tested was calculated and standard error determined.

Ethical Clearance for Study Performed

The following section of the PG4 form presents the ethics level rating of this study (Level 1), as per the DUT Ethics and Biosafety Research Committee.

aspects, **297**: 63-70.fve

Section C: Ethics
Note: Ethics requirements are faculty specific. Kindly ensure that you are aware of and have complied with the relevant ethics requirements.

Tick as appropriate:

Humans		Organisations		Animals		Environment	
Yes	No X	Yes	No X	Yes	No X	Yes	No X

Indicate Category (X)

1.	Exempt from Ethics and Biosafety Research Committee Review (straightforward research without ethical problems)	X
2.	Expedited review (minimal risk to humans, animals or environment)	
3.	Full Ethics and Biosafety Research Committee review recommended (possible risk to humans, animals, environment, or a sensitive research area)	
4.	Full Ethics and Biosafety Research Committee review required (risk to humans, animals, environment, or a sensitive research area)	

Attach Addendums (if any)

Please initial alongside if the project is to be registered as secret

[redacted]

PG4a_2010